Cover Page

Universiteit Leiden

The handle http://hdl.handle.net/1887/20426 holds various files of this Leiden University dissertation.

Author: Commandeur, Suzan
Title: Organotypic in vitro models of human cutaneous squamous cell carcinoma
Issue Date: 2013-01-16

Organotypic *in vitro* models of human cutaneous squamous cell carcinoma

Suzan Commandeur

Organotypic *in vitro* models of human cutaneous squamous cell carcinoma
© Suzan Commandeur, 2013

All rights reserved. No part of this thesis may be reproduced, stored or transmitted in any way without prior written permission of the copyright owner.

ISBN:	9789088915505
Cover design:	Suzan Commandeur
Photo on front cover:	Application of test compound on *in vitro* human skin model. © Aat Mulder
Lay out:	Suzan Commandeur
Printed by:	Proefschriftmaken.nl || Uitgeverij BOXPress
Published by:	Uitgeverij BOXPress, 's-Hertogenbosch

The research presented in this thesis was performed at the Department of Dermatology of the Leiden University Medical Center, The Netherlands.

The research presented in this thesis was financially supported by ZonMw, the Netherlands Organisation for Health Research and Development.

Financial support for the publication of this thesis was kindly provided by Stichting Stimuleringsfonds Alternatieven voor Dierproeven, Stichting Proefdiervrij, Animal Free Research, Aeon Astron Europe B.V., GlaxoSmithKline B.V., LEO Pharma B.V., Galderma B.V., Louis Widmer Nederland B.V., Astellas B.V., Fagron B.V. and Merz GmbH.

Organotypic *in vitro* skin models of human cutaneous squamous cell carcinoma

Proefschrift

ter verkrijging van
de graad van Doctor aan de Universiteit Leiden,
op gezag van de Rector Magnificus Prof. Mr. P.F. van der Heijden,
volgens besluit van het College voor Promoties
te verdedigen op woensdag 16 januari 2013
klokke 16.15 uur

door

Suzan Commandeur
geboren te Delft
in 1983

Promotiecommissie

Promotor	Prof. Dr. R. Willemze
Co-promotores	Dr. A. El Ghalbzouri Dr. C.P. Tensen
Overige leden	Prof. Dr. S. Gibbs *VU University Medical Centre (VUmc), Amsterdam*
	Prof. Dr. J.A. Bouwstra *Leiden Amsterdam Centre for Drug Research (LACDR), Leiden*
	Prof. Dr. L.H.F. Mullenders

Voor Jaap

Contents

	List of abbreviations	9
Chapter 1	General introduction	11
Chapter 2	An in vitro three-dimensional model of primary human cutaneous squamous cell carcinoma *Exp Dermatol. 2009 Oct;18(10):849-56.*	37
Chapter 3	Functional characterization of cancer associated fibroblasts of human cutaneous squamous cell carcinoma *Exp Dermatol. 2011 Sep;20(9):737-42.*	59
Chapter 4	Replacement of animal-derived collagen matrix by human fibroblast-derived dermal matrix for human skin equivalent products *Biomaterials. 2009 Jan;30(1):71-8.*	77
Chapter 5	Gene expression analysis of squamous cell carcinoma of immunosuppressed transplant recipients. *Submitted*	101
Chapter 6	Epidermal growth factor receptor activation and inhibition in 3D in vitro models of normal skin and human cutaneous squamous cell carcinoma in vitro. *Cancer Science (accepted)*	131
Chapter 7	General discussion	147
Chapter 8	Nederlandse samenvatting	162
	List of publications	170
	Curriculum vitae	172
	Short summary	174

List of abbreviations

6-4PP	6-4 photoproducts
AE	air-exposed
AEC	3-amino-9-ethylcarbazole
AK	actinic keratosis
BAF	B allele frequency
BCC	basal cell carcinoma
BM	basement membrane
BP	biological processes
BSA	bovine serum albumin
CAF	cancer-associated fibroblast
CPD	cyclobutane-pyrimidine dimers
cnLOH	copy neutral LOH
CNV	copy number variation
DAB	3,3'-diamino- benzidine
DED	de-epidermized dermis
DEG	differentially expressed gene
DEJ	dermal-epidermal junction
DEP	differentially expressed probe
DMEM	Dulbecco's modified Eagle medium
ECM	extracellular matrix
EGF	epidermal growth factor
EGFR	epidermal growth factor receptor
ELISA	enzyme linked immunosorbent assay
ESC	epidermal stem cell
FBS	fetal bovine serum
FC	fold change
FDR	false discovery rate
FDM	fibroblast-derived matrix
FGF	fibroblast growth factor
GO	gene ontology
GSEA	geneset enrichment analysis
GWEA	genome-wide expression analysis
HGF	hepatocyte growth factor
HPV	human papilloma virus
HSE	human skin equivalent
HRP	horseradish peroxidase
LOH	loss of heterozygosity
KEGG	Kyoto encyclopedia of genes and genomes
KGF	keratinocyte growth factor
MMP	matrix metalloproteinase
NF	normal fibroblast
NFκB	nuclear factor κB
NHDF	normal human dermal fibroblast
NHEK	normal human epidermal keratinocyte
NMF	natural moisturizing factor
NMSC	non-melanoma skin cancer
NS	normal skin
OTR	organ transplant recipient
PBS	phosphate buffered saline
PCA	principal component analysis
PCR	polymerase chain reaction
PDGF	platelet-derived growth factor
PGSEA	parametric GSEA
QPCR	quantitative RT-PCR
RANKL	receptor activator of NF-κB ligand
RSN	robust spline normalization
RT-PCR	reversed transcriptase PCR
SB	stratum basale
SC	stratum corneum
SCC	squamous cell carcinoma
SNP	single nucleotide polymorphism
SS	stratum spinosum
STR	short tandem repeat
TF	transcription factor
TFBS	transcription factor binding site
TGF-β	transforming growth factor β
TSG	tumor suppressor gene
UVR	ultraviolet radiation
VST	variance-stabilizing transformation

1

General introduction

Cutaneous squamous cell carcinoma (SCC)

Cutaneous SCC in society

Incidence of cutaneous SCC

Skin cancer is the most common type of cancer in fair-skinned Caucasian populations. Each year, there are two to three million new cases worldwide and skin cancer incidence rates outnumber those of all other major cancers combined in the United States (US).[1-5] In The Netherlands, over 20 000 new cases of skin cancer were diagnosed in 2000.[6] In 2005, this number was projected to increase by 80% to more than 37 000 per year in 2015.[6] However, current estimations of the Dutch Cancer Society have already reached 36 000 new cases of skin cancer per year for 2012, pointing out that the incidence of skin cancer among the Dutch population grows even more rapidly than foreseen.[7] The majority of skin cancers are carcinomas, also referred to as keratinocyte skin cancers or non-melanoma skin cancers (NMSC), comprising basal cell carcinoma (BCC) and squamous cell carcinoma (SCC). In general, the absolute incidence of BCC is about five times the incidence of SCC, with an annual 2011 estimate of 27 000 cases of BCC and 5 400 cases of SCC in The Netherlands, comprising about 75% and 15% of all skin cancer diagnoses in the Netherlands, respectively.[7] Despite the lower incidence of SCC compared to BCC, SCCs have a greater propensity for invasion, local recurrence and metastasis.[8] This problem is particularly dramatic in organ transplant recipients (OTRs) receiving immune suppressive medication to prevent graft rejection.[9] Based on standardized incidence ratios for the Northern regions of Europe and the US, the risk for cutaneous SCC in these patients is approximately 70 times increased compared to the general population in those regions.[10] Cutaneous SCC are often claimed to be more aggressive in OTRs than in immune competent individuals, but this statement is currently insufficiently supported by literature.[11-13] Increased development of successive lesions is particularly pronounced in renal transplant recipients, having a 75% risk of developing another cutaneous SCC within 5 years after diagnosis of the first lesion, compared to a risk of only 20% of developing another SCC within 5 years in the general population.[14]

Risk factors for cutaneous SCC

In addition to immune suppression in OTRs, cutaneous SCC is also increased in patients whose immune system is otherwise compromised, e.g. by immune deficiency diseases and chemotherapy.[15] Other exposure-related risk factors for development of cutaneous SCC include ultra-violet radiation (UVR) exposure, radiotherapy and smoking.[16] Although the absolute risk of UVR exposure is relatively low, massive and prolonged sun exposure of the

population make this the most well-known and most relevant risk factor for cutaneous SCC.[17] An indirect viral risk factor for cutaneous SCC, in specific genus β human papilloma virus (β-HPV), is suspected.[18-20] However, recent findings suggest that it is unlikely that any currently known virus is commonly responsible for induction or maintenance of cutaneous SCC.[21] Host-related risk factors for cutaneous SCC include increased age, male gender and light skin color.[17] Furthermore, chronic ulcers, chronic inflammatory lichen sclerosis, burn wounds and various specific genetic traits also increase the risk for cutaneous SCC.[17]

Management of cutaneous SCC

Management of cutaneous SCC in OTRs exists in preventive patient education minimizing excessive sun exposure, intensive skin surveillance, active early-stage treatment of all premalignant lesions and surgical removal of established carcinomas.[22, 23] Premalignant lesions are generally cleared by topical lesion-directed cryotherapy and/or field-directed topical treatment.[24] Established SCCs are mostly surgically excised and histologically examined.[25, 26] Although cutaneous SCCs can often be successfully removed and are rarely lethal, their UVR exposure-related high incidence on the face, their rapid growth and their removal in itself may be cosmetically disfiguring, negatively impacting the quality of life of cutaneous SCC patients.[27] The cost associated with treatment of SCC is substantial. In 2004, the total direct cost associated with the treatment of NMSC in the US was $1.5 billion.[28] Taken together, although cutaneous SCC does not present a large mortality risk, its high and rising prevalence and expense of treatment render this skin cancer a major public health problem.

Pathology of cutaneous SCC

Cutaneous SCC originates from a malignant population of proliferating keratinocytes in the suprabasal layers of the epidermis. These skin tumors can develop *de novo* or from the precursor lesion actinic keratosis (AK). AKs, or solar keratoses, are premalignant, dysplastic, intra-epidermal lesions (Figure 1). Approximately 8% of AKs ultimately progress to SCC.[24] During this process, the tumor expands through the basement membrane (BM) and invades the underlying dermis (Figure 1). Cutaneous SCC and its precursor lesions are predominantly located on sun-exposed areas of the skin, including the face, scalp, lip, forearms and back of the hands. It is therefore not surprising that UVR exposure is the predominant driver in the pathogenesis of cutaneous SCC. UVR exerts its oncogenic effects directly through DNA damage, and indirectly through local and systemic immune suppression. Direct UVR induced DNA damage involves dimerization of successive pyrimidine bases resulting in cyclobutane-pyrimidine dimers (CPDs) and 6-4 photoproducts (6-4PP). During DNA replication, these dimers may lead to specific point mutations (mostly cytosine to thymine transitions) and double strand breaks in the DNA,

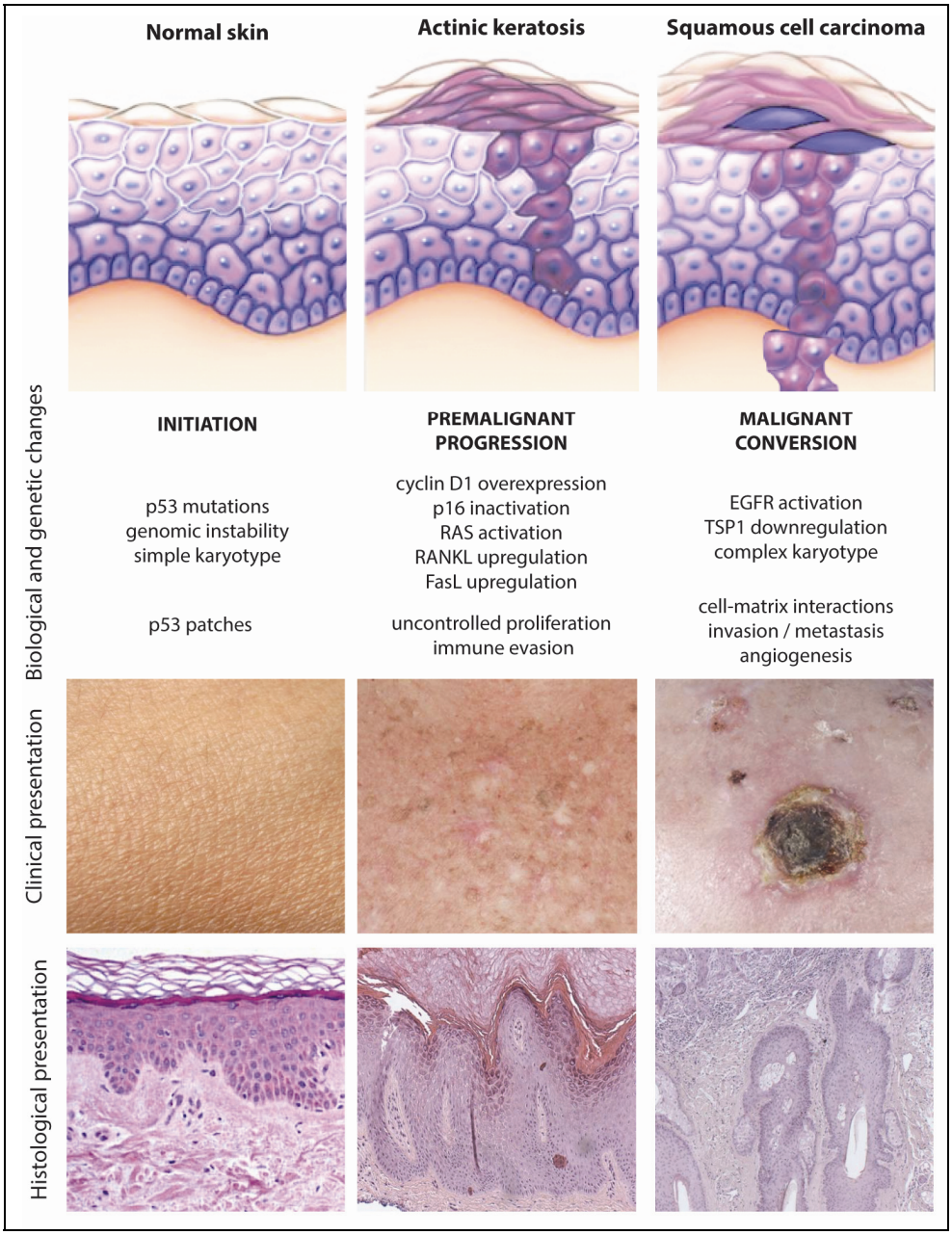

Figure 1 | Overview of genetic, biological, clinical and histological changes in initiation, premalignant progression and malignant conversion of normal skin to actinic keratosis and cutaneous squamous cell carcinoma. Images adapted and reused with permission (Nancy Heim of the Columbia University Medical Center (schematics), iStockphoto/Eugene Llacuna (normal skin), Department of Dermatology of the Leiden University Medical Center).

the latter of which may also induce chromosomal aberrations.[29] When left unrepaired, UVR-induced DNA damage accumulates over many years and leads to actual mutations in cellular DNA, altering genes regulating normal cellular growth. Importantly, inactivating UVR-induced mutations in the p53 tumor suppressor gene are very common early events in SCC carcinogenesis, both in immune competent individuals and in immune suppressed OTRs.[30-32] These p53 mutations result in unchecked mitosis (cell cycle deregulation) and loss of apoptosis in affected epidermal keratinocytes, allowing for clonal expansion and formation of premalignant lesions (Figure 1). Upon further UVR exposure, genomic instability increases and additional genetic lesions may accumulate in these cells, including inactivation of the CDKN2A (p16 INK4A) tumor suppressor gene, overexpression of the cell cycle regulator cyclin D1 gene and activation of the proliferative RAS pathway – events all associated with progression of AK to SCC (Figure 1).[33-36] As mutations in the RAS family of proto-oncogenes are rare events in cutaneous SCCs, increased RAS signaling may result from amplification of its gene locus and increased expression and activation of upstream factors including the transmembrane tyrosine kinase epidermal growth factor receptor (EGFR).[37] EGFR overexpression has been inconsistently found in 0% to 78% of cutaneous SCCs and may result from highly variable numerical aberrations or genetic amplifications. However, increased EGFR activation and upregulated EGFR signaling have been consistently found in 25% to 100% of cutaneous SCCs.[36, 38-40] EGFR is directly activated by its ligands as well as through decreased dephosphorylation by UVR.[41] Indeed, EGFR ligands have been found upregulated in cutaneous SCCs when compared to adjacent normal skin.[40] Of all genetic aberrations characteristic of cutaneous SCC, many have been found at the chromosomal level, as supported by complex karyotypes with large numbers of allelic imbalances often displayed by immune competent AKs and SCCs.[42-45] Genetic and phenotypic differences between SCCs may be explained by functional equivalence of various genetic changes, allowing a large number of genotypes to be tumorigenic. Furthering on this concept, intratumoral (genetic) diversity may result from multiple genetic clones existing in different regions and at different times within the same tumor.

In addition to DNA damage, UVR exposure induces both systemic and local immune suppression in the skin. UVR-induced soluble mediators tempering the systemic immune response include cis-urogenic acid and interleukin 10.[46] UVR exposure results in local immune suppression in epidermal keratinocytes by upregulation of the receptor activator of NF-κB ligand (RANKL), thereby inducing dendritic cell-mediated proliferation of regulatory T cells (Tregs), which in turn locally reduce the peritumoral immunological response by effector T cells in the skin.[47] In addition, epidermal Langerhans cells are reduced in number and function upon UVR exposure, hampering their response to transformed cells.[46] Furthermore, cutaneous AK and SCC cells display simultaneous

downregulation of cell death receptor Fas (CD95) and upregulation of Fas ligand (FasL), providing them with an active defense from systemic Fas-expressing immune effector cells.[48, 49] Adding to this, UVR and viral infections (e.g. HPV) are suggested to synergistically support oncogenesis in the skin.[50-52]

Tumor-stroma interactions in cutaneous SCC

Microenvironmental barriers to proliferation

The process of cutaneous SCC initiation, progression, invasion and eventually metastasis does not occur in isolation, as the (pre)malignant epidermal cells are surrounded by their microenvironment. Moreover, epidermal cells need to overcome various microenvironmental barriers in order to expand and eventually invade the dermis. These barriers select for specific adaptive cellular properties during the different stages of carcinogenesis. Ultimately, such microenvironmental barriers define the sequence with which hallmarking phenotypical and genotypical changes occur during SCC carcinogenesis.[53] In normal epidermis, detachment-induced apoptosis (anoikis) and contact inhibition are dominant proliferation barriers. Resistance to these barriers confers early properties of premalignant epidermal cells that are hallmarked by genetic aberrations in cell cycle regulators, resulting in insensitivity to anti-growth signals and uncontrolled proliferation. Then, independent growth signaling caused by upregulated expression of growth factors and/or receptors enable premalignant cells to overcome normal proliferation limits. In cutaneous SCC, this is mostly reflected by upregulation of the proliferative RAS pathway, including increased activation of EGFR and increased transcription of EGFR ligands.[39, 40]

Invasion through the basement membrane

The development of invasive SCC is not simply accomplished by unrestricted proliferation of the cancer cell population, but rather requires an active collaboration of malignant epidermal SCC cells and various dermal components. Epidermal cells are anchored to and separated from the underlying dermis by an intact basement membrane (BM), in which the basal layer (basal lamina) facing the epidermis and the reticular layer (lamina reticularis) facing the dermis are fused (Figure 2). The basal lamina typically harbors laminins, integrins, entactins, dystroglycans and an underlying network of collagen type IV fibrils, whereas the reticular layer mainly contains collagen type I and collagen type III fibers. The two layers are connected by collagen type VII anchoring fibrils and microfibrils. Through the BM, substrates, metabolites and signaling molecules are exchanged between the epidermis and the dermis. The dermis consists of extracellular matrix (ECM),

containing large amounts of collagen type I, collagen type IV and fibronectin, in which fibroblasts, immune cells and vasculature reside. The BM acts as a mechanical barrier preventing premalignant cells from invading the dermis and deeper tissues.

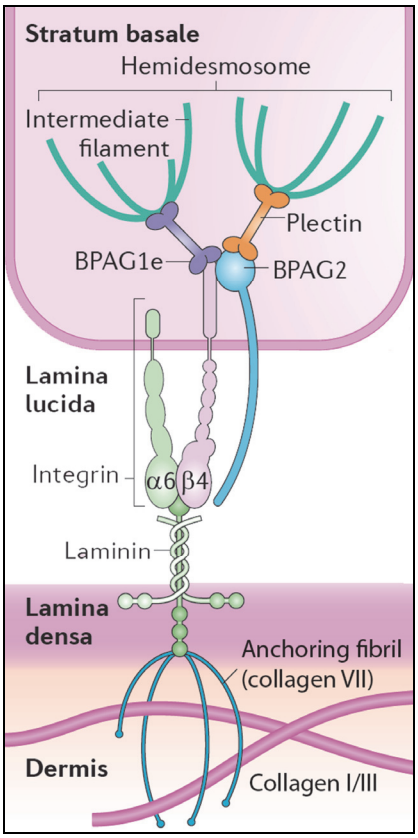

Figure 2 | Schematic representation of the basement membrane (BM) separating the epidermis from the dermis in human skin. The BM is composed of the lamina lucida and lamina densa. Hemidesmosomes anchor keratinocytes from the basal layer to the BM, mainly through the interaction of laminin 332 with the $\alpha_6\beta_4$ integrin receptor and the transmembrane protein bullous pemphigoid antigen 2 (BPAG2, also known as collagen XVII). This interaction also relays signals from the epidermal and extraepidermal environment to a network of keratin intermediate filaments. Hemidesmosomes are tethered to intermediate filaments by the plakin family members plectin and BPAG1e.. Anchoring of the epidermis to the dermis depends on the interaction of laminin 332 with collagen VII, the major component of anchoring fibrils that extend from the BM into the dermis. Adapted with permission from Macmillan Publishers Ltd: Nature Reviews Molecular Cell Biology, Simpson et al, copyright (2011).

Cancer-associated fibroblasts

Cutaneous tumor invasion is a manifestation of disrupted epidermal homeostasis resulting from interactions between the epidermal cancer cells and their stromal counterparts in the dermis, mainly represented by cancer-associated fibroblasts (CAFs).[54] In literature, these cells are also termed tumor-associated fibroblasts, reactive stromal fibroblasts, activated fibroblasts, myofibroblasts, peritumoral fibroblasts, pericytes or fibrocytes.[55-58] CAFs have been found responsible for breakdown of BM structures and dermal ECM remodeling in concert with epithelial cancer cells, thereby facilitating tumor invasion. [53, 59, 60] The functional contribution of CAFs to carcinogenesis is supported by their structural properties, as their phenotype is similar to fibroblasts associated with wound healing (Figure 3). To synthesize large amounts of ECM constituents, CAFs typically contain a large euchromatic nucleus with one or two nucleoli and a prominent rough endoplasmic reticulum and Golgi apparatus.[53] These changes in nuclear volume and cellular composition are partly driven by pro-fibrotic growth factors released by the cancer cells and include transforming growth factor-β (TGF-β), epidermal growth factor (EGF), platelet-derived growth factor (PDGF) and fibroblast growth factor (FGF), all of which are key mediators of fibroblast activation and tissue fibrosis. In turn, cutaneous SCC-associated CAFs themselves have been shown to produce increased amounts of growth factors including hepatocyte growth factor (HGF) and ECM-degrading proteases such as matrix metalloproteinase 2 (MMP2), MMP3, MMP9 and MMP10, facilitating increased ECM turnover and remodeling.[61-64] Many growth factors bind to dermal ECM components like proteoglycans, fibronectin and vitronectin.[65] This renders the dermal ECM a reservoir of growth factors that can be released upon ECM degradation, thereby establishing stable gradients of growth factors supporting tumorigenesis. The extensive crosstalk between cancer cells and their activated stroma ultimately leads to increased tumor cell motility, for which BM and dermal ECM degradation is a substrate. Beyond invasion, cancer cells may acquire metastatic properties, thereby successfully overcoming other microenvironmental barriers including hypoxia and ischaemia, often marked by increased angiogenesis. Late-stage invasion of cutaneous SCC cells into subcutaneous tissues is indeed characterized by increased stromal angiogenic responses and increased density of both blood and lymphatic vessels, which have not been found in the dermis of normal skin, AKs and less aggressive, early-stage SCCs.[66-68] Although metastasis is rare in cutaneous SCC, it is hallmarked by increased angiogenesis at the invasive tumor front in immune suppressed OTRs.[12, 69]

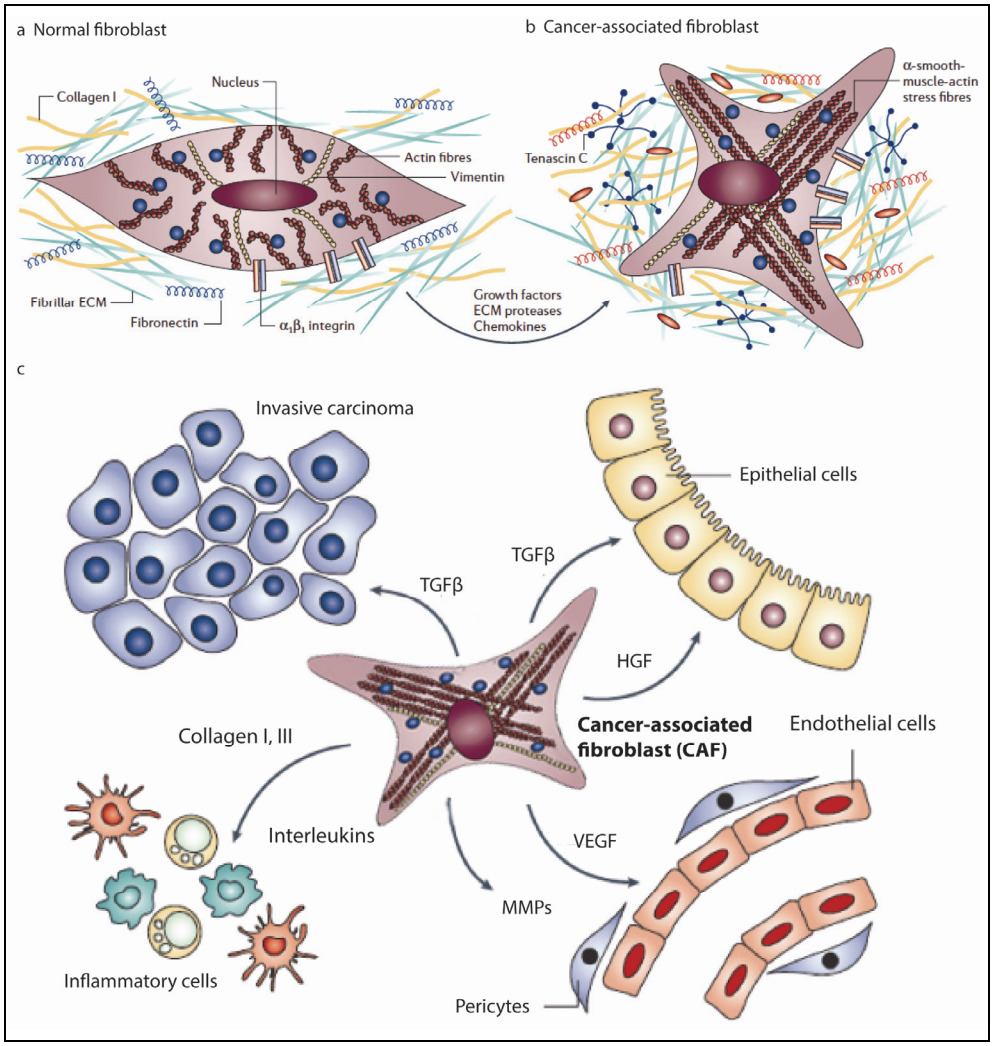

Figure 3 | In human skin, normal fibroblasts are embedded in the fibrillar extracellular matrix (ECM) of the dermis, which largely consists of type I collagen and fibronectin (a). Upon interaction with epithelial tumor cells, cancer-associated fibroblasts (CAFs) acquire an activated phenotype, which is associated with α-smooth-muscle actin expression and enhanced secretion of ECM proteins (b). In the tumor stroma, CAFs communicate with cancer cells, resident epithelial cells, endothelial cells, pericytes and inflammatory cells through the secretion of growth factors and chemokines (c). Through the increased deposition of collagens and modulation of the inflammatory response, CAFs induce and maintain a potentially oncogenic microenvironment. Adapted with permission from Macmillan Publishers Ltd, copyright 2006.[53]

Modeling cutaneous squamous cell carcinoma

In vivo SCC models

To develop rational preventive and therapeutic strategies and to study functional consequences of genetic aberrations found in clinical research, basic research models are needed. Experimental models for cutaneous SCC include *in vivo* and *in vitro* models. *In vivo* models are living, intact animals in which human disease is studied without the risk of harming human beings. For cutaneous SCC, traditional *in vivo* models are based on chemically, radiation- or virally induced carcinogenesis in mice. An old but still widely used approach is the two-stage model of chemical skin carcinogenesis, in which genotoxic agents are applied to murine skin for tumor initiation, followed by repeated exposure to a mitogenic tumor promoter to induce hyperplasia.[70] The affected skin forms mainly benign papillomas, some of which eventually progress to cutaneous SCC.[71] In radiation-induced skin carcinogenesis models, mice develop cutaneous SCCs upon repeated UVR exposure without prior chemical tumor initiation. The immune competent outbred hairless albino mouse strain SKH1-*hr* is the most widely used model organism to study UVR-induced cutaneous SCC.[72] Upon chronic UVR exposure, these mice develop cutaneous SCC resembling human cutaneous SCC both at the morphological and molecular level.[73] Virally induced *in vivo* skin carcinogenesis models include transgenic mice with expression of specific regions of the HPV8 genes, leading to spontaneous development of papillomas, dysplasia and SCC of the skin.[74] Expression of specific HPV38 genes greatly increases their susceptibility to chemical and UVR-induced skin carcinogenesis.[75] Another approach to study skin carcinogenesis *in vivo* is intradermal or subcutaneous injection or surface transplantation of human cancer cell line xenografts into immunodeficient mice.[76-78] Severe combined immunodeficient (scid) mice, immune deficient Rag1 mice and athymic nude mice are often used for such xenograft models.[79] Genetically engineered mice with germline alterations further add to the spectrum of model organisms available for studying cutaneous SCC.[80] Refined genetically engineered models include mosaic or conditional models, in which a latent allele is phenotypically inactive until stimulated in a tissue- and time-specific manner with exogenous chemicals or viruses, often utilizing the Cre-lox recombination system.[81, 82] Examples of successfully combined approaches include surface transplantation with genetically engineered human SCC cell lines and UVR-induction of SCC in a xenograft mouse model.[78, 83] All *in vivo* models available have certain features that render them suitable for studying a specific research question (Table 1).

Table 1 | Key features of *in vivo* models of human cutaneous SCC.

In vivo model	Transformed cell origin[1]	Genetically defined[2]	Intact immunity[3]	Relevant microenvironment[4]	Genomic instability[5]
Chemical carcinogenesis	Mouse or human*	No	Possible*	Yes	Possible*
UVR-induced carcinogenesis	Mouse or human*	No	Possible*	Yes	Yes
Viral carcinogenesis (human papillomavirus, HPV)	Mouse	Yes	Yes	No	Unknown
Xenograft (injected or transplanted)	Human	Possible	No	No	Yes
Genetically engineered	Mouse	Yes	Yes	Yes	No
Genetically engineered (non-germline)	Mouse	Yes	Yes	Yes	No

[1] **Transformed cell origin** defines whether the model carcinomas consist of either human or animal cells.
[2] **Genetically defined** states whether the genetic background of the host animal is fully known.
[3] **Intact immunity** defines whether the host animal has an intact immune system.
[4] **Relevant microenvironment** defines the similarity of the surrounding tumor stroma to that in human SCC.
[5] **Genomic instability** defines the similarity of the genomic instability of the tumors to that found in human SCC.
* When combined with xenograft approaches, human cells may be used at the expense of intact immunity.

In vitro SCC models

Primary cells and cell lines

The natural complexity of living organisms present in *in vivo* models is a great barrier to the identification and functional study of individual biological components. Therefore, *in vitro* models are used in which components of an organism that have been isolated from their native biological context permit simplified and more accessible analyses than can be done with whole organisms. To study human cutaneous SCC *in vitro*, both two- and three-dimensional tissue culture approaches are available. Two-dimensional monolayer cell cultures are either based on primary cells or cell lines. Primary cutaneous SCC cell cultures are notoriously difficult to establish, and can be obtained either by direct primary SCC explant culture or enzymatic isolation of primary SCC cells.[84] The resulting primary monolayer SCC cell cultures are often very heterogenic, have a limited lifespan and mostly require feeder layers of immortalized dermal fibroblasts.[85] However, upon successful *in vitro* propagation, primary cutaneous SCC cell cultures may retain the ability to proliferate indefinitely, thereby establishing immortal SCC cell lines. These cultures provide useful subsets of precisely defined stages of tumorigenic differentiation. To date, only a limited number of cutaneous SCC cell lines are available (Table 2). Among these, the MET1 to MET4 cell lines represent a clonally related progression series of cutaneous SCC, as these cell lines are derived from a primary cutaneous SCC, two recurrences and a metastasis from a single patient. Furthermore, genetic engineering of the HaCaT cell line, originating from spontaneously immortalized healthy human keratinocytes, resulted in a series of malignant tumorigenic and even metastatic variants.[86, 87] Such cell line series representing different stages of skin carcinogenesis enable the *in vitro* study of sequential acquisition of transformation-related traits. In addition, using such SCC cell lines, both phenotypic and genetic characteristics can be correlated to their direct clinical origin.

Three-dimensional *in vitro* SCC models

Isolated cultures of primary SCC cells and established SCC cell lines lack any microenvironmental context. Therefore, co-cultures of either primary SCC cells or SCC cell lines and dermal human fibroblasts are performed to study the interaction between both cell types.[88] Also, either primary SCC cells or SCC cell lines can be cultured in ECM-like matrices (e.g. Matrigel®, Cultrex®) to study the interaction between SCC cells and ECM components *in vitro*.[89] However, such SCC models still lack a fully organized representation of the relevant human SCC microenvironment. More advanced *in vitro* models of cutaneous SCC are therefore represented by three-dimensional cell culture systems, integrating SCC cells in a relevant microenvironment. In literature, these models

Table 2 | Characteristics of human cutaneous SCC cell lines currently available.

Cell line	Tumor stage	Origin	Characteristics	Reference
SCC-12B2	Primary, well-differentiated	Male OTR (60), immune suppression, face	- p53 mutated - poorly differentiated - cystic in mice	Rheinwald et al (1981)[85]
SCC-12F2			- p53 mutated - well-differentiated - not tumorigenic in mice	
SCC-13	Primary, well-differentiated	Female OTR (56), radiotherapy, face	- p53 mutated - well-differentiated - feeder layer dependent - cystic in mice	
HSC-1	Primary, poorly differentiated	Male (75), untreated, dorsal hand (HSC-1), ear (HSC-5)	- p53 status unknown - not tumorigenic in mice	Kondo et al (1981)[90]
HSC-5	Primary, highly differentiated			Hozumi et al (1990)[91]
SCL-I	Primary, moderately differentiated	Female (74), untreated, face	- p53 mutated - moderately tumorigenic in mice	Boukamp et al (1982)[92]
SCL-II	Primary, poorly differentiated	Male (91), radiotherapy, face	- p53 mutated - not tumorigenic in mice	Tilgen et al (1983)[93]
HaCaT	None (healthy skin)	Male (62), upper back (distant melanoma periphery)	- spontaneously immortalized - UVR-specific p53 mutations - chromosomal aberrations characteristic of human SCC	Boukamp et al (1988)[94]
A388.6TG.c2	Primary	Male (86), location unknown	generated and selected by exposing a primary SCC to carcinogenic chemicals	Gioeli et al (1997)[95]
MET1	Primary, invasive, moderately differentiated	Male OTR (36), immune suppression, dorsal hand (MET1-3), axillary lymph node (MET4)	- no p53 mutations - poorly differentiated - tumorigenic in mice	Proby et al (2000)[96] Popp et al (2000)[97]
MET2	Recurrence, deeply invasive, poorly differentiated			
MET3				
MET4	Metastasis, poorly differentiated			

are designated three-dimensional, full-thickness, organotypic, (bio)engineered or reconstructed human skin cancer models, equivalents, constructs or rafts.

Three-dimensional *in vitro* human SCC models contain an epidermal compartment and a dermal compartment (Figure 4). The epidermal compartment may harbor any epidermal representation of human SCC, including genetically or chemically transformed primary keratinocytes, established SCC cell lines or complete primary SCC explants. The dermal compartment of three-dimensional SCC models may be composed of any biological or artificial matrix representing human dermis, including rat-tail type I collagen, human fibroblast-derived matrix (FDM), de-epidermized human dermis (DED) or artificial matrix. The dermal matrix may be either acellular or seeded with any type of human stromal cell, including healthy or disease-associated human fibroblasts, endothelial cells or immune cells. The epidermal and dermal compartments of three-dimensional SCC models are ideally separated by a functional BM, allowing for the study of SCC invasion. In general, the dermal compartment is prepared and seeded with stromal cells before adding the epidermal compartment. Depending on the type of matrix, this may take one to four weeks. In this phase, the culture medium is optimized towards creating a dermal microenvironment capable of fully supporting the prospective epidermal compartment. For example, human fibroblast-derived matrix is prepared during four weeks in standard fibroblast medium supplemented with high concentrations of ascorbic acid (vitamin C) to stimulate ECM formation.[98] Next, the epidermal compartment is added to the culture system. The cultures are then kept submerged in culture medium to promote attachment of epidermal cells to the dermal compartment and to stimulate proliferation of the epidermal cells to form a three-dimensional multilayered epidermis. This submerged culture period typically covers four to seven days allowing a functional BM to form. Culture medium in this phase is typically supplemented with fetal bovine serum (FBS) or equivalent non-animal additives to promote proliferation. Subsequently, the three-dimensional models are cultured at the air-liquid interface, leaving the epidermal compartment air-exposed to stimulate cellular differentiation.[99, 100] The air-exposed culture period typically spans two weeks, but may range from one to twenty weeks depending on the type of model and the research question. The culture medium of three-dimensional SCC models in the air-exposed culture phase is supplemented with various agents specifically stimulating proliferation, differentiation and maintenance of the epidermal compartment, including serum, hormones (e.g. insulin, hydrocortisone), vitamins (e.g. ascorbic acid, retinoids), fatty acids (e.g. palmitic acid, arachidonic acid) and growth factors (e.g. EGF, keratinocyte growth factor (KGF)). Typical examples of three-dimensional *in vitro* cutaneous SCC models include those generated by Borchers et al (1997), Gioeli et al (1997), Ponec et al (2000), Martins et al (2009) and Obrigkeit et al

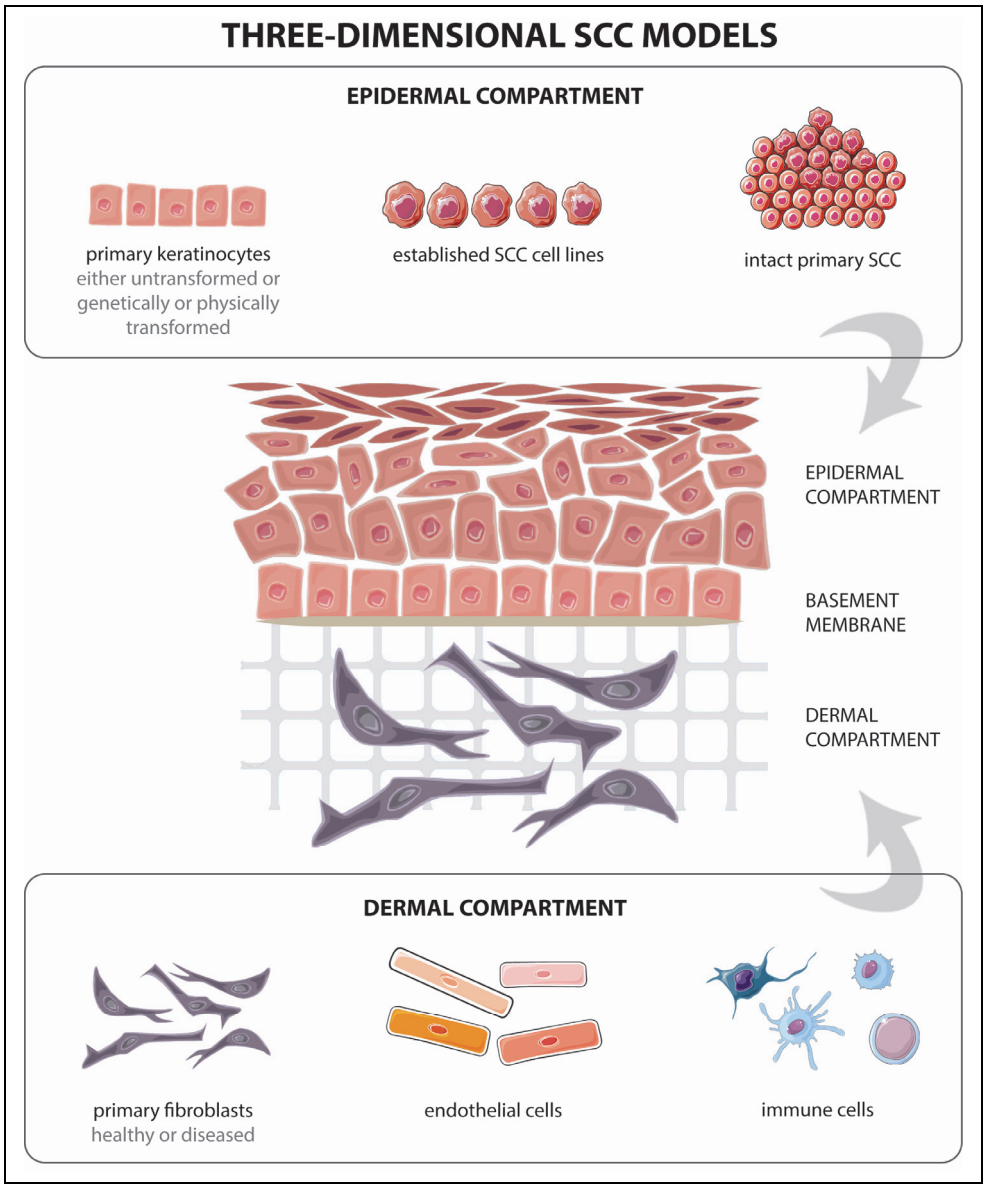

Figure 4 | Three-dimensional *in vitro* cutaneous SCC models offer great versatility. The epidermal compartment can be generated with any epidermal representation of human SCC, including (transformed) primary keratinocytes, SCC cell lines or primary SCC explants. The dermal compartment can be any biological or artificial matrix representing human dermis, acellular or seeded with any type of human stromal cell, including healthy or disease-associated human fibroblasts, endothelial cells or immune cells.

(2009) (Table 3).[95, 101-104] Without exception, these models have been generated with SCC cell lines in their epidermal compartment and all but one were cultured with relatively high amounts (10%) of FBS. Altogether, various cell-based models are currently available to study human cutaneous SCC *in vitro*. These models all have their own characteristics regarding the number of cell types involved, representation of a relevant microenvironment, reproducibility, experimental time span and availability (Table 4). As with *in vivo* models for cutaneous SCC, the *in vitro* model of choice can be matched to each specific research question.

Table 3 | Historical overview of three-dimensional *in vitro* cutaneous SCC models.

	EPIDERMAL COMPARTMENT	DERMAL COMPARTMENT	CULTURE SPECS
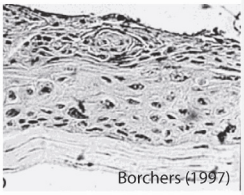 Borchers (1997)	Ha-*ras* transformed HaCaT II-4 cell line	rat tail collagen seeded with normal human dermal fibroblasts	**Regimen** 1 day submerged 14 days air-exposed **Medium** 10% FCS
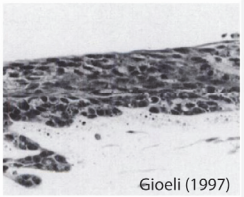 Gioeli (1997)	SCC cell line A388.6TG.c2	rat tail collagen seeded with normal human fibroblasts	**Regimen** 1 day submerged 14 days air-exposed **Medium** 10% FCS
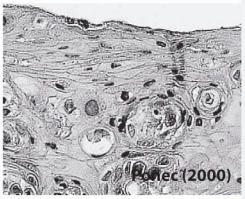 Rheinwald (2000)	SCC cell line SCC-12F2	rat tail collagen seeded with normal human dermal fibroblasts	**Regimen** 1 day submerged 21days air-exposed **Medium** 5% > 1% > 0% FCS
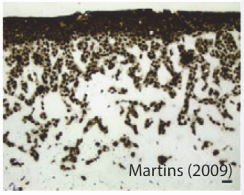 Martins (2009)	SCC cell line MET1 with siRNA-mediated collagen VII knockdown	rat tail collagen mixed with Matrigel (1:1) seeded with normal human dermal foreskin fibroblasts	**Regimen** 1 day submerged 10 days air-exposed **Medium** 10% FCS 10 ng/ml EGF
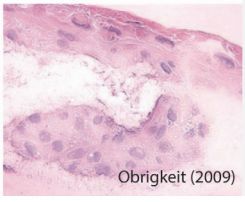 Obrigkeit (2009)	normal human epidermal foreskin keratinocytes + SCC cell line SCC-12	rat tail (?) collagen seeded with normal human dermal foreskin fibroblasts	**Regimen** 1 week submerged 5 days air-exposed **Medium** 10% FCS 10 ng/ml EGF

Table 4 | Key features of *in vitro* models of human cutaneous SCC.

In vitro model	Microenvironment [1]	Reproducibility [2]	Timespan [3]	Availability [4]
Two-dimensional (2D) models				
Primary SCC cells	-	low	weeks	low
SCC cell lines	-	high	infinite	high
Co-culture of SCC cells and fibroblasts	stromal fibroblasts	medium	weeks	medium*
Three-dimensional (3D) models				
ECM with SCC cells e.g. Matrigel®, Cultrex®	ECM (non-human) BM (disorganized)	medium/high*	days	medium*
3D SCC model	ECM, BM, stromal cells	medium/high*	weeks/months	medium*
Ex vivo primary SCC	-	low	days	low

[1] **Microenvironment** | extracellular matrix (ECM), basement membrane (BM), stromal cells.
[2] **Reproducibility** | determined by good laboratory practice (GLP) and heterogeneity of material.
[3] **Timespan** | experimental window, equivalent to *in vitro* viability of the model.
[4] **Availability** | primarily determined by dependence on primary human material.
* Dependent on SCC cell type incorporated in the model: primary cells limit reproducibility and availability.

In vitro SCC models as alternatives to animal experimentation

Animal experimentation and the 3Rs concept

The only direct approach to study human cutaneous SCC is through clinical research. However, experimentation on human subjects is limited by ethical and technical constraints. Therefore, indirect *in vivo* and *in vitro* approaches are used for experimental research without harming human beings. The use of *in vivo* models is subject to ethical debates on inhumane animal experimentation. Researchers are obliged to weigh the distress imposed on animals during the experiment against the expected gain in knowledge. Elimination of inhumane practices from animal experimentation is generally discussed under the three headings of reduction, refinement and replacement of humane technique – the three Rs introduced by William Russell and Rex Burch in 1959.[105] Reduction covers any decrease in the numbers of animals used to obtain information of a given amount and precision. So, reduction methods obtain comparable levels of

information from fewer animals or more information from the same number of animals. Refinement covers any decrease in the incidence or severity of inhumane procedures. Therefore, refinement methods alleviate or minimize potential pain, suffering and distress and enhance animal well-being. Replacement covers the substitution of conscious living animals for insentient material. Replacement methods therefore achieve a given purpose without conducting any scientific procedure on animals. The 3Rs concept is currently fully implemented in standard procedures for designing animal experiments.[106, 107]

Since the 1980's, efforts to reduce animal experimentation have been gaining momentum under the pressure of animal welfare groups and public opinion. In 1986, a European Union (EU) directive on the protection of animals used for experimental purposes officially banned animal experiments whenever a scientifically approved alternative exists.[108] Ever since, the number of animals used for experiments more than halved. However, recent reports show that despite this absolute decrease, the number of genetically modified animals rises drastically.[106] In The Netherlands, over 560.000 animals were used for scientific experiments in 2010. About 16% of these animals were genetically modified mice. In addition, almost 500.000 animals were wasted in the process of obtaining animals of only one desired sex, maintenance of specific strains or unforeseen disease. More than 70% (359.347) of these waste animals were genetically modified mice, indicating the disproportionately high pressure of genetic engineering on the total number of animals used and pointing out the persisting relevance of reducing animal experimentation.

Replacement in studying cutaneous SCC

The fidelity of mice as model organisms for human skin cancer is limited; the murine skin differs from human skin in structure and function. Architecturally, the murine epidermis with densely-distributed hair follicles and without sweat glands contrasts with the human epidermis. The epidermal thickness of normal human skin, comprising 6 to 10 cell layers together covering over 100 μm more than triples that of murine skin, which generally contains only 3 cell layers spanning less than 25 μm.[109] Functionally, mouse skin has greater percutaneous absorption and a decreased barrier function in comparison to human skin and mice have effective cutaneous wound regeneration without scarring, while human skin is subject to extensive hypertrophy upon wounding.[109, 110] Furthermore, the metabolic rate of mice, including epidermal turnover, is faster than in humans.[109] For example, SKH1-*hr* mice have been shown to contract their SCCs approximately 250 times faster than humans at comparable daily UVR dosages, offering obvious experimental advantages, but limiting their representation of human SCC.[111] Extrapolation of experimental data obtained in mice to human cancer can be further hindered by differences in oncogenic signaling, which may cause known human tumor suppressor

genes to elicit a different spectrum of tumors in mice than in humans.[112, 113] Besides intrinsic differences between *in vivo* and *in vitro* models, experimental efficiency, as defined by the balance between time, cost and information yield, is often in favor of *in vitro* methods. Moreover, *in vitro* cell culture models represent important replacement techniques for experimentation on human cutaneous SCC. Especially three-dimensional *in vitro* SCC models harboring multiple interacting cell types in a relevant microenvironment offer great alternatives to animal SCC models. These *in vitro* SCC models are highly discriminative, as they reproduce one or more particular features of human cutaneous SCC in detail, e.g. invasion, hyperproliferation or epidermal dysplasia. The design of every experiment to investigate human cutaneous SCC should therefore focus on the model with the highest experimental efficiency, which is the most discriminative and the least inhumane for that particular research question. Hence, a robust and reliable *in vitro* model of human cutaneous SCC is a highly desirable experimental vehicle to investigate human cutaneous SCC development and therapeutic responses.

Thesis aim and outline

The aim of the research described in this thesis was to develop an *in vitro* model of human cutaneous squamous cell carcinoma (SCC) for ultimately screening potential therapeutic compounds. To this end, we first maintained intact primary human cutaneous SCCs of immune suppressed organ transplant recipients (OTRs) on three-dimensional rat-tail collagen matrices seeded with normal human dermal fibroblasts (NHDFs). We also cultured human cutaneous SCC cell lines on NHDF-seeded rat-tail collagen matrices. The resulting invasive primary SCC models and SCC cell line models are characterized in **Chapter 2**. To study the contribution of the microenvironment to the invasive potential of our *in vitro* SCC models, we modulated the composition of the dermal compartment in two ways. Firstly, we replaced the NHDFs in the dermal matrix by primary human cancer-associated fibroblasts (CAFs) isolated from primary cutaneous SCCs of immune suppressed OTRs. *In vitro* SCC cell line models based on these SCC-associated CAFs are described in **Chapter 3**. Secondly, we replaced the rat-tail collagen matrix by normal human dermal fibroblast-derived matrix (FDM), resulting in a fully human dermal microenvironment as covered by **Chapter 4**. To validate our primary *in vitro* SCC cultures as models of human cutaneous SCC, we performed molecular profiling of primary cutaneous SCCs, allowing the comparison with their counterparts expanded *in vitro*. **Chapter 5** identifies the pathways and genomic alterations present in primary cutaneous SCCs of immune suppressed OTRs and their precursor lesions. As upregulation of the RAS pathway has been found in SCCs of both immune suppressed and immunocompetent individuals, we used our *in vitro* SCC models to investigate the effects of erlotinib, a small molecule inhibitor of the epidermal growth factor receptor (EGFR) tyrosine kinase upstream of RAS. This proof of principle for the therapeutic screening potential of our *in vitro* SCC models is described in **Chapter 6**. The results presented in this thesis are summarized and discussed in **Chapter 7**.

References

1. Gloster, H.M., Jr. & Neal, K. Skin cancer in skin of color. *J Am Acad Dermatol* **55**, 741-60 (2006).
2. INTERSUN Programme. *World Health Organization* (2011).
3. Rogers, H.W. et al. Incidence estimate of nonmelanoma skin cancer in the United States, 2006. *Arch Dermatol* **146**, 283-7 (2010).
4. Cancer Facts & Figures 2010. *American Cancer Society* (2010).
5. Williams, H. et al. Epidemiology of skin diseases in Europe. *Eur J Dermatol* **16**, 212-8 (2006).
6. de Vries, E., van de Poll-Franse, L.V., Louwman, W.J., de Gruijl, F.R. & Coebergh, J.W. Predictions of skin cancer incidence in the Netherlands up to 2015. *Br J Dermatol* **152**, 481-8 (2005).
7. Skin cancer. *Dutch Cancer Society* (2011).
8. Carucci, J.A. et al. In-transit metastasis from primary cutaneous squamous cell carcinoma in organ transplant recipients and nonimmunosuppressed patients: clinical characteristics, management, and outcome in a series of 21 patients. *Dermatol Surg* **30**, 651-5 (2004).
9. Ulrich, C., Kanitakis, J., Stockfleth, E. & Euvrard, S. Skin cancer in organ transplant recipients--where do we stand today? *Am J Transplant* **8**, 2192-8 (2008).
10. Wisgerhof, H.C. in Dermatology (Leiden University, Leiden, 2011).
11. Barrett, W.L., First, M.R., Aron, B.S. & Penn, I. Clinical course of malignancies in renal transplant recipients. *Cancer* **72**, 2186-9 (1993).
12. Martinez, J.C. et al. Defining the clinical course of metastatic skin cancer in organ transplant recipients: a multicenter collaborative study. *Arch Dermatol* **139**, 301-6 (2003).
13. Winkelhorst, J.T., Brokelman, W.J., Tiggeler, R.G. & Wobbes, T. Incidence and clinical course of de-novo malignancies in renal allograft recipients. *Eur J Surg Oncol* **27**, 409-13 (2001).
14. Wisgerhof, H.C. et al. Subsequent squamous- and basal-cell carcinomas in kidney-transplant recipients after the first skin cancer: cumulative incidence and risk factors. *Transplantation* **89**, 1231-8 (2010).
15. Wilkins, K. et al. Cutaneous malignancy and human immunodeficiency virus disease. *J Am Acad Dermatol* **54**, 189-206; quiz 207-10 (2006).
16. De Hertog, S.A. et al. Relation between smoking and skin cancer. *J Clin Oncol* **19**, 231-8 (2001).
17. 't Hoen, M. & Nijsten, T.E.C. Epidemiologie van het plaveiselcelcarcinoom. *Nederlands Tijdschrift voor Dermatologie en Venereologie* **16**, 380-383 (2006).
18. Bouwes Bavinck, J.N. et al. Multicenter study of the association between betapapillomavirus infection and cutaneous squamous cell carcinoma. *Cancer Res* **70**, 9777-86 (2010).
19. Feltkamp, M.C., de Koning, M.N., Bavinck, J.N. & Ter Schegget, J. Betapapillomaviruses: innocent bystanders or causes of skin cancer. *J Clin Virol* **43**, 353-60 (2008).
20. Proby, C.M. et al. A case-control study of betapapillomavirus infection and cutaneous squamous cell carcinoma in organ transplant recipients. *Am J Transplant* **11**, 1498-508 (2011).
21. Arron, S.T., Ruby, J.G., Dybbro, E., Ganem, D. & Derisi, J.L. Transcriptome Sequencing Demonstrates that Human Papillomavirus Is Not Active in Cutaneous Squamous Cell Carcinoma. *J Invest Dermatol* **131**, 1745-53 (2011).
22. Berg, D. & Otley, C.C. Skin cancer in organ transplant recipients: Epidemiology, pathogenesis, and management. *J Am Acad Dermatol* **47**, 1-17; quiz 18-20 (2002).
23. Stasko, T. et al. Guidelines for the management of squamous cell carcinoma in organ transplant recipients. *Dermatol Surg* **30**, 642-50 (2004).
24. Feldman, S.R. & Fleischer, A.B., Jr. Progression of actinic keratosis to squamous cell carcinoma revisited: clinical and treatment implications. *Cutis* **87**, 201-7 (2011).
25. Euvrard, S., Kanitakis, J. & Claudy, A. Skin cancers after organ transplantation. *N Engl J Med* **348**, 1681-91 (2003).
26. Jemec, G.B. & Holm, E.A. Nonmelanoma skin cancer in organ transplant patients. *Transplantation* **75**, 253-7 (2003).
27. Rhee, J.S., Matthews, B.A., Neuburg, M., Burzynski, M. & Nattinger, A.B. Creation of a quality of life instrument for nonmelanoma skin cancer patients. *Laryngoscope* **115**, 1178-85 (2005).
28. Bickers, D.R. et al. The burden of skin diseases: 2004 a joint project of the American Academy of Dermatology Association and the Society for Investigative Dermatology. *J Am Acad Dermatol* **55**, 490-500 (2006).

29. Garinis, G.A. et al. Transcriptome analysis reveals cyclobutane pyrimidine dimers as a major source of UV-induced DNA breaks. *EMBO J* **24**, 3952-62 (2005).
30. Brash, D.E. et al. A role for sunlight in skin cancer: UV-induced p53 mutations in squamous cell carcinoma. *Proc Natl Acad Sci U S A* **88**, 10124-8 (1991).
31. McGregor, J.M. et al. p53 mutations implicate sunlight in post-transplant skin cancer irrespective of human papillomavirus status. *Oncogene* **15**, 1737-40 (1997).
32. Ziegler, A. et al. Sunburn and p53 in the onset of skin cancer. *Nature* **372**, 773-6 (1994).
33. Brown, V.L. et al. p16INK4a and p14ARF tumor suppressor genes are commonly inactivated in cutaneous squamous cell carcinoma. *J Invest Dermatol* **122**, 1284-92 (2004).
34. Pelisson, I., Soler, C., Chardonnet, Y., Euvrard, S. & Schmitt, D. A possible role for human papillomaviruses and c-myc, c-Ha-ras, and p53 gene alterations in malignant cutaneous lesions from renal transplant recipients. *Cancer Detect Prev* **20**, 20-30 (1996).
35. van der Schroeff, J.G., Evers, L.M., Boot, A.J. & Bos, J.L. Ras oncogene mutations in basal cell carcinomas and squamous cell carcinomas of human skin. *J Invest Dermatol* **94**, 423-5 (1990).
36. Toll, A. et al. Epidermal growth factor receptor gene numerical aberrations are frequent events in actinic keratoses and invasive cutaneous squamous cell carcinomas. *Exp Dermatol* **19**, 151-3 (2010).
37. Mauerer, A., Herschberger, E., Dietmaier, W., Landthaler, M. & Hafner, C. Low incidence of EGFR and HRAS mutations in cutaneous squamous cell carcinomas of a German cohort. *Exp Dermatol* (2011).
38. Rebello, P. et al. Pharmacokinetics of CAMPATH-1H in BMT patients. *Cytotherapy* **3**, 261-7 (2001).
39. Fogarty, G.B., Conus, N.M., Chu, J. & McArthur, G. Characterization of the expression and activation of the epidermal growth factor receptor in squamous cell carcinoma of the skin. *Br.J.Dermatol.* **156**, 92-98 (2007).
40. Rittie, L. et al. Differential ErbB1 signaling in squamous cell versus basal cell carcinoma of the skin. *Am.J.Pathol.* **170**, 2089-2099 (2007).
41. El Abaseri, T.B., Putta, S. & Hansen, L.A. Ultraviolet irradiation induces keratinocyte proliferation and epidermal hyperplasia through the activation of the epidermal growth factor receptor. *Carcinogenesis* **27**, 225-231 (2006).
42. Ashton, K.J., Weinstein, S.R., Maguire, D.J. & Griffiths, L.R. Chromosomal aberrations in squamous cell carcinoma and solar keratoses revealed by comparative genomic hybridization. *Arch Dermatol* **139**, 876-82 (2003).
43. Purdie, K.J. et al. Single nucleotide polymorphism array analysis defines a specific genetic fingerprint for well-differentiated cutaneous SCCs. *J Invest Dermatol* **129**, 1562-8 (2009).
44. Purdie, K.J. et al. Allelic imbalances and microdeletions affecting the PTPRD gene in cutaneous squamous cell carcinomas detected using single nucleotide polymorphism microarray analysis. *Genes Chromosomes Cancer* **46**, 661-9 (2007).
45. Rehman, I., Takata, M., Wu, Y.Y. & Rees, J.L. Genetic change in actinic keratoses. *Oncogene* **12**, 2483-90 (1996).
46. Norval, M. The mechanisms and consequences of ultraviolet-induced immunosuppression. *Prog Biophys Mol Biol* **92**, 108-18 (2006).
47. Loser, K. et al. Epidermal RANKL controls regulatory T-cell numbers via activation of dendritic cells. *Nat Med* **12**, 1372-9 (2006).
48. Erb, P., Ji, J., Kump, E., Mielgo, A. & Wernli, M. Apoptosis and pathogenesis of melanoma and nonmelanoma skin cancer. *Adv Exp Med Biol* **624**, 283-95 (2008).
49. Satchell, A.C., Barnetson, R.S. & Halliday, G.M. Increased Fas ligand expression by T cells and tumour cells in the progression of actinic keratosis to squamous cell carcinoma. *Br J Dermatol* **151**, 42-9 (2004).
50. Hall, L., Struijk, L., Neale, R.E. & Feltkamp, M.C. Re: Human papillomavirus infection and incidence of squamous cell and basal cell carcinomas of the skin. *J Natl Cancer Inst* **98**, 1425-6 (2006).
51. Jackson, S., Harwood, C., Thomas, M., Banks, L. & Storey, A. Role of Bak in UV-induced apoptosis in skin cancer and abrogation by HPV E6 proteins. *Genes Dev* **14**, 3065-73 (2000).
52. Karagas, M.R. et al. Human papillomavirus infection and incidence of squamous cell and basal cell carcinomas of the skin. *J Natl Cancer Inst* **98**, 389-95 (2006).
53. Kalluri, R. & Zeisberg, M. Fibroblasts in cancer. *Nat Rev Cancer* **6**, 392-401 (2006).
54. De Wever, O. & Mareel, M. Role of tissue stroma in cancer cell invasion. *J.Pathol.* **200**, 429-447 (2003).
55. Bhowmick, N.A., Neilson, E.G. & Moses, H.L. Stromal fibroblasts in cancer initiation and progression. *Nature* **432**, 332-337 (2004).
56. Desmouliere, A., Guyot, C. & Gabbiani, G. The stroma reaction myofibroblast: a key player in

the control of tumor cell behavior. *Int.J.Dev.Biol.* **48**, 509-517 (2004).
57. Kellermann, M.G. et al. Myofibroblasts in the stroma of oral squamous cell carcinoma are associated with poor prognosis. *Histopathology* **51**, 849-853 (2007).
58. Spaeth, E.L. et al. Mesenchymal stem cell transition to tumor-associated fibroblasts contributes to fibrovascular network expansion and tumor progression. *PLoS.One.* **4**, e4992 (2009).
59. Lengyel, E. et al. Induction of M(r) 92,000 type IV collagenase expression in a squamous cell carcinoma cell line by fibroblasts. *Cancer Res.* **55**, 963-967 (1995).
60. Sato, T. et al. Enhancement of membrane-type 1-matrix metalloproteinase (MT1-MMP) production and sequential activation of progelatinase A on human squamous carcinoma cells co-cultured with human dermal fibroblasts. *Br.J.Cancer* **80**, 1137-1143 (1999).
61. Boyd, S. et al. MMP-10 (Stromelysin-2) and MMP-21 in human and murine squamous cell cancer. *Exp.Dermatol.* **18**, 1044-1052 (2009).
62. Chebassier, N., Leroy, S., Tenaud, I., Knol, A.C. & Dreno, B. Overexpression of MMP-2 and MMP-9 in squamous cell carcinomas of immunosuppressed patients. *Arch.Dermatol.Res.* **294**, 124-126 (2002).
63. McCawley, L.J., Wright, J., LaFleur, B.J., Crawford, H.C. & Matrisian, L.M. Keratinocyte expression of MMP3 enhances differentiation and prevents tumor establishment. *Am.J.Pathol.* **173**, 1528-1539 (2008).
64. Tsukifuji, R., Tagawa, K., Hatamochi, A. & Shinkai, H. Expression of matrix metalloproteinase-1, -2 and -3 in squamous cell carcinoma and actinic keratosis. *Br.J.Cancer* **80**, 1087-1091 (1999).
65. Hynes, R.O. The extracellular matrix: not just pretty fibrils. *Science* **326**, 1216-9 (2009).
66. Strieth, S., Hartschuh, W., Pilz, L. & Fusenig, N.E. Angiogenic switch occurs late in squamous cell carcinomas of human skin. *Br J Cancer* **82**, 591-600 (2000).
67. Cernea, C.R. et al. Angiogenesis and skin carcinomas with skull base invasion: a case-control study. *Head Neck* **26**, 396-400 (2004).
68. Moussai, D. et al. The human cutaneous squamous cell carcinoma microenvironment is characterized by increased lymphatic density and enhanced expression of macrophage-derived VEGF-C. *J Invest Dermatol* **131**, 229-36 (2011).
69. O'Grady, A., O'Kelly, P., Murphy, G.M., Leader, M. & Kay, E. COX-2 expression correlates with microvessel density in non-melanoma skin cancer from renal transplant recipients and immunocompetent individuals. *Hum Pathol* **35**, 1549-55 (2004).
70. Slaga, T.J. Overview of tumor promotion in animals. *Environ Health Perspect* **50**, 3-14 (1983).
71. Glick, A. et al. The high-risk benign tumor: evidence from the two-stage skin cancer model and relevance for human cancer. *Mol Carcinog* **46**, 605-10 (2007).
72. de Gruijl, F.R. & Forbes, P.D. UV-induced skin cancer in a hairless mouse model. *Bioessays* **17**, 651-60 (1995).
73. Benavides, F., Oberyszyn, T.M., VanBuskirk, A.M., Reeve, V.E. & Kusewitt, D.F. The hairless mouse in skin research. *J Dermatol Sci* **53**, 10-8 (2009).
74. Marcuzzi, G.P. et al. Spontaneous tumour development in human papillomavirus type 8 E6 transgenic mice and rapid induction by UV-light exposure and wounding. *J Gen Virol* **90**, 2855-64 (2009).
75. Viarisio, D. et al. E6 and E7 from beta HPV38 cooperate with ultraviolet light in the development of actinic keratosis-like lesions and squamous cell carcinoma in mice. *PLoS Pathog* **7**, e1002125 (2011).
76. Park, Y.W. et al. AEE788, a dual tyrosine kinase receptor inhibitor, induces endothelial cell apoptosis in human cutaneous squamous cell carcinoma xenografts in nude mice. *Clin Cancer Res* **11**, 1963-73 (2005).
77. Streit, M. et al. Overexpression of thrombospondin-1 decreases angiogenesis and inhibits the growth of human cutaneous squamous cell carcinomas. *Am J Pathol* **155**, 441-52 (1999).
78. Burnworth, B. et al. The multi-step process of human skin carcinogenesis: a role for p53, cyclin D1, hTERT, p16, and TSP-1. *Eur J Cell Biol* **86**, 763-80 (2007).
79. Nomura, T. et al. Induction of cancer, actinic keratosis, and specific p53 mutations by UVB light in human skin maintained in severe combined immunodeficient mice. *Cancer Res* **57**, 2081-4 (1997).
80. Heyer, J., Kwong, L.N., Lowe, S.W. & Chin, L. Non-germline genetically engineered mouse models for translational cancer research. *Nat Rev Cancer* **10**, 470-80 (2010).
81. Caulin, C. et al. An inducible mouse model for skin cancer reveals distinct roles for gain- and loss-of-function p53 mutations. *J Clin Invest* **117**, 1893-901 (2007).
82. Martinez-Cruz, A.B. et al. Spontaneous squamous cell carcinoma induced by the somatic inactivation of retinoblastoma and

Trp53 tumor suppressors. *Cancer Res* **68**, 683-92 (2008).
83. Atillasoy, E.S., Elenitsas, R., Sauter, E.R., Soballe, P.W. & Herlyn, M. UVB induction of epithelial tumors in human skin using a RAG-1 mouse xenograft model. *J Invest Dermatol* **109**, 704-9 (1997).
84. Watt, S.A. et al. Integrative mRNA profiling comparing cultured primary cells with clinical samples reveals PLK1 and C20orf20 as therapeutic targets in cutaneous squamous cell carcinoma. *Oncogene* (2011).
85. Rheinwald, J.G. & Beckett, M.A. Defective terminal differentiation in culture as a consistent and selectable character of malignant human keratinocytes. *Cell* **22**, 629-632 (1980).
86. Boukamp, P. et al. Step-wise progression in human skin carcinogenesis in vitro involves mutational inactivation of p53, rasH oncogene activation and additional chromosome loss. *Oncogene* **11**, 961-9 (1995).
87. Mueller, M.M. et al. Tumor progression of skin carcinoma cells in vivo promoted by clonal selection, mutagenesis, and autocrine growth regulation by granulocyte colony-stimulating factor and granulocyte-macrophage colony-stimulating factor. *Am J Pathol* **159**, 1567-79 (2001).
88. Prunieras, M., Delescluse, C. & Regnier, M. The culture of skin. A review of theories and experimental methods. *J Invest Dermatol* **67**, 58-65 (1976).
89. De Angelis, T., Noe, A., Chatterjee, M. & Mulholland, J. Stromelysin-1 activation correlates with invasiveness in squamous cell carcinoma. *J Invest Dermatol* **118**, 759-66 (2002).
90. Kondo, S. & Aso, K. Establishment of a cell line of human skin squamous cell carcinoma in vitro. *Br J Dermatol* **105**, 125-32 (1981).
91. Hozumi, Y., Kondo, S., Shimoura, T. & Aso, K. Human squamous cell carcinoma from skin: establishment and characterization of a new cell line (HSC-5). *J Dermatol* **17**, 143-8 (1990).
92. Boukamp, P. et al. Phenotypic and genotypic characteristics of a cell line from a squamous cell carcinoma of human skin. *J Natl Cancer Inst* **68**, 415-27 (1982).
93. Tilgen, W. et al. Preservation of morphological, functional, and karyotypic traits during long-term culture and in vivo passage of two human skin squamous cell carcinomas. *Cancer Res* **43**, 5995-6011 (1983).
94. Boukamp, P. et al. Normal keratinization in a spontaneously immortalized aneuploid human keratinocyte cell line. *J Cell Biol* **106**, 761-71 (1988).
95. Gioeli, D., Conway, K. & Weissman, B.E. Localization and characterization of a chromosome 11 tumor suppressor gene using organotypic raft cultures. *Cancer Res* **57**, 1157-65 (1997).
96. Proby, C.M. et al. Spontaneous keratinocyte cell lines representing early and advanced stages of malignant transformation of the epidermis. *Exp.Dermatol.* **9**, 104-117 (2000).
97. Popp, S. et al. Genetic characterization of a human skin carcinoma progression model: from primary tumor to metastasis. *J.Invest Dermatol.* **115**, 1095-1103 (2000).
98. El Ghalbzouri, A., Commandeur, S., Rietveld, M.H., Mulder, A.A. & Willemze, R. Replacement of animal-derived collagen matrix by human fibroblast-derived dermal matrix for human skin equivalent products. *Biomaterials* **30**, 71-78 (2009).
99. Asselineau, D., Bernhard, B., Bailly, C. & Darmon, M. Epidermal morphogenesis and induction of the 67 kD keratin polypeptide by culture of human keratinocytes at the liquid-air interface. *Exp Cell Res* **159**, 536-9 (1985).
100. Boelsma, E., Verhoeven, M.C. & Ponec, M. Reconstruction of a human skin equivalent using a spontaneously transformed keratinocyte cell line (HaCaT). *J Invest Dermatol* **112**, 489-98 (1999).
101. Russell, W.M. & Burch, R.L. The Principles of Humane Experimental Technique (Methuen, London, 1959).
102. Zo Doende 2010. *nieuwe Voedsel en Waren Autoriteit* (2012).
103. Workman, P. et al. Guidelines for the welfare and use of animals in cancer research. *Br J Cancer* **102**, 1555-77 (2010).
104. in Official Journal of the European Communities 1-29 (1986).
105. Khavari, P.A. Modelling cancer in human skin tissue. *Nat Rev Cancer* **6**, 270-80 (2006).
106. Menon, G.K. New insights into skin structure: scratching the surface. *Adv Drug Deliv Rev* **54 Suppl 1**, S3-17 (2002).
107. Rebel, H. et al. Early p53-positive foci as indicators of tumor risk in ultraviolet-exposed hairless mice: kinetics of induction, effects of DNA repair deficiency, and p53 heterozygosity. *Cancer Res* **61**, 977-83 (2001).
108. Hahn, W.C. & Weinberg, R.A. Modelling the molecular circuitry of cancer. *Nat Rev Cancer* **2**, 331-41 (2002).
109. Hamad, N.M. et al. Distinct requirements for Ras oncogenesis in human versus mouse cells. *Genes Dev* **16**, 2045-57 (2002).

2

An *in vitro* three-dimensional model of primary human cutaneous squamous cell carcinoma

Suzan Commandeur, Frank R. de Gruijl, Rein Willemze, Cornelis P. Tensen and Abdoelwaheb El Ghalbzouri

Department of Dermatology, Leiden University Medical Center, Leiden, the Netherlands

Experimental Dermatology 2009;18(10):849-856

Abstract

Squamous cell carcinomas (SCC) represent a substantial clinical problem because of increases, frequent recurrences and successive de novo tumors, especially in organ transplant recipients. To improve upon the current surgical and other non-selective therapies, a validated organotypic *in vitro* model of primary human SCC needs to be developed. Such a model will have obvious advantages over current cell line and animal based approaches, and may render the latter partly obsolete. In a first approach, an explant technique of primary SCC biopsies onto dermal constructs was used to emulate tumor expansion in an *in vitro* model. Histological analysis revealed the formation of nests of squamous cells, mimicking an invasive morphological feature of primary SCC. Immunohistochemical analysis comprised an array of markers characteristic of keratinocyte (hyper) proliferation (K6, K16, K17 and Ki67), differentiation (K1, K10 and involucrin), basement membrane (collagen types IV and VII, integrins a6 and b4 and laminin 332) and SCC (K4, K13 and Axl). The generated human SCC models displayed disturbed differentiation and keratins associated with hyperproliferation, but a low frequency of Ki67 positive cells. Basement membrane composition of the *in vitro* SCC model resembled that of normal skin. These results show for the first time that *in vitro* modelling of three-dimensional growth of primary cutaneous human SCC is feasible. This model may provide a platform to develop refined preventive and curative treatments and thereby gain understanding of SCC pathogenesis.

Introduction

Cutaneous squamous cell carcinoma (SCC) is a malignant tumor of epidermal keratinocytes characterized by invasive growth into the dermis. After basal cell carcinoma, SCC is the most common malignancy in white populations with epidemic incidence rates currently ranging from 18 per 100.000 person years in the Netherlands up to 395 per 100.000 person years in Australia, and predicted to have increased by 80% in the Netherlands in 2015.[1, 2] Actinic keratoses (AK) are precursor lesions of SCC and precede the biological continuum ranging from carcinoma in situ to invasive SCC. The clinical problem of SCC is particularly dramatic in immunosuppressed individuals: in a population of Australian immune suppressed kidney transplant recipients, the cumulative incidences of SCC after 5, 11 and 20 years have increased to 3%, 16% and 41%, respectively.[3] Our clinic closely monitors and treats organ transplant patients presenting with skin carcinomas. The current study focuses on SCCs from this group of patients.

Since medical intervention is always required for treatment of primary, successive and recurrent cutaneous SCCs, refined therapies focused on precursor lesions are highly desirable. Well-targeted specific therapeutic agents could serve this purpose, based on essential knowledge on cutaneous SCC carcinogenesis. The development of a representative *in vitro* skin carcinoma model system allows for a better understanding of fundamental carcinogenesis mechanisms and may serve as a validated pre-screening platform for candidate drugs. Traditional *in vivo* models rely on the use of chemical, genetic or mechanical induction or propagation of carcinogenesis in mice.[4-8] Current *in vitro* approaches are limited to the use of cell lines, which have commonly undergone multiple adaptations to long-term culture, resulting in a clonal selection of a subpopulation of cells from primary heterogeneous tumors. This may compromise a true representation of primary skin cancer. *In vitro* SCC progression models involve the transformed HaCaT cell line, the MET1 to MET4 cell lines derived from primary and recurrent cutaneous SCC and metastases thereof and the benign Ha-Ras mutated murine keratinocyte cell line 308 that is capable of transformation *in vitro*.[7, 9-11] More refined approaches are based on human skin equivalents, comprising three-dimensional systems in which a natural skin tissue context is reconstructed. These model systems have the advantage of harboring different cell types in a local environment that is highly similar to that of the *in vivo* tissue. Thus, these model systems will more closely emulate cellular processes than conventional monolayer cultures.[12, 13] But again, SCC cell line based human skin equivalents harbor the drawback of an artificially selected clone of tumor cells, rendering primary SCC biopsies more suitable for SCC modeling *in vitro*. Earlier studies show that phenotypic defects in genetic skin disorders persist in organotypic skin cultures,

e.g. with the hereditary blister disease epidermolysis bullosa simplex.[14] Based on these findings, we reasoned that three-dimensional modeling of human cutaneous SCC of immunocompromised organ-transplant recipients should be possible by using cells from primary human cutaneous SCCs. Here we present the generation of such a model, which was subsequently characterized for the presence of putative SCC markers as well as markers specific for keratinocyte activation, proliferation and differentiation and basement membrane (BM) formation.

Methods

Patient material

Three primary excisional well-differentiated cutaneous SCC biopsies from different renal transplant patients were freshly collected. Of these biopsies, one part was processed for diagnosis while the remainder was used for explant culture. Two native skin biopsies originating from the buttock of immunocompromised renal transplant patients and two native skin biopsies originating from mamma reduction surplus skin of immunocompetent individuals were freshly collected and served as control explants. In addition, three archived well-differentiated SCC samples from the institutional Department of Pathology were used as reference material for immunohistochemical analyses. All samples used were collected with written informed consent of the patient according to the Declaration of Helsinki after approval of the medical ethical committee of the Leiden University Medical Center. Furthermore, two SCC cell lines representing the tumorigenic populations of cutaneous SCCs (SCC-12B2 and SCC-13) were included. These cell lines were kindly provided by Dr. J.G. Rheinwald.[15] Clinical specifications of all starting materials are provided in Table 1.

Fibroblast culture

For isolation of normal human dermal fibroblasts (NHDFs), dermis was obtained through overnight incubation of fresh mamma reduction surplus skin with dispase II (Roche Diagnostics, Almere, the Netherlands). Fibroblasts were isolated from the dermis through incubation with a solution consisting of collagenase II (Invitrogen, Breda, the Netherlands) and dispase II (ratio 1:3 and 3 ml/g dermis) at 37°C for 2 hours. The cells were filtered using a 70 µm cell strainer (BD Biosciences, Breda, the Netherlands), and cultured in fibroblast medium at 37°C and 5% CO_2 until subconfluency. Fibroblast medium consisted of Dulbecco's modified Eagle's medium (DMEM, Gibco/Invitrogen, Breda, the Netherlands) supplemented with 5% fetal bovine serum (FBS, HyClone/Greiner, Nurtingen, Germany), 100 U ml^{-1} penicillin and 100 µg ml^{-1} streptomycin (Invitrogen,

Table 1 | Clinical specifications of starting materials.

Specimen	Gender	Age	Localization	Diagnosis	Background	Treatment
Control samples for explant culture and immunohistochemistry						
Normal skin	F	26	Breast	Healthy	Mamma reduction	-
Normal skin	F	43	Breast	Healthy	Mamma reduction	-
Normal skin	M	73	Buttock	Healthy	Renal transplant	Pred / Aza
Normal skin	M	54	Buttock	Healthy	Renal transplant	Pred / Aza
Confirmation samples for immunohistochemistry						
Primary tumor	F	51	Back	SCC	Renal transplant	Pred / Aza
Primary tumor	F	58	Coeur	SCC	Renal transplant	Pred / Aza
Primary tumor	F	51	Lower leg	SCC	Renal transplant	Pred / Aza
Tumor samples for explant culture and immunohistochemistry						
Primay tumor	M	50	Upper arm	SCC	Renal transplant	Pred / Aza
Primary tumor	M	76	Upper arm	SCC	Renal transplant	Pred / Aza
Primary tumor	F	55	Lower leg	SCC	Renal transplant	Pred / Aza
Cell lines for reference culture and immunohistochemistry						
SCC-12B2	M	60	Face	SCC	Renal transplant	Immune suppr.
SCC-13	F	56	Face	SCC	Renal transplant	Radiation

F, female; M, male; SCC, squamous cell carcinoma; Pred, prednisone; Aza, azathioprine; Immune suppr, unspecified immune suppression.

Breda, the Netherlands). Culture medium was refreshed every three days. Fibroblast passages two to four have been used for the experiments.

SCC cell line culture

SCC cell lines were cultured on lethally irradiated murine 3T3 fibroblasts in standard keratinocyte medium at 37°C and 7.3% CO_2 until subconfluency. Standard keratinocyte medium consisted of DMEM and Ham's F12 medium in a 3:1 ratio, supplemented with 5% FBS, 0.5 µM hydrocortisone, 1 µM isoproterenol, 0.1 µM insulin (Sigma-Aldrich, Zwijndrecht, the Netherlands), 100 U/ml penicillin and 100 µg/ml streptomycin. Culture medium was refreshed every three days.

Explant cultures

Upon arrival, the three fresh SCC biopsies from immune-suppressed individuals were rinsed three times in sterile phosphate buffered saline (PBS). Thereafter the biopsies were incubated overnight at 4°C in PBS supplemented with penicillin-streptamycin solution (300 U/ml) and amphotericin B (Fungizone, 5 µL/ml, Gibco/Invitrogen). Next, the biopsies were rinsed three times with sterile PBS. For generation of explant cultures, dermal equivalents were constructed as described earlier.[12, 16, 17] In brief, rat tail collagen was seeded with $1.25x10^5$ NHDF per milliliter and incubated for a period of one week under submerged conditions. Thereafter, the SCC biopsies were placed onto the collagen matrices. All explants (skin cancer and healthy skin biopsies) were cultured at the air-liquid interface under serum-free conditions. The SCC models were cultured for three weeks in serum-free keratinocyte medium as described above, supplemented with 53 µM selenious acid, 10 mM L-serine, 10 µM L-carnitine, 7 µg/ml β-dextrin, 1 µM dL-α-tocopherol-acetate, 100 µg/ml ascorbic acid phosphate and a lipid supplement containing 25 µM palmitic acid, 30 µM linoleic acid, 7 µM arachidonic acid and $2.4x10^{-5}$ M bovine serum albumin (Sigma-Aldrich, Zwijndrecht, The Netherlands).

Human skin equivalents

Human skin equivalents (HSEs) using keratinocytes from two SCC cell lines were generated as described earlier.[13] Briefly, dermal equivalents containing NHDFs were seeded with $5x10^4$ keratinocytes cm^{-2} from cell lines SCC-12B2 and SCC-13. The HSEs were incubated overnight under submerged conditions in standard keratinocyte medium. The next day, cultures were lifted to the air-liquid interface and medium was replaced by the same keratinocyte medium as described above for the explant cultures, but with reduced FBS (1%). From the second day, serum was omitted and HSEs were cultured for three to four weeks while medium was refreshed every three days.

Immunohistochemical analysis

After the culture period, skin equivalents were split in two fragments for immunohistochemical analyses. One part was snap-frozen in liquid nitrogen while the other part was fixed in 4% paraformaldehyde, dehydrated and paraffin embedded. Formalin fixed, paraffin embedded primary SCC archive material was obtained from the Department of Pathology of the Leiden University Medical Center. Global histological analysis was performed on 5 µm sections through staining with haematoxylin and eosin (HE). Immunohistochemistry was performed on 5 µm sections and all samples were analyzed for the presence of a set of markers specific for keratinocyte proliferation, differentiation and BM composition. Immunohistochemical analysis of collagen types IV (clone PHM12, Chemicon, Temecula CA) and VII (clone LH7.2, Dr. I.M. Leigh, London, UK), integrin subunits α_6 (clone JEB5, Dr. A Sonnenberg, Amsterdam, The Netherlands) and β_4 (clone 3E1, Telios Pharmaceuticals, San Diego CA), involucrin (clone SY5, Santa Cruz Biotechnology, Santa Cruz CA), Ki67 (clone MIB1, DAKO, Glostrup, Germany), laminin 332 (clone BM165, Dr. A. Aumailley, Cologne, Germany), keratin 1 (clone LHK1, Dr. I.M. Leigh, London, UK), keratin 4 (clone 6B10, Dr. G.N.P. van Muijen, Leiden, The Netherlands), keratin 6 (clone Ks6.KA12, Sanbio BV, Uden, The Netherlands), keratin 13 (clone 1C7, Dr. G.N.P. van Muijen, Leiden, The Netherlands) and keratin 17 (clone CKE3, Sigma, Saint Louis MO) was performed on 5 µm frozen sections that were air-dried overnight and fixed in acetone for 10 min. Paraffin embedded cultures were sectioned and 5 µm sections were deparaffinized in ethanol and rehydrated in preparation of immunohistochemical analysis of Axl (clone C20, Santa Cruz Biotechnology, Santa Cruz CA), keratin 10 (clone DEK10, Neomarkers, Fremont CA) and keratin 16 (clone LL025, Dr. I.M. Leigh, London, UK). After incubation with secondary antibodies, sections were stained with streptavidin-biotinylated horseradish peroxidase complex (ABComplex/HRP, DakoCytomation, Glostrup, Denmark), as described by the supplier. All sections were counterstained with haematoxylin.

Estimation of proliferation index

To determine the proliferation index, the number of Ki67 positive nuclei from the total number of basal cells (x100%) was used. A minimum of 100 basal cells was counted in sections of two different samples at a magnification of 200×. The resulting data are expressed as the mean of the two independent experiments ± SD (error bars).

Results

Invasive behavior in biopsy and cell line based skin cancer models

Fresh skin biopsies of both healthy and SCC origin were cultured on fibroblast-seeded collagen matrices at the air-liquid interface under serum-free conditions. During a four-week culture period, biopsy-associated keratinocytes migrated and proliferated over the dermal equivalent in a lateral fashion (Figure 1a). Cross sections of all explant cultures revealed spreading of the epidermis with viable cell-layers including the stratum basale, stratum spinosum, stratum granulosum and the stratum corneum. Furthermore, invasive behavior of a subpopulation of expanded SCC-associated keratinocytes was observed in two of three SCC explant models. These keratinocytes were capable of forming invasive nests in the dermal equivalent, originating from observed epidermal protrusions (Figure 1b-e). These invasive nests were seen in the direct vicinity of the original tumor biopsy as well as in dermal parts more distant from the original tumor biopsy. Skin equivalents generated with cell line SCC-12B2 showed extensive invasion into the dermal equivalent (Figure 1f), while cell line SCC-13 showed disturbed attachment of the epidermal keratinocytes to the dermal equivalent (Figure 1g). None of these features were observed in explant cultures of healthy skin biopsies of both immunocompetent and immunocompromised individuals.

Immunohistochemical SCC model characterization

To further characterize the SCC explant cultures, immunohistochemical analyses were performed on its epidermal outgrowth, targeting various protein specific markers for keratinocyte activation, proliferation and differentiation and BM formation. Results of all immunohistochemical analyses are summarized in Table 2.

Generated SCC models display hyperproliferative features

To assess the activation and proliferation status of keratinocytes in the cultures, expression of activation and hyperproliferation-specific keratins K6, K16 and K17 and proliferation-specific nuclear protein Ki67 was analyzed. In normal epidermis, none of the activation-specific keratins were detected (Figure 2a) and 13% ± 0.7% of basal cells stained positive for Ki67. Explant models of normal skin of immunocompetent individuals showed suprabasal staining of K6 and slight suprabasal staining of K16, while K17 was not detected and 15% ± 3% of basal cells stained positive for Ki67. Explant models of normal skin from immunocompromised patients showed slight suprabasal staining of K6 and subcorneal staining of K16 and K17 (Figure 2b). Epidermis, but not squamous cell nests of primary SCC stained strongly positive for K6, K16, K17 (Figure 2e) and Ki67 (62% ± 25%), lining the

Figure 1 | Haematoxylin–eosin (HE) staining of a skin cancer explant model, generated by culturing a squamous cell carcinoma (SCC) biopsy on a fibroblast-seeded collagen matrix (a). Explant models exhibit formation of squamous nests in the dermal compartment (a, indicated with arrows and b), originating from epidermal protrusions (c–e). Human skin equivalents were generated with SCC cell lines SCC-12B2 (f) and SCC-13 (g). Scale bars indicate 100 µm.

Table 2 | Summarized results of all immunohistochemical stainings on squamous cell carcinoma (SCC) explant models, primary SCC, normal skin explant models of organ transplant recipients (NS-OTR), primary normal skin of healthy individuals (NS-H), normal skin explant models of healthy individuals and SCC-12B2 and SCC-13 human skin equivalents (HSE). SC, stratum corneum; SS, stratum spinosum; SB, stratum basale; DEJ, dermal-epidermal junction.

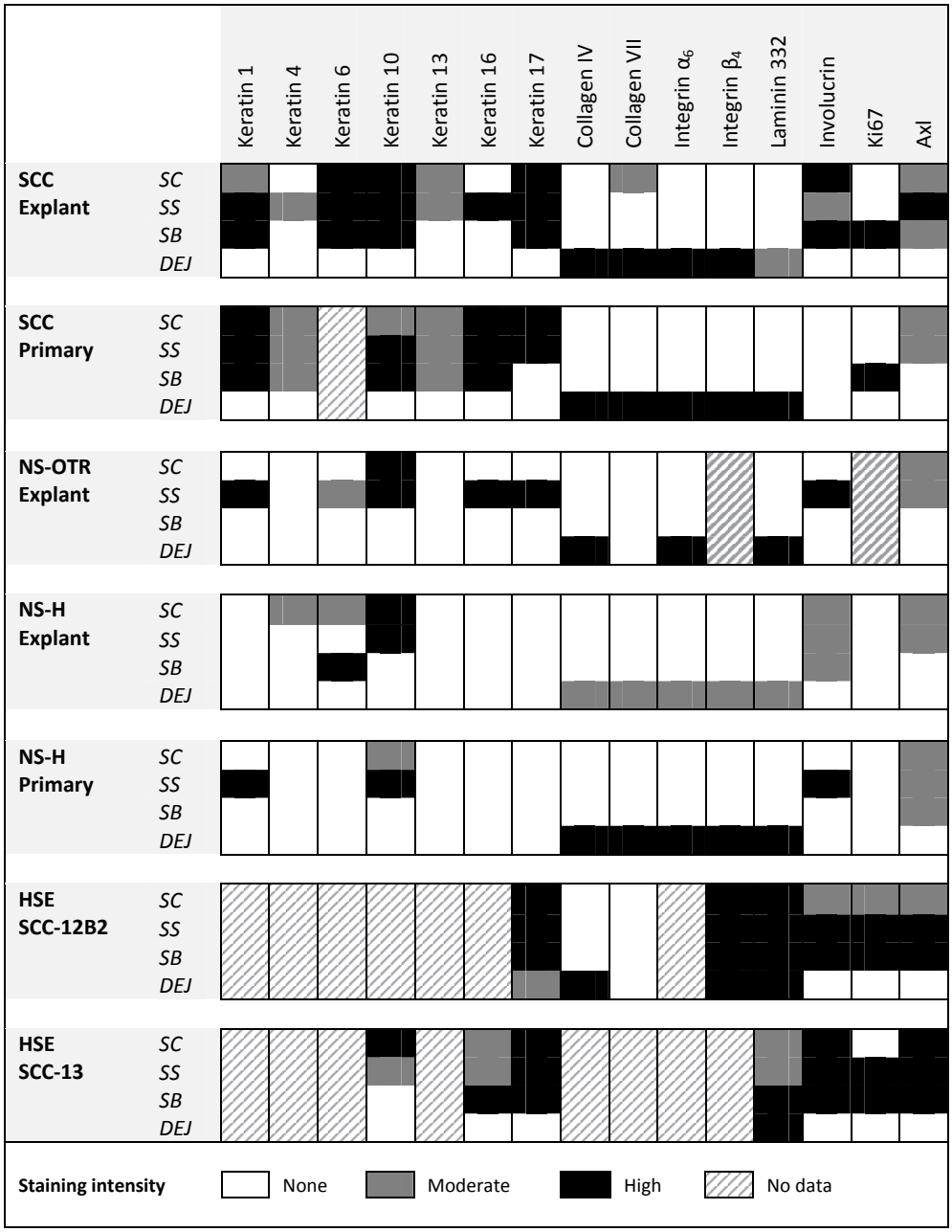

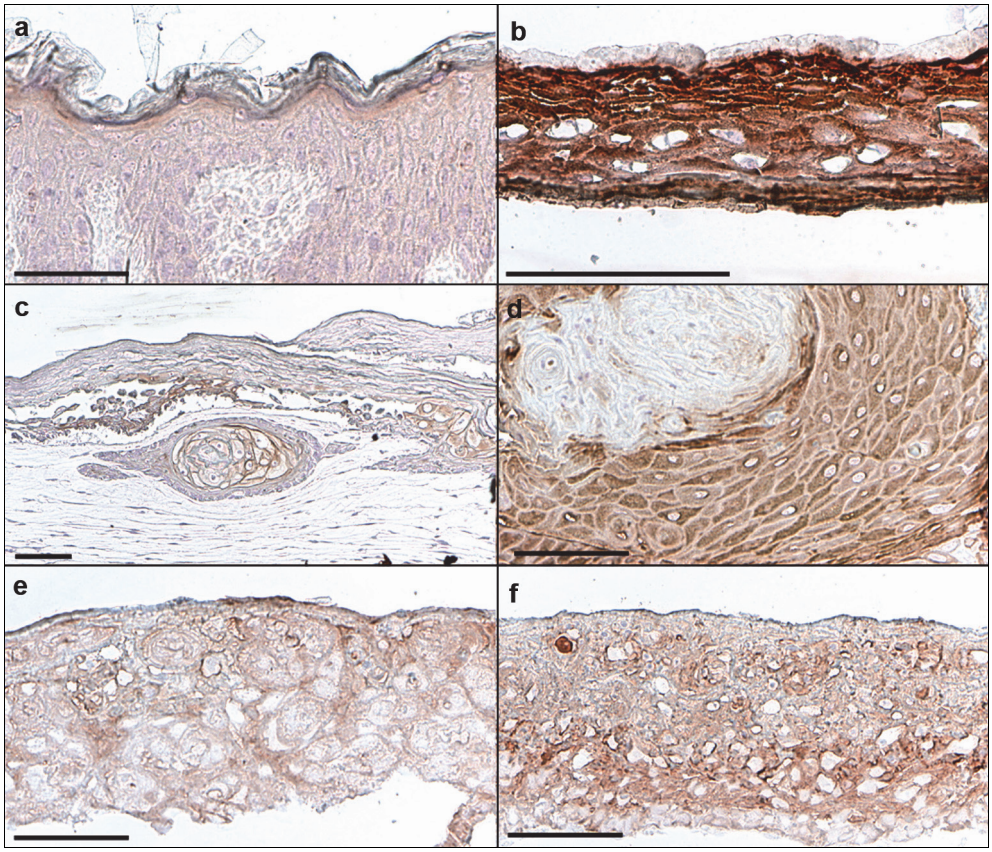

Figure 2 | Immunohistochemical staining of epidermal hyperproliferation marker keratin 17 (K17) in normal skin of immunocompetent indivuals (a) and immunocompromised individuals (b), squamous cell carcinoma (SCC) explant model (c, d), primary SCC (e) and human skin equivalents generated with SCC cell lines SCC-12B2 (f) and SCC-13 (g). Counterstained with haematoxylin. Scale bars indicate 100 µm.

proliferative edges of the invasive SCCs. The staining pattern of the SCC explant cultures resembled that of primary SCC with a strong K6 and K17 (Figure 2 c,d) staining throughout the epidermis and suprabasal staining of K16. Ki67 staining was present in 12% ± 2% of basal cells of SCC explant models. Skin equivalents generated with the SCC cell lines SCC-12B2 and SCC-13 stained positive for K17, which was present throughout all epidermal layers. SSC-13 showed a more pronounced expression of K17 in the basal cell layers (Figure 2f,g). Ki67 was present throughout all cell layers of SCC-12B2 and SCC-13 in 39% ± 8% and 82% ± 3% of cells, respectively.

Disturbed differentiation in SCC models

To gain more insight in the differentiation of keratinocytes in the cultures, immunohistochemical analyses were performed, focusing on differentiation-specific keratins K1, K4, K10 and K13, as well as on the terminal differentiation marker involucrin. In normal skin, K1 and K10 are expressed throughout the first suprabasal layers of the epidermis, indicating a normal proliferation program (Figure 3a,b). This staining pattern of K10, but not of K1, was also observed in explant models of normal skin of immunocompetent individuals (Figure 3e,f). In primary SCC however, both K1 and K10 were abundantly expressed in the cytoplasm of both basal and suprabasal keratinocytes (Figure 3j,k). The SCC explant model also showed strong basal expression of both K1 and K10, similar to primary SCC (Figure 3n,o). Furthermore, K1 was weakly detected in the suprabasal layers of the SCC explant model, whereas K10 was abundantly present in these layers of this model. K4 and K13 are both absent in normal skin and in normal skin explant models (Figure 3c,d,g,h). In all primary SCC and SCC explant skin models, both K4 and K13 were expressed in all cell layers (Figure 3l,m,p,q). In normal skin, involucrin is only expressed in the upper layers of the epidermis. In explanted normal skin of both immunocompetent and immunocompromised individuals, involucrin was also strongly expressed in the stratum corneum. In primary SCC, involucrin was abundant, without clear spatial restrictions, excluding the basal cell layers, but with greatest intensity in the cornified center of squamous cell nests. SCC explant models exhibited an involucrin staining pattern resembling that of primary SCC, with staining of all suprabasal layers as well as prominent staining in invasive squamous nests. Human skin equivalents of SCC cell lines SCC-12B2 and SCC-13 were only stained for K10 and involucrin. K10 was virtually absent in the model seeded with SCC-12B2 and present throughout the entire epidermis of the model seeded with SCC-13 (data not shown). Diffuse cytoplasmic staining of involucrin was shown in all epidermal layers of SCC-12B2 models and in focal areas of SCC-13 models (data not shown).

Normal basement membrane in SCC models

In order to assess the composition of the BM and associated cell adhesion molecules, immunohistochemical analysis was performed for collagen type IV, collagen type VII, laminin 332, integrin α_6 and integrin β_4 (data not shown). In normal skin of immunocompetent individuals and explants thereof, both collagen types IV and VII, laminin 332 and integrin $\alpha_6\beta_4$ were confined to the epidermal-dermal junction (EDJ). Explant models of normal skin of immunocompromised individuals showed similar staining, but lacked collagen type VII staining. Primary SCC showed considerable variation in the presence of these molecules both within and between tumors. In some cases, the presence of collagen type IV along the EDJ was disrupted or completely absent, while in

Figure 3 | Immunohistochemical staining of differentiation-specific keratins K1, K10, K4 and K13 in normal skin (a–d), normal skin explant models of immunocompetent individuals (e–h), primary SCC (i–m) and SCC explant models (m–p). Rows indicate the various samples (from top to bottom: normal skin; NS, normal skin explant models; NSX, primary SCC and SCC explant models; SCCX) and columns indicate the various markers (from left to right: K1, K10, K4, K13). Explant models were cultured for 4 weeks under airexposed and serum-free conditions prior to processing for immunohistochemical analysis. Counterstained with haematoxylin. Scale bars indicate 100 µm.

other cases the immunolocalization and intensity were similar to that in normal skin. Collagen type VII staining was often absent in primary SCC, but focal expression of varying intensity in proliferating fields of tumorigenic keratinocytes was observed as well. Expression of laminin 332 was not evaluated in primary SCC. The integrin subunit α_6 was not detected in primary SCC, whereas the integrin β_4 subunit was highly abundant in most tumors, particularly lining squamous cell nests. In explant models of SCC, the detection of collagen types IV and VII, laminin 332 and integrin $\alpha_6\beta_4$ was confined to the EDJ, indicating a fully formed BM. However, these BM molecules were also present at the circumference of the dermal squamous cell nests observed in SCC explant models. Models incorporated with the highly invasive SCC-12B2 cell line stained positive for collagen type IV lining the numerous areas of dermal invasion. Collagen type VII however was not detected in these cultures, whereas both laminin 332 and integrin subunit β_4 were clearly present throughout all the epidermal compartments. In models seeded with SCC-13, lacking a proper dermal-epidermal attachment, collagen type IV was not detected, while collagen type VII was detected abundantly in the entire epidermal layer. Laminin 332 and integrin subunit β_4 were both present along the EDJ and in the basal region.

Axl is expressed both in SCC models and primary SCC

As a candidate for involvement in SCC development and progression, we evaluated the presence of Axl in our current *in vitro* skin cancer model. In both native skin and explanted normal skin of both immunocompetent and immunocompromised individuals, no epidermal staining of Axl was observed (Figure 4a,b). Primary SCC and SCC explant models showed significant cytoplasmic staining of Axl in keratinocytes throughout the epidermis, particularly in more differentiated areas surrounding keratin pearls and in subcorneal layers (Figure 4c,d).

Discussion

In this study we used a skin explant method for the development and characterization of refined organotypic *in vitro* SCC models. Starting with primary human SCC biopsies of immune-suppressed individuals, we were able to create a three-dimensional skin equivalent harboring both keratinocytes and fibroblasts in a well-controlled microenvironment.

Global histology of SCC models revealed extensive lateral migration and proliferation of biopsy-associated keratinocytes, constituting an epidermal sheet of several cell layers. In addition, a subpopulation of expanded SCC-associated keratinocytes formed squamous cell nests in the dermal equivalent of some SCC models, which was never observed in

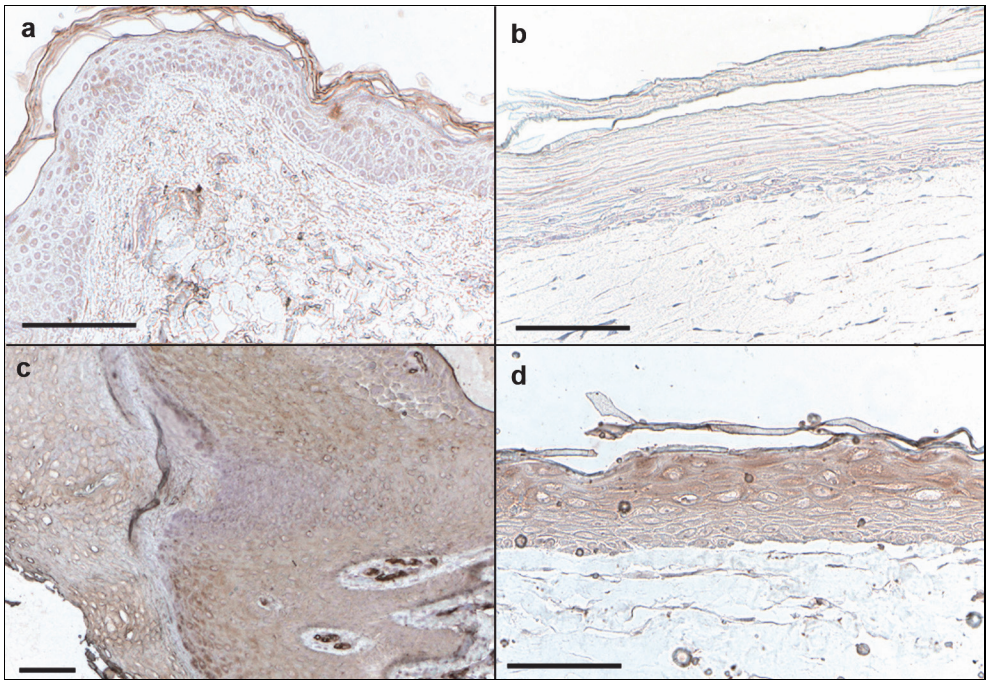

Figure 4 | Immunohistochemical staining of putative squamous cell carcinoma (SCC) marker Axl in normal skin (a), normal skin explant model (b), primary SCC (c) and SCC explant model (d). Explant models were cultured for 4 weeks under air-exposed and serum-free conditions prior to processing for immunohistochemical analysis. Counterstained with haematoxylin. Scale bars indicate 100 µm.

healthy control material. These squamous cell nests resembled those of invasive well-differentiated primary SCC, with well ordered islands and keratin pearls.[18] Furthermore, immunohistochemical analyses showed that keratinocytes in the SCC explant model were in an activated state, indicated by abundant expression of intermediate filament keratins K6, K16 and K17. These keratins are known to occur in the process of keratinocyte activation, which is characterized by hyperproliferation, migration, extensive cytoskeleton adaptation and BM component formation.[19] These keratins are known to be absent in healthy epidermis, but present in hyperproliferative epithelial cells in pathologic conditions, including chronic wounds, psoriasis and cutaneous squamous SCC.[19-22] Interestingly, explant models of normal buttock skin of immunocompromised renal transplant patients also stained positive for both K16 and K17, indicating that normal skin of these individuals might be in an activated state. This may be due to the immunosuppressive therapy of the patients concerned, consisting of the purine synthesis inhibitor azathioprine in combination with prednisone. Future research on higher numbers of immunocompromised normal skin explant cultures is needed to confirm this

observation. Detection of cell-cycling specific marker Ki67 of SCC explant models resembled that of normal skin and was not comparable to that of primary SCC. This implicates that the proliferation index of SCC models was normalized in culture. SCC explant models exhibited distorted expression of differentiation-specific keratins K1 and K10, indicating an aberrant differentiation pattern that was also seen in primary SCC. In addition, in primary SCC and *in vitro* skin cancer models differentiation-specific keratins K4 and K13 were present. Both keratins have been shown to be absent in normal skin.[23] Aberrant staining of K1, K4, K10 or K13 was not observed in normal skin explants derived from immunocompetent or immunocompromised donors. SCC explant models showed a terminal differentiation pattern that is similar to primary SCC, characterized by patchy cytoplasmic staining but with increased intensity in invasive squamous nests.[24, 25] As a soluble protein precursor of the cross-linked envelope found in normal stratum corneum, involucrin was detected in the suprabasal layers of normal skin and explant cultures thereof, derived from both immunocompetent and immunocompromised donors.[24-26] The current SCC explant model presented with a fully functional and continuous BM, displaying all of its main components including collagen types IV and VII, laminin 332 and integrin $\alpha_6\beta_4$. The squamous cells nests observed in these *in vitro* SCC models showed a similar pattern, implicating the functionality of these keratinocytes to form a normal BM surrounding these invasive areas.

Although our *in vitro* SCC explant model displayed invasive behavior by the formation of squamous nests, extensive invasion as seen in primary SCC is not present. This may be due to the facts that our culture conditions were not specifically selective for tumor cells and that the dermal equivalents in these models were seeded with fibroblasts of healthy origin, providing a healthy microenvironment. Recent advances in cell biology indicate the vital importance of cancer-associated fibroblasts in tumor-stroma interactions and invasion of SCC.[27] Thus, the squamous cell nests observed in our model may reflect the invasive capacity of lesional keratinocytes alone, or perhaps supported by few biopsy-associated fibroblasts, or the limited effects of SCC-associated keratinocytes on healthy fibroblasts seeded in the dermal equivalent. Of interest, skin models seeded with SCC cell line SCC-12B2 showed extensive invasion of the dermal compartment, which was also seeded with fibroblasts of healthy origin. This may support a mechanism in which epidermal keratinocytes provide molecular cues to associated dermal fibroblasts, which in turn enable tumor invasion. Therefore, incorporation of SCC-associated fibroblasts in the current model may improve the invasive characteristics of primary SCC-derived keratinocytes.

Furthermore, the current *in vitro* SCC explant model deviated from primary SCC in the lack of aberrations in composition and function of their BM. The most important components of the human cutaneous BM include collagen types IV and VII in anchoring fibrils, and laminin 332 and integrin $\alpha_6\beta_4$ in anchoring filaments, which are all confined to a continuous EDJ in normal skin.[28, 29] SCC however, showed striking aberrations in localization and intensity of BM components and presented with great variability within and between tumors. These differences have been demonstrated to be correlated with the differentiation status and the degree of keratinization of primary SCC. In well-differentiated and highly keratinized SCC, laminin 332 and collagen type IV were strongly expressed in the tumor nest near the BM without loss of continuity.[30] In poorly differentiated and poorly keratinized SCC, these proteins were largely lost, suggesting that these SCC cause greater enzymatic degradation of BM components than well-differentiated SCC. This hypothesis is supported by a study in which a negative correlation was demonstrated between protease activity and the level of cellular differentiation in SCC.[31] Positive correlation between BM degrading activity of tumor cell lines and their metastatic potential *in vivo* has been established as well, demonstrating that poorly differentiated tumors have a higher potential to metastasize than well-differentiated ones.[32] In addition to this concept of tumor metastasis facilitation by protease degradation of the BM and other components of the host extracellular matrix, an important role is indicated for other components of the extracellular matrix, including fibronectin and collagen type VII.[33, 34] Moreover, extracellular cues of the tumor microenvironment are required for the complex processes of tumor growth and cellular or tissue invasion.[34, 35] Permeation of the BM is a central determinant of malignancy in a wide array of epithelial cancers, including breast, prostate, lung, kidney and skin.[36] The importance of laminin 332 in this process has been widely demonstrated in SCC *in vivo*, showing that the collagen type VII non collagenous domain is required for SCC tumorigenesis and that the expression of both laminin 332 and integrin β_4 correlate with tumor invasion, progression and prognosis of RAS-driven epithelial tumors.[6, 37-39]

Recently, studies aimed at the identification of genes that are differentially expressed in SCC revealed the overexpression of the transmembrane receptor tyrosine kinase Axl in these tumors.[40] In normal skin of both immunocompetent and immunocompromised donors and explants thereof, Axl was virtually absent in the epidermis. In primary SCC however, Axl was highly present both membranous and cytoplasmic, and this staining pattern was also found in skin cancer explant models. In earlier studies, Axl was shown to have transforming potential and was found to be upregulated in metastatic SCC cell lines MET1 and MET4 when compared to premalignant SCC cell line PM1 and frequently overexpressed in primary SCC when compared to normal skin and BCC.[11, 40] These findings

were supported by previous studies in murine SCC where Axl overexpression was also noted.[41] Axl has been shown to modulate a number of cellular processes including adhesion, migration and proliferation. Also, Axl was shown to confer resistance of SCC cells to apoptosis.[42] Further studies are suggested to elucidate the potential role of Axl in SCC, as it may represent a novel therapeutic target for intervention in skin cancer development.

In conclusion, the *in vitro* expanded human SCC models presented here exhibited a normal proliferative character based on the Ki67 proliferation index, but highly increased expression of activation-associated keratins K6, K16 and K17, and presented with invasive behavior through the *in vitro* formation of invasive nests of keratinocytes. In addition, differentiation of the *in vitro* SCC models was disturbed, based on altered expression of differentiation-specific keratins 1, 4, 10 and 13, and of the putative SCC-specific Axl protein. Concerning BM composition and related invasion, *in vitro* SCC representation was still limited, leaving room for improvement of the tumor-stroma interaction in the current *in vitro* SCC explant model. Further validation of these and future *in vitro* SCC models will be focused on the role of SCC fibroblasts in SCC formation and genomic analysis to assess whether SCC specific genetic aberrations are maintained *in vitro*. Ultimately, development of the present model may help to extend the basic understanding of the pathogenic mechanisms of SCC in the clinically relevant group of immunocompromised organ-transplant recipients. Subsequently, it may lead to identification of novel therapeutic targets by exploration of reversal or prevention of tumor development in the organotypic *in vitro* human skin carcinoma models. Finally, this work may add significantly to advances in the field of alternatives to animal experimentation in skin cancer research, thereby meeting moral dilemmas and increasing opposition.

Acknowledgements

The authors would like to thank J.N. Bouwes Bavinck MD PhD, and H.C. Wisgerhof MD, for providing the primary SCC material that was used for this study.

References

1. de Vries, E., van de Poll-Franse, L.V., Louwman, W.J., de Gruijl, F.R. & Coebergh, J.W. Predictions of skin cancer incidence in the Netherlands up to 2015. *Br.J.Dermatol.* **152**, 481-488 (2005).
2. Staples, M.P. et al. Non-melanoma skin cancer in Australia: the 2002 national survey and trends since 1985. *Med.J.Aust.* **184**, 6-10 (2006).
3. Bouwes Bavinck, J.N. et al. The risk of skin cancer in renal transplant recipients in Queensland, Australia. A follow-up study. *Transplantation* **61**, 715-721 (1996).
4. Atillasoy, E.S., Elenitsas, R., Sauter, E.R., Soballe, P.W. & Herlyn, M. UVB induction of epithelial tumors in human skin using a RAG-1 mouse xenograft model. *J.Invest Dermatol.* **109**, 704-709 (1997).
5. Brown, K. & Balmain, A. Transgenic mice and squamous multistage skin carcinogenesis. *Cancer Metastasis Rev.* **14**, 113-124 (1995).
6. Dajee, M. et al. NF-kappaB blockade and oncogenic Ras trigger invasive human epidermal neoplasia. *Nature* **421**, 639-643 (2003).
7. Eicher, S.A. et al. Evaluation of topical gene therapy for head and neck squamous cell carcinoma in an organotypic model. *Clin.Cancer Res.* **2**, 1659-1664 (1996).
8. Slaga, T.J., Budunova, I.V., Gimenez-Conti, I.B. & Aldaz, C.M. The mouse skin carcinogenesis model. *J.Investig.Dermatol.Symp.Proc.* **1**, 151-156 (1996).
9. Gupta, A., Rosenberger, S.F. & Bowden, G.T. Increased ROS levels contribute to elevated transcription factor and MAP kinase activities in malignantly progressed mouse keratinocyte cell lines. *Carcinogenesis* **20**, 2063-2073 (1999).
10. Popp, S. et al. Genetic characterization of a human skin carcinoma progression model: from primary tumor to metastasis. *J.Invest Dermatol.* **115**, 1095-1103 (2000).
11. Proby, C.M. et al. Spontaneous keratinocyte cell lines representing early and advanced stages of malignant transformation of the epidermis. *Exp.Dermatol.* **9**, 104-117 (2000).
12. El Ghalbzouri, A., Lamme, E. & Ponec, M. Crucial role of fibroblasts in regulating epidermal morphogenesis. *Cell Tissue Res.* **310**, 189-199 (2002).
13. Ponec, M. et al. The formation of competent barrier lipids in reconstructed human epidermis requires the presence of vitamin C. *J Invest Dermatol* **109**, 348-55 (1997).
14. El Ghalbzouri, A., Jonkman, M., Kempenaar, J. & Ponec, M. Recessive epidermolysis bullosa simplex phenotype reproduced in vitro: ablation of keratin 14 is partially compensated by keratin 17. *Am.J.Pathol.* **163**, 1771-1779 (2003).
15. Rheinwald, J.G. & Beckett, M.A. Defective terminal differentiation in culture as a consistent and selectable character of malignant human keratinocytes. *Cell* **22**, 629-632 (1980).
16. El Ghalbzouri, A. et al. Fibroblasts facilitate re-epithelialization in wounded human skin equivalents. *Lab Invest* **84**, 102-112 (2004).
17. Smola, H., Thiekotter, G. & Fusenig, N.E. Mutual induction of growth factor gene expression by epidermal-dermal cell interaction. *J Cell Biol* **122**, 417-29 (1993).
18. Bloor, B.K., Seddon, S.V. & Morgan, P.R. Gene expression of differentiation-specific keratins in oral epithelial dysplasia and squamous cell carcinoma. *Oral Oncol.* **37**, 251-261 (2001).
19. Freedberg, I.M., Tomic-Canic, M., Komine, M. & Blumenberg, M. Keratins and the keratinocyte activation cycle. *J.Invest Dermatol.* **116**, 633-640 (2001).
20. Moll, R., Franke, W.W., Schiller, D.L., Geiger, B. & Krepler, R. The catalog of human cytokeratins: patterns of expression in normal epithelia, tumors and cultured cells. *Cell* **31**, 11-24 (1982).
21. Smits, T. et al. Aneuploidy and proliferation in keratinocytic intraepidermal neoplasias. *Exp.Dermatol.* **16**, 81-86 (2007).
22. Yoshikawa, K., Katagata, Y. & Kondo, S. Relative amounts of keratin 17 are higher than those of keratin 16 in hair-follicle-derived tumors in comparison with nonfollicular epithelial skin tumors. *J.Invest Dermatol.* **104**, 396-400 (1995).
23. Richard, G., De, L.V., Didona, B., Bale, S.J. & Compton, J.G. Keratin 13 point mutation underlies the hereditary mucosal epithelial disorder white sponge nevus. *Nat.Genet.* **11**, 453-455 (1995).
24. Murphy, G.F., Flynn, T.C., Rice, R.H. & Pinkus, G.S. Involucrin expression in normal and neoplastic human skin: a marker for keratinocyte differentiation. *J.Invest Dermatol.* **82**, 453-457 (1984).
25. Said, J.W., Sassoon, A.F., Shintaku, I.P. & Banks-Schlegel, S. Involucrin in squamous and basal cell carcinomas of the skin: an immunohistochemical study. *J.Invest Dermatol.* **82**, 449-452 (1984).

26. Kalinin, A.E., Kajava, A.V. & Steinert, P.M. Epithelial barrier function: assembly and structural features of the cornified cell envelope. *Bioessays* **24**, 789-800 (2002).
27. Gaggioli, C. et al. Fibroblast-led collective invasion of carcinoma cells with differing roles for RhoGTPases in leading and following cells. *Nat.Cell Biol.* **9**, 1392-1400 (2007).
28. Merker, H.J. Morphology of the basement membrane. *Microsc.Res.Tech.* **28**, 95-124 (1994).
29. Timpl, R. Macromolecular organization of basement membranes. *Curr.Opin.Cell Biol.* **8**, 618-624 (1996).
30. Oguro, K. et al. Immunohistochemical alterations in basement membrane components of squamous cell carcinoma. *J.Invest Dermatol.* **96**, 250-254 (1991).
31. Tsuboi, R. et al. Comparison of proteinase activities in squamous cell carcinoma, basal cell epithelioma, and seborrheic keratosis. *J.Invest Dermatol.* **90**, 869-872 (1988).
32. Liotta, L.A. et al. Metastatic potential correlates with enzymatic degradation of basement membrane collagen. *Nature* **284**, 67-68 (1980).
33. Chang, C. & Werb, Z. The many faces of metalloproteases: cell growth, invasion, angiogenesis and metastasis. *Trends Cell Biol.* **11**, S37-S43 (2001).
34. Waterman, E.A. et al. A laminin-collagen complex drives human epidermal carcinogenesis through phosphoinositol-3-kinase activation. *Cancer Res.* **67**, 4264-4270 (2007).
35. Marinkovich, M.P. Tumour microenvironment: laminin 332 in squamous-cell carcinoma. *Nat.Rev.Cancer* **7**, 370-380 (2007).
36. Friedl, P. & Wolf, K. Tumour-cell invasion and migration: diversity and escape mechanisms. *Nat.Rev.Cancer* **3**, 362-374 (2003).
37. Janes, S.M. & Watt, F.M. New roles for integrins in squamous-cell carcinoma. *Nat.Rev.Cancer* **6**, 175-183 (2006).
38. Ortiz-Urda, S. et al. Type VII collagen is required for Ras-driven human epidermal tumorigenesis. *Science* **307**, 1773-1776 (2005).
39. Rodeck, U., Fertala, A. & Uitto, J. Anchorless keratinocyte survival: an emerging pathogenic mechanism for squamous cell carcinoma in recessive dystrophic epidermolysis bullosa. *Exp.Dermatol.* **16**, 465-467 (2007).
40. Green, J. et al. Overexpression of the Axl tyrosine kinase receptor in cutaneous SCC-derived cell lines and tumours. *Br.J.Cancer* **94**, 1446-1451 (2006).
41. Loercher, A. et al. Nuclear factor-kappaB is an important modulator of the altered gene expression profile and malignant phenotype in squamous cell carcinoma. *Cancer Res.* **64**, 6511-6523 (2004).
42. Papadakis, E., Vyas, J.J. & O'Toole, E.A. A role for the Receptor Tyrosine Kinase, Axl, in Cutaneous Squamous Cell Carcinoma Survival *J.Invest Dermatol.* **127**, Abstract 571 (2007).

3

Functional characterization of cancer-associated fibroblasts of human cutaneous squamous cell carcinoma

Suzan Commandeur, Suet Huy Ho, Frank R. de Gruijl, Rein Willemze, Cornelis P. Tensen and Abdoelwaheb El Ghalbzouri

Department of Dermatology, Leiden University Medical Center, Leiden, the Netherlands

Experimental Dermatology 2011;20(9):737-742

Abstract

Cutaneous squamous cell carcinoma (SCC) is the second most common type of skin cancer in the Caucasian population worldwide, having a propensity for invasion, local recurrence and metastasis. Stromal cancer-associated fibroblasts (CAFs) are suspected to play an important role in SCC carcinogenesis. In this study, we characterized CAFs isolated from primary cutaneous SCCs and compared them to normal fibroblasts (NFs) isolated from healthy dermis. Human skin CAFs in monolayers displayed different morphology, increased proliferation and migration compared to NFs. CAFs caused strong contraction of collagen matrices in which they were seeded and released high levels of the extracellular matrix component pro-collagen I. CAFs decreased proliferation and differentiation in the epidermis of human skin equivalents (HSEs) seeded with SCC cell lines, without affecting basement membrane composition. Finally, CAFs significantly increased invasion and dermal-epidermal detachment of SCC cell lines SCC-12B2 and SCC-13, respectively, when cultured in HSEs. These distinct features of CAFs point out a specific role in cutaneous SCC development.

Introduction

Cutaneous squamous cell carcinoma (SCC) is the second most common type of skin cancer worldwide, after basal cell carcinoma (BCC).[1] Although the absolute incidence of SCC is only about one-third of the incidence of BCC, SCCs have a greater propensity for invasion, local recurrence and metastasis.[2] This problem is particularly dramatic in organ transplant recipients treated with immune suppressants.[3] Despite a variety of treatment options, there is a need for more specific inhibitors of invasion and metastasis of cutaneous SCCs.

In normal skin, tissue homeostasis is maintained by extensive crosstalk between epidermal keratinocytes, dermal fibroblasts and the extracellular matrix (ECM). Analogously, cutaneous tumor invasion as a manifestation of disrupted epidermal homeostasis results from complex interactions between the epidermal cancer cells and their surrounding stroma, consisting of ECM, cancer-associated fibroblasts (CAFs), immune cells and vasculature.[4] CAFs are considered important players in epithelial tumor progression and invasion.[5] In concert with epithelial cancer cells, CAFs are responsible for ECM deposition and remodelling.[6-8] These properties are considered supportive of tumor progression and invasion, which involves active ECM remodelling and breakdown of basement membrane (BM) structures that separate epidermal from dermal skin compartments.

By definition, CAFs are fibroblasts residing in the tumor stroma, either in direct contact with or in the vicinity of epithelial cancer cells. In literature, these cells are also termed tumor-associated fibroblasts, reactive stroma fibroblasts, activated fibroblasts, myofibroblasts, peritumoral fibroblasts, pericytes or fibrocytes.[9-12] CAFs are generally accredited myofibroblastic properties and characteristically express alpha smooth muscle actin (α-SMA), a cytoplasmic component unusually present in myofibroblast stress fibres, which play an important role in cell adhesion, tension and contractility.[10, 13] As increased stromal α-SMA expression is clinically associated with increased invasiveness of oral and cervical SCC, colorectal carcinoma and breast carcinoma, it is often used as an experimental CAF selection marker.[11, 13-17] In addition, CAFs may be differentiated from normal fibroblasts (NFs) based on their expression of specific fibroblast surface proteins (e.g. fibroblast-activated protein, FAP) and increased production of tumor-promoting growth factors (e.g. hepatocyte growth factor, HGF) and proteins associated with invasion, remodeling and (neo)vascularization (e.g. stromal cell–derived factor 1).[5, 12]

Despite many efforts in characterizing CAFs, studies on CAFs in cutaneous SCC have not been published. The aim of the present study was to define the morphological and

functional characteristics of CAFs that spontaneously expanded from primary cutaneous SCC. To this end, we compared the morphological, migratory, proliferative and contractile properties of CAFs and NFs from healthy dermis, as well as the effects of CAFs on ECM formation. In addition, the effects of CAFs on BM formation and invasion of SCC cell lines in human skin equivalents (HSEs) were investigated.

Methods

Patient material

Five primary well-differentiated cutaneous SCCs were freshly collected from different renal transplant patients (median age 58 years, two women and three men, all treated with prednisone and azathioprin). One part of each lesion was processed for diagnosis, while the remainder was used for isolation of CAFs. Diagnoses were routinely confirmed by the Pathology Department of the Leiden University Medical Center. All tumor samples used were collected with written informed consent of the patient according to the Declaration of Helsinki after approval of the medical ethical committee of the Leiden University Medical Center. Fresh mamma reduction skin of three healthy female individuals (median age 31 years) was used for isolation of NFs and normal human epidermal keratinocytes (NHEKs). This surplus material was obtained in accordance with the Dutch Law on Medical Treatment Agreement. In addition, two SCC cell lines, SCC-12B2 (isolated from a facial SCC on a 60-year-old male kidney transplant patient) and SCC-13 (isolated from a facial SCC on a 56-year-old female kidney transplant patient), were included. These cell lines were previously kindly provided by Dr J.G. Rheinwald.[18]

Fibroblast culture

Normal fibroblasts were isolated from healthy skin as described earlier.[19] For isolation of CAFs, fresh SCCs from immunesuppressed individuals were rinsed three times in sterile phosphate buffered saline (PBS) upon arrival. The biopsies were incubated for several hours at room temperature in PBS supplemented with penicillin–streptamycin (300 U/ml) and amphotericin B (Fungizone, 5 µl/ml; Gibco/Invitrogen, Breda, the Netherland). Next, the biopsies were rinsed three times with sterile PBS, cut into small pieces, explanted in a dish and cultured for approximately 2 weeks at 37°C and 5% CO_2 until fibroblast monolayer cultures were established. Fibroblast medium consisted of CnT-05 medium (CELLnTEC, Bern, Switzerland) containing 5% fetal bovine serum (FBS, HyClone/Greiner, Nurtingen, Germany) and supplemented with penicillin–streptamycin (300 U/ml) and amphotericin B (5 µl/ml). Medium was refreshed every 3 days. Fibroblast passages 3 to 6 have been used for the experiments.

Keratinocyte culture

Normal human epidermal keratinocytes were isolated as described earlier.[20] Cell lines SCC-12 and SCC-13 were cultured on lethally irradiated murine 3T3 fibroblasts. Keratinocytes were cultured in standard keratinocyte medium consisting of DMEM and Ham's F12 medium in a 3:1 ratio, supplemented with 5% FBS, 0.5 µM hydrocortisone, 1 µM isoproterenol, 0.1 µM insulin (Sigma-Aldrich, Zwijndrecht, the Netherlands) and 100 U/ml penicillin–streptamycin. Keratinocytes were cultured at 37°C and 7.3% CO_2. Culture medium was refreshed every 3 days. First-passage NHEKs were used for experiments.

Human skin equivalents

Human skin equivalentss were generated as described earlier.[21] Briefly, dermal equivalents were generated by seeding rat-tail collagen (3.2 mg/ml, isolated in-house) with $1.25x10^5$ fibroblasts/ml, which were incubated for a period of 1 week under submerged conditions in fibroblast medium at 37°C and 5% CO_2. Subsequently, dermal equivalents were seeded with $5x10^4$ keratinocytes/cm^2 (either NHEK, SCC-12B2 or SCC-13). HSEs were incubated overnight under submerged conditions at 37°C and 7.3% CO_2 in standard keratinocyte medium as described earlier. After 3 days, FBS was reduced to 1%. Two days thereafter, FBS was omitted and HSEs were cultured at the air–liquid interface for 2 weeks, while medium was refreshed every 3 days.

Fibroblast morphology, proliferation and migration

Monolayer cultures of two NF donors and five CAF donors were regularly observed and photographed with a phase-contrast microscope camera to determine their morphological characteristics at various confluences and passages. To monitor proliferation, manual cell counts were performed per phase-contrast microscope field in duplo for 7 days. To determine the migratory behavior of the fibroblasts, a scratch assay was performed. Scratches were made in duplo into subconfluent cell layers using a P200 pipette tip, creating cell-free zones. Cultures were washed extensively with PBS and incubated at 37°C and 5% CO_2 in standard fibroblast culture medium for 2 days. Position-matched phase-contrast microscope images were acquired at 0, 14, 18 and 42h. Cell migration into the cell-free zones was quantified using ImageJ freeware version 1.41 (http://rsbweb.nih.gov/ij/).

Collagen contraction

Fibroblasts from two NF donors and five CAF donors were seeded into 3.2 mg/ml rat-tail collagen matrices on 3.0 µm pore size six-well transwell membrane inserts (Corning Life Sciences, Amsterdam, the Netherlands) at a seeding density of $1.25x10^5$ fibroblasts/ml. After incubation for 1 week under submerged conditions in fibroblast medium at 37°C and

5% CO_2, macroscopic pictures of all cultures were acquired. Collagen shrinkage was quantified using ImageJ freeware version 1.41 (http://rsbweb.nih.gov/ij/).

Immunocytochemistry

Fibroblasts (both NFs and CAFs) were cultured as confluent monolayers on sterile eight-chamber glass slides (Lab-Tek II, Nalge Nunc International, Rochester, NY, USA). Cultures were fixed in ice-cold methanol and acetone (1:1) and stained for α-SMA (1:50, clone 1A4; Abcam, Cambridge, UK) according to standard cryosection procedures using a streptavidin-biotinylated horseradish peroxidase (HRP) complex (GE Healthcare, Buckinghamshire, UK) and 3-amino-9-ethylcarbazole (AEC). To determine the percentage of α-SMA-positive cells, the number of α-SMA-positive cells was divided by the total number of nuclei (x100%). A minimum of 80 cells was counted in four different locations at a 100× magnification. The resulting data are expressed as the mean of the four counts ±SD.

Pro-collagen I deposition

Quantification of human pro-collagen type I in the culture medium of fibroblasts cultured on membrane inserts was performed by enzyme-linked immunosorbent assay (ELISA, MetraCICP ELISA kit; Quidel Corporations, San Diego, CA, USA) according to the manufacturer's instructions. Culture medium was collected at each refreshment throughout a 5-week culture period. Measurements were taken and data analysis was performed according to the manufacturer's procedure. The data are expressed as ng/ml culture medium with mean and SD of triplicate measurements of specimens originating from two independent cultures.

Histology and immunohistochemistry

After culture, HSEs were partly archived as formalin-fixed paraffin-embedded material, while the other part was snap-frozen in liquid nitrogen. For histological analysis, 5-lm sections of HSEs were stained with haematoxylin and eosin. Immunohistochemical analysis of Ki67 (1:100, clone MIB1; Abcam), involucrin (1:200, clone SY5; Dako, Glostrup, Denmark), collagen type IV (1:75, clone MAB1430; Chemicon, Melbourne, Vic., Australia) and laminin 332 (1:200, clone BM165, personal gift from Dr A. Aumailley, Cologne, Germany) was performed on 5-µm HSE cryosections that were air-dried overnight and fixed in acetone for 10 min. After incubation with the secondary antibody (biotinylated goat anti-mouse IgG; DakoCytomation, Glostrup, Denmark), sections were stained with streptavidin-biotinylated HRP complex and AEC. All sections were counterstained with haematoxylin.

Quantification of proliferation index

To determine the proliferation index of the HSEs cultured with SCC cell lines, the number of Ki67-positive nuclei from a total number of 100 epidermal cells (x100%) was counted. Per section, counts were performed in three different locations at a magnification of 200×. Results were expressed as the mean of the three counts ±SD (error bars).

Quantification of invasion and BM-detachment

For HSEs in which cell line SCC-12B2 was cultured on either NFs or CAFs, invasion was quantified by calculating two parameters: the maximal invasion depth ratio and the total dermal area.[22, 23] The maximal invasion depth ratio is defined as the distance of the deepest invading cell from the epidermal surface divided by the total distance from the epidermal surface to the filter. As such, a higher maximal invasion depth ratio indicates more invasive behaviour. The total dermal area is defined as the complete remaining area of dermal equivalent in which no epidermal cells have invaded. A larger total dermal area indicates less invasive behaviour. For HSEs in which cell line SCC-13 was cultured on either NFs or CAFs, detachment from the BM was quantified by calculating the total length of direct dermal–epidermal contact. All parameters defined earlier were calculated per microscopic field. Three representative areas of each section were digitally recorded at 100× magnification with a Zeiss Axiocam color (model 412-312; Carl Zeiss B.V., Sliedrecht, the Netherlands) camera connected to a Zeiss Axioplan 2 upright light microscope. For each parameter, three measurements per recording were taken using ImageJ freeware version 1.41.

Statistics

Statistical significance of differences in non-categorized, continuous measurements was determined using the two-tailed Student's t-test for unpaired samples.

Results

Morphology, migration and proliferation distinguish CAFs from NFs

The morphology of both CAFs and NFs was determined by microscopic observation of monolayer cultures. CAFs appeared quite undifferentiated, which was marked by long spindle-shaped cells and limited visual contact inhibition. This distinguished them from NFs, displaying visual contact inhibition and a predominant star shape, indicating a more differentiated nature. Although these morphological differences between the two groups of CAFs and NFs were retained in parallel experiments, in-group heterogeneity was always observed between individual cultures originating from different donors. Morphological differences between CAFs and NFs decreased with increased passaging. Fibroblast

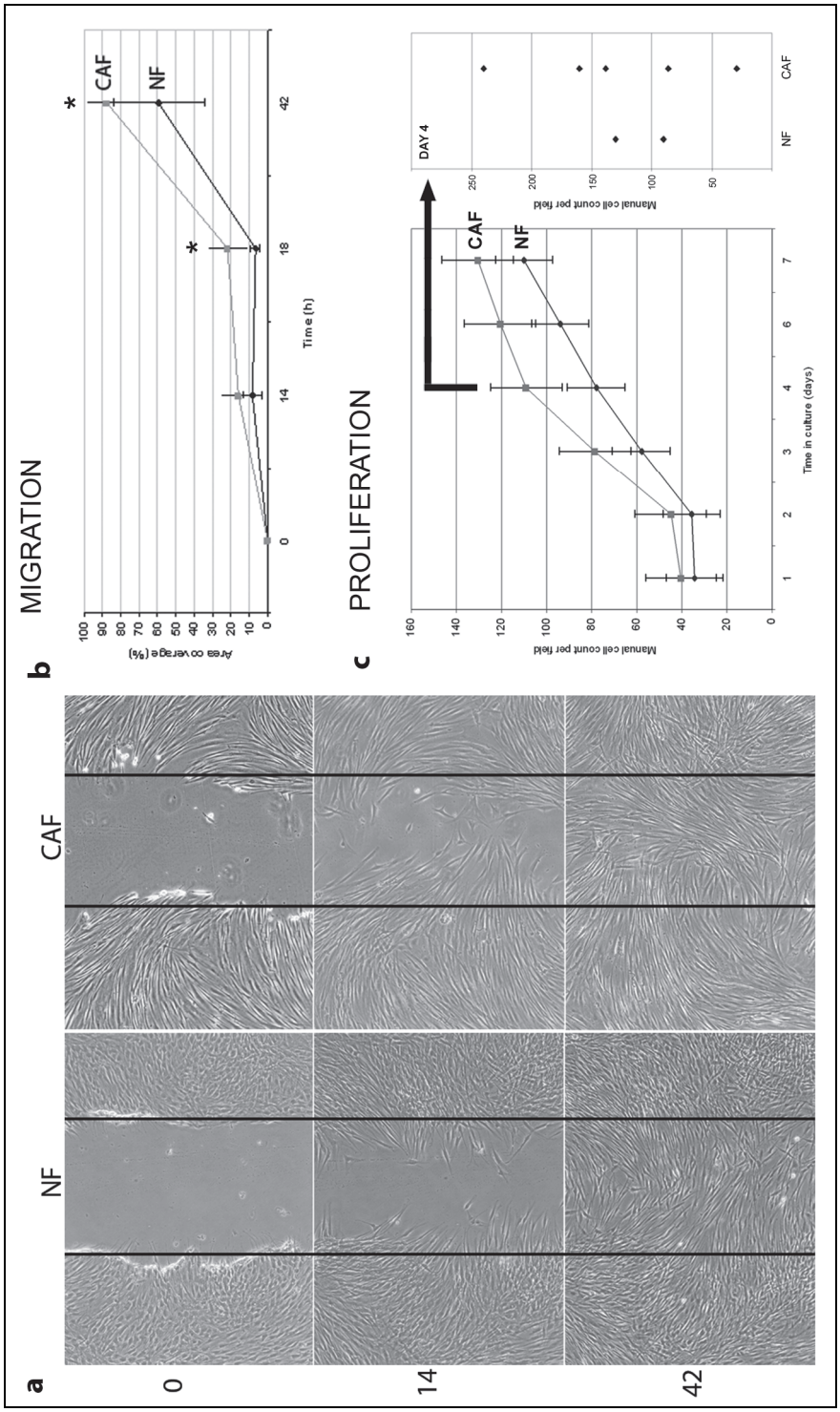

Figure 1 | (a) Photographs of a scratch assay in monolayer cultures of normal fibroblasts (NF) and cancer-associated fibroblasts (CAF) at 0, 18 and 42 h after scratching. (b) Graph of time course of recovery of the scratched area by NF and CAF (asterisk denotes $P < 0.05$). (c) Proliferation of NF and CAF. Left panel: manual cell counts per microscopic field. Right panel: CAF cell counts showing considerable variation, shown for day 4.

migration was assessed in a scratch assay. CAFs and NFs recover scratched areas of identical width after 42h to 88% (±11%) and 59% (±25%), respectively (Figure 1a,b). The migratory capacity of CAFs significantly exceeded that of NFs from 18h on (Figure 1b). Furthermore, CAFs proliferated 28% (±9%) faster than NFs, as reflected by cell counts per microscopic field of view at 2, 3, 4, 6 and 7 days after seeding (Figure 1c, left panel). However, this difference in proliferation between NFs and CAFs was not statistically significant. Considerable variation was found in the cell counts between NFs and CAFs (Figure 1c, right panel).

CAFs induce increased collagen contraction

The contractile properties of CAFs and NFs were evaluated in a collagen contraction experiment. Collagen contraction by CAFs significantly more than quadrupled collagen contraction by NFs (Figure 2a). This was quantified by a dramatic difference in shrinkage of floating fibroblast-seeded collagen matrices, as the average area of CAF-seeded matrices was only 28% (± 2.4%) of that of NF-seeded matrices. Immunohistochemical analysis of

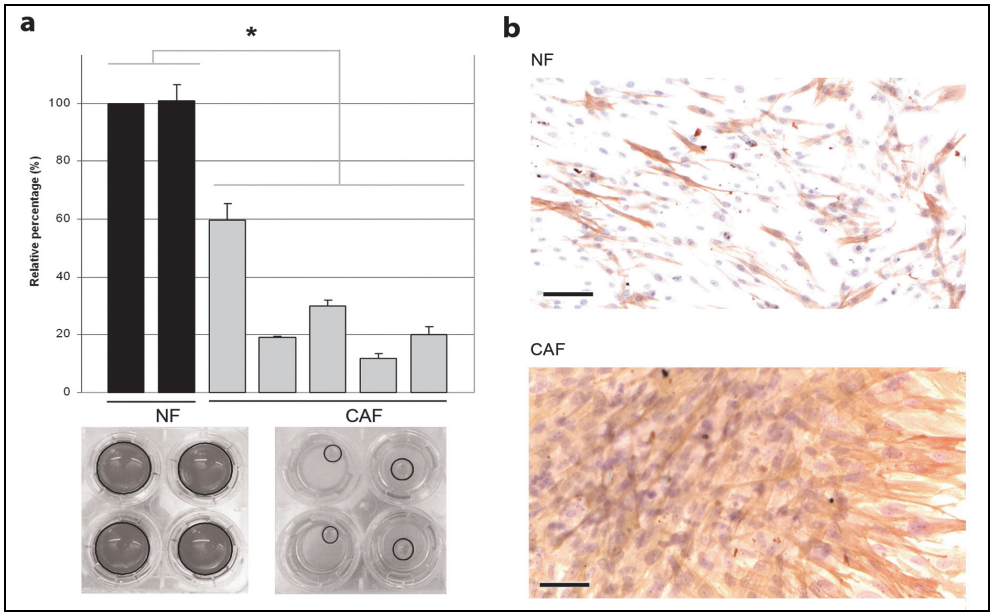

Figure 2 | (a) Graph of the collagen contraction by normal fibroblasts (NF, n = 2) and cancer-associated fibroblasts (CAF, n = 5), measured by the relative area coverage of floating fibroblast-seeded collagen matrices. The difference between NFs and CAFs is statistically significant (asterisk denotes $P < 0.01$). In the photographs below the graph, collagen matrix circumferences are demarcated by black circles. (b) Immunohistochemical staining of alpha smooth muscle actin α-SMA) on NF and CAF. Scale bars indicate 100 µm.

the contraction-related protein a-SMA revealed 100% positive staining of CAFs cultured in a monolayer, while NFs cultured under identical conditions showed only 32% (±5%) α-SMA-positive cells (Figure 2b).

Pro-collagen I production is increased in CAFs

To evaluate ECM-formation, pro-collagen type I was measured by ELISA in duplo in culture medium of NFs and CAFs collected throughout a 5-week culture period. A significant increase in pro-collagen type I secretion was measured during the first 3 weeks in both NFs and CAFs ($P < 0.05$) (Figure 3). However, pro-collagen type I secretion by CAFs significantly exceeded that of NFs after 1, 3 and 5 weeks (Figure 3). The maximum concentration of pro-collagen type I produced by CAFs (347 ± 31 ng/ml) was 50% higher than that of NFs (230 ± 27 ng/ml).

CAFs enhance tumorigenic characteristics of SCC cell lines

To evaluate CAFs functionally, HSEs were cultured using dermal equivalents seeded with either NFs or CAFs, on which either NHEKs, cell line SCC-12B2 or SCC-13 keratinocytes were cultured. This resulted in HSEs with SCC-characteristics, as these cell lines are known for their extensive dermal invasion (SCC-12B2) and dermal-epidermal detachment (SCC-

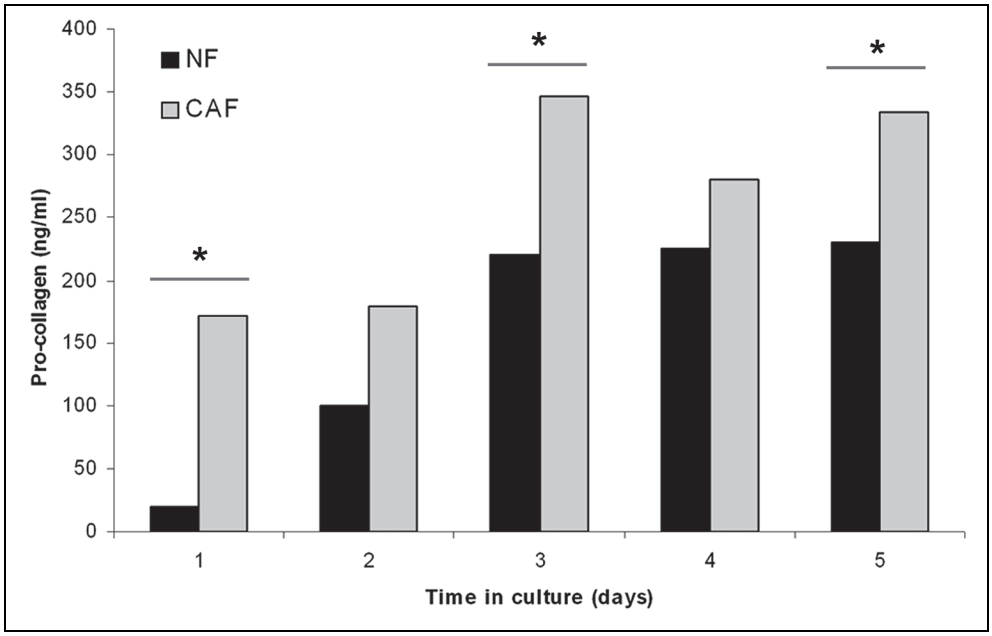

Figure 3 | Enzyme-linked immunosurbent assays (ELISA) results of human pro-collagen type I levels in culture medium of normal fibroblasts (NF) and cancer associated fibroblasts (CAF) (asterisk denotes $P<0.05$).

13).[18, 20] When cultured on either NF-seeded (Figure 4a) or CAF-seeded (Figure 4b) dermal equivalents, NHEKs generated a fully differentiated, normal epidermis with several cell layers. NF-based SCC-12B2 HSEs showed extensive dermal invasion (Figure 4d). However, when cultured on CAF-based dermal equivalents, invasion of SCC-12B2 cells was highly increased (Figure 4e). This was reflected by a significant difference in the maximal invasion depth ratio per microscopic field of both models, which was 0.72 (±0.07) in NFbased SCC-12B2 HSEs and 0.91 (±0.04) in CAF-based SCC-12B2 HSEs (Figure 4c, P = 0.02). Moreover, the difference in total dermal cross-sectional area of both models was striking, as 6.50 mm^2 (±0.25 mm^2) of dermal area per microscopic field remains in NFbased SCC-12B2 HSEs, while only 0.63 mm^2 (±0.24 mm^2) of dermal area per microscopic field was left in CAF-

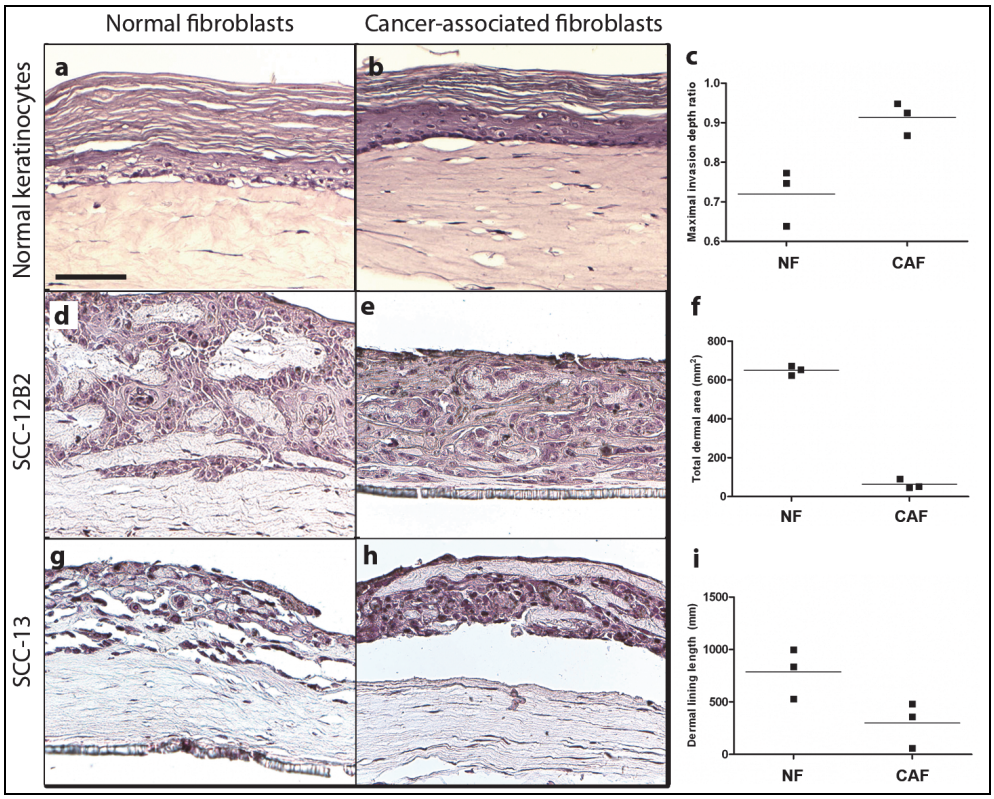

Figure 4 | Haematoxylin-eosin (HE) staining of human skin equivalents of normal human epidermal keratinocytes (NHEK, a,b) SCC-12B2 (d,e) and SCC-13 (g,h) on a collagen matrix seeded with normal fibroblasts (NF) (a,d,g) or cancer associated fibroblasts (CAF) (b,e,h). Scale bars indicate 100 µm. The maximal invasion depth ratio of SCC-12B2 is significantly higher in CAF-based HSEs than in NF-based HSEs (c, P=0.02). The remaining total dermal area is significantly lower in CAF-based HSEs than in NF-based HSEs (f, P < 0.001). Detachment of SCC-13 is higher in CAF-based HSEs compared to NF-based HSEs, as quantified by the dermal lining length (i, P=0.06).

based SCC-12B2 HSEs (Figure 4f, P < 0.001). This tendency also held for SCC-13 HSEs, as CAF-based HSEs showed increased dermal-epidermal detachment, which is a characteristic of SCC-13 cells in HSEs (Figure 4g,h). We quantified the dermal lining length as a measure of dermal–epidermal detachment, which was 7.8 mm (±2.3 mm) per microscopic field in NF-based SCC-13 HSEs and 3.0 mm (±2.2 mm) per microscopic field in CAF-based SCC-13 HSEs (Figure 4i, P = 0.06).

CAFs decrease proliferation in human SCC skin models

Proliferation rates in SCC-12B2 HSEs and in SCC-13 HSEs based either on NFs or CAFs were assessed by routine quantification of immunohistochemical staining of the nuclear Ki67 protein, which is associated with cell cycling (Figure 5a). NF-based SCC-12B2 HSEs showed a proliferation rate of 0.39 (±0.09) (P < 0.05). The proliferation rate of CAF-based SCC-12B2 HSEs significantly decreased to 0.20 (±0.05, P < 0.05). NF-based SCC-13 HSEs showed a proliferation rate of 0.29 (±0.08), but when cultured on CAFs, proliferation decreased to 0.14 (±0.01), but this difference was not statistically significant (P = 0.06).

CAFs affect terminal differentiation but not BM-formation in human SCC HSE

Terminal differentiation of SCC-12B2 and SCC-13 in HSEs based on either NFs or CAFs was assessed by immunohistochemical staining of involucrin. In normal skin and in either NF- or CAFbased NHEK HSEs, involucrin was present in the subcorneal stratum granulosum and fades downwards in the stratum spinosum (data not shown). Involucrin was widely distributed in NF-based SCC-12B2 HSEs, in accordance with their characteristic morphological disorganization (Figure 5b). Involucrin staining decreased in both SCC-12B2 and SCC-13 HSEs when cultured on CAFs, indicating an overall decrease in terminal differentiation (Figure 5b). BM composition was assessed by immunohistochemical staining of collagen IV and laminin 332 (formerly known as laminin 5). In normal skin and HSEs based on either NFs of CAFs, both proteins were present in the BM, demarcating the epidermal–dermal lining (data not shown). In SCC-12B2 HSEs either based on NFs or CAFs, both collagen IV and laminin 332 marked several dermal–epidermal linings, including some of those in invasive areas (Figure 5c,d). In SCC-13 HSEs based on either NFs or CAFs, collagen IV was virtually absent (Figure 5c). Furthermore, these models showed scattered laminin 332 staining throughout their epidermal cell compartment, irrespective of whether NFs or CAFs were used in the HSE (Figure 5d).

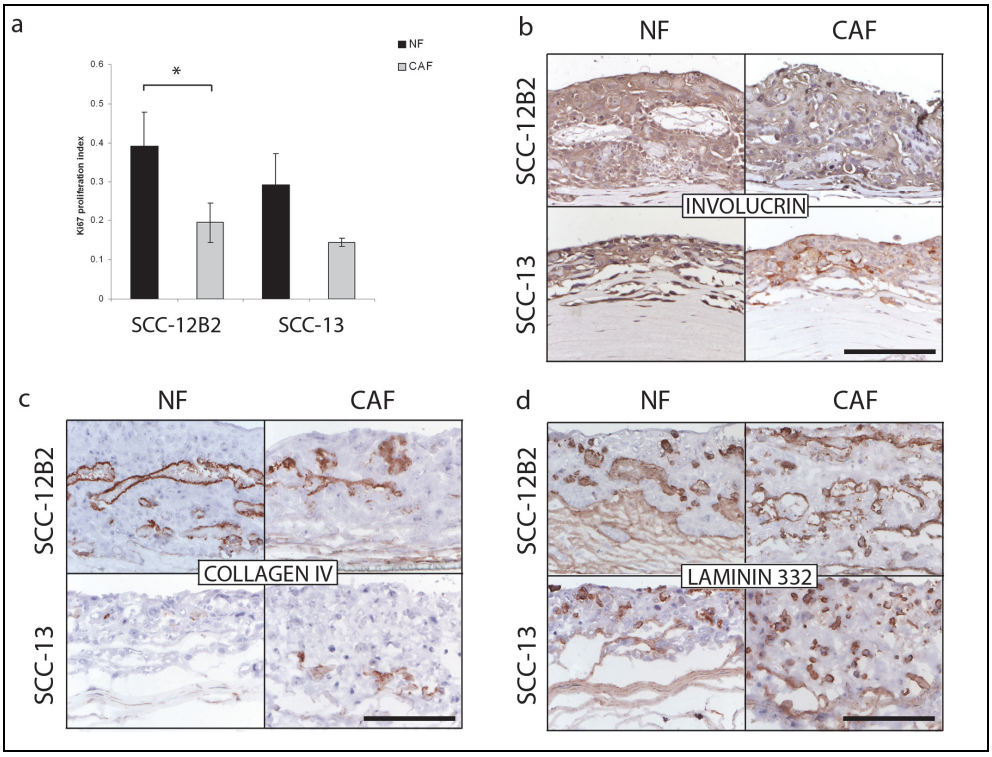

Figure 5 | Human skin equivalents (HSEs) of normal human epidermal keratinocytes (NHEK), SCC-12B2 and SCC-13 were cultured on a collagen matrix seeded with either normal fibroblasts (NFs) or cancer-associated fibroblasts (CAFs) and immunohistochemically stained for Ki67 (a), involucrin (b), collagen IV (c) and laminin 332 (d). Proliferation as quantified by Ki67 staining was lower in CAF-based HSEs than in NF-based HSEs (a, asterisk denotes $P < 0.05$). Collagen IV staining is virtually absent in SCC-13 HSEs (c) and staining of involucrin (b), collagen IV (c) and laminin 332 (d) was independent of NF or CAF in the collagen matrix. Scale bars indicate 200 µm.

Discussion

As significant players in the tumor microenvironment, CAFs have extensively been shown to promote tumor formation and progression in several epithelial tumors.[6, 9] This implies that CAFs are different from their normal counterpart fibroblasts that do not actively promote tumor formation and progression. However, studies on CAFs associated with cutaneous SCCs have never been published before. In this work, we showed that CAFs isolated from primary cutaneous SCCs have morphological characteristics (long, spindle shaped, no contact inhibition) that distinguish them from dermal NFs (short, star shaped, contact inhibition). These findings are in line with morphological characteristics of CAFs

originating from oral SCC reported earlier.[24] The heterogeneity we observed within groups of both CAFs and NFs originating from different donors may be explained by the fact that in general, fibroblasts occur in morphologically and functionally heterogeneous subpopulations, even within a single tissue.[25] This also holds for CAFs, which reflect the heterogeneity of the carcinoma they are associated with, corresponding to their various origins and physiological admixture with normal fibroblasts in various states of differentiation.[24, 26, 27] In addition, morphological CAF characteristics faded with increased passaging, limiting experimentation with these cells.

Furthermore, we showed that CAFs phenotypically differ from NFs by their increased proliferative, migratory and contractile properties. In particular, increased α-SMA expression is in agreement with earlier findings and is considered a CAF-marker, representing an activated stromal myofibroblast population.[24, 28] α-SMA was detected in all CAFs and only in a minor fraction of NFs. Functionality of α-SMA on CAFs was demonstrated by a contraction assay performed in an ECM-like collagen matrix, in which the CAFs contracted the matrix significantly more than NFs. Further research into specific cytoskeletal changes may elucidate differences in actual cell contractility of CAFs and NFs. Furthermore, CAFs showed significantly increased migration in a scratch assay, although a slight contribution of increased proliferation of the CAFs cannot be excluded.

Production of the ECM component pro-collagen type I was significantly increased in CAFs, physically supporting their increased proliferation and migration, as was shown earlier for wound healing myofibroblasts.[29] Increased ECM synthesis by CAFs may enhance tumor progression and invasion *in vivo*. This feature of skin CAFs may be utilized *in vitro*, as CAF-derived matrix can replace animal-derived or artificial dermal equivalents to further mimic the human microenvironment of cutaneous SCCs.[30, 31] As cutaneous SCCs are known to produce increased levels of matrix degrading enzymes (e.g. matrix metalloproteinase 10, MMP-10), an *in vitro* model system with CAF-derived ECM would allow for further investigating the interaction between skin carcinoma cells and the stroma.[32]

We have assessed the functional effects of CAFs on cutaneous SCC cell lines SCC-12B2 and SCC-13 in HSEs. SCC-12B2 keratinocytes characteristically show invasion when cultured in HSEs, which is significantly increased by CAFs. In literature, similar effects have been described for transformed oral keratinocytes and immortalized and genetically engineered oesophageal epithelial cells cultured in corresponding CAF-based HSEs.[33, 34] In SCC- 13 HSEs, CAFs increased dermal–epidermal detachment, which is a characteristic of this cell line when cultured in a HSE. The BM composition *in vitro* was not markedly affected by CAFs. The absence of collagen IV in SCC-13 HSEs fits the SCC-13 hallmark of dermal–

epidermal detachment. Furthermore, decreased involucrin staining as a marker of terminal differentiation corresponded with a general reciprocal correlation between carcinoma aggressiveness and differentiation.[35] Unexpectedly, CAFs decreased cellular proliferation of SCC cell lines in HSEs as marked by nuclear Ki67 staining after 2 weeks of culturing. This might be explained by CAF-induced microenvironmental changes other than those studied in this work, e.g., cellular senescence in or secretion of soluble factors by either epithelial or mesenchymal cells.[36]

In conclusion, fibroblasts associated with human cutaneous SCC differ from normal HSEs with respect to their morphological and functional characteristics, facilitating selection of living subpopulations of stromal SCC cells to study skin carcinogenesis *in vitro*. Invasion and dermal–epidermal detachment of SCC cell lines SCC-12B2 and SCC-13 increased under the influence of a CAFcontaining microenvironment. In this study, HSEs have proved useful in studying cutaneous SCC–stroma interactions *in vitro* and may serve as vehicles to develop refined therapeutics to SCC.

Acknowledgements

The authors thank J.N. Bouwes Bavinck, MD, PhD, and H.C. Wisgerhof, MD from the Department of Dermatology of the Leiden University Medical Center for providing the primary SCCs that were used for this study. In addition, the authors thank L. Eweje MSc from the Department of Drug Delivery Technology of the Leiden/Amsterdam Center for Drug Research for critically reading the paper.

References

1. Erb, P. et al. Role of apoptosis in basal cell and squamous cell carcinoma formation. *Immunol.Lett.* 100, 68-72 (2005).
2. Carucci, J.A. et al. In-transit metastasis from primary cutaneous squamous cell carcinoma in organ transplant recipients and nonimmunosuppressed patients: clinical characteristics, management, and outcome in a series of 21 patients. *Dermatol.Surg.* 30, 651-655 (2004).
3. Ulrich, C., Kanitakis, J., Stockfleth, E. & Euvrard, S. Skin cancer in organ transplant recipients--where do we stand today? *Am.J.Transplant.* 8, 2192-2198 (2008).
4. De Wever, O. & Mareel, M. Role of tissue stroma in cancer cell invasion. *J.Pathol.* 200, 429-447 (2003).
5. Orimo, A. et al. Stromal fibroblasts present in invasive human breast carcinomas promote tumor growth and angiogenesis through elevated SDF-1/CXCL12 secretion. *Cell* 121, 335-348 (2005).
6. Kalluri, R. & Zeisberg, M. Fibroblasts in cancer. *Nat.Rev.Cancer* 6, 392-401 (2006).
7. Lengyel, E. et al. Induction of M(r) 92,000 type IV collagenase expression in a squamous cell carcinoma cell line by fibroblasts. *Cancer Res.* 55, 963-967 (1995).
8. Sato, T. et al. Enhancement of membrane-type 1-matrix metalloproteinase (MT1-MMP) production and sequential activation of progelatinase A on human squamous carcinoma cells co-cultured with human dermal fibroblasts. *Br.J.Cancer* 80, 1137-1143 (1999).
9. Bhowmick, N.A., Neilson, E.G. & Moses, H.L. Stromal fibroblasts in cancer initiation and progression. *Nature* 432, 332-337 (2004).
10. Desmouliere, A., Guyot, C. & Gabbiani, G. The stroma reaction myofibroblast: a key player in the control of tumor cell behavior. *Int.J.Dev.Biol.* 48, 509-517 (2004).
11. Kellermann, M.G. et al. Myofibroblasts in the stroma of oral squamous cell carcinoma are associated with poor prognosis. *Histopathology* 51, 849-853 (2007).
12. Spaeth, E.L. et al. Mesenchymal stem cell transition to tumor-associated fibroblasts contributes to fibrovascular network expansion and tumor progression. *PLoS.One.* 4, e4992 (2009).
13. Liang, P. et al. Myofibroblasts correlate with lymphatic microvessel density and lymph node metastasis in early-stage invasive colorectal carcinoma. *Anticancer Res.* 25, 2705-2712 (2005).
14. Finak, G. et al. Stromal gene expression predicts clinical outcome in breast cancer. *Nat.Med.* 14, 518-527 (2008).
15. Kawashiri, S. et al. Significance of stromal desmoplasia and myofibroblast appearance at the invasive front in squamous cell carcinoma of the oral cavity. *Head Neck* 31, 1346-1353 (2009).
16. Li, Q., Huang, W. & Zhou, X. Expression of CD34, alpha-smooth muscle actin and transforming growth factor-beta1 in squamous intraepithelial lesions and squamous cell carcinoma of the cervix. *J.Int.Med.Res.* 37, 446-454 (2009).
17. Sappino, A.P., Skalli, O., Jackson, B., Schurch, W. & Gabbiani, G. Smooth-muscle differentiation in stromal cells of malignant and non-malignant breast tissues. *Int.J.Cancer* 41, 707-712 (1988).
18. Rheinwald, J.G. & Beckett, M.A. Tumorigenic keratinocyte lines requiring anchorage and fibroblast support cultures from human squamous cell carcinomas. *Cancer Res.* 41, 1657-1663 (1981).
19. Commandeur, S., de Gruijl, F.R., Willemze, R., Tensen, C.P. & El Ghalbzouri, A. An in vitro three-dimensional model of primary human cutaneous squamous cell carcinoma. *Exp Dermatol* 18, 849-56 (2009).
20. Ponec, M. et al. The formation of competent barrier lipids in reconstructed human epidermis requires the presence of vitamin C. *J.Invest Dermatol.* 109, 348-355 (1997).
21. El Ghalbzouri, A., Gibbs, S., Lamme, E., Van Blitterswijk, C.A. & Ponec, M. Effect of fibroblasts on epidermal regeneration. *Br.J.Dermatol.* 147, 230-243 (2002).
22. Nurmenniemi, S. et al. A novel organotypic model mimics the tumor microenvironment. *Am.J.Pathol.* 175, 1281-1291 (2009).
23. Nystrom, M.L. et al. Development of a quantitative method to analyse tumour cell invasion in organotypic culture. *J.Pathol.* 205, 468-475 (2005).
24. Liu, Y. et al. Separation, cultivation and biological characteristics of oral carcinoma-associated fibroblasts. *Oral Dis.* 12, 375-380 (2006).
25. Nolte, S.V., Xu, W., Rennekampff, H.O. & Rodemann, H.P. Diversity of fibroblasts--a review on implications for skin tissue engineering. *Cells Tissues.Organs* 187, 165-176 (2008).

26. Haviv, I., Polyak, K., Qiu, W., Hu, M. & Campbell, I. Origin of carcinoma associated fibroblasts. *Cell Cycle* 8, 589-595 (2009).
27. Sugimoto, H., Mundel, T.M., Kieran, M.W. & Kalluri, R. Identification of fibroblast heterogeneity in the tumor microenvironment. *Cancer Biol.Ther.* 5, 1640-1646 (2006).
28. Olumi, A.F. et al. Carcinoma-associated fibroblasts direct tumor progression of initiated human prostatic epithelium. *Cancer Res.* 59, 5002-5011 (1999).
29. Gabbiani, G. The myofibroblast in wound healing and fibrocontractive diseases. *J.Pathol.* 200, 500-503 (2003).
30. Amatangelo, M.D., Bassi, D.E., Klein-Szanto, A.J. & Cukierman, E. Stroma-derived three-dimensional matrices are necessary and sufficient to promote desmoplastic differentiation of normal fibroblasts. *Am.J.Pathol.* 167, 475-488 (2005).
31. El Ghalbzouri, A., Commandeur, S., Rietveld, M.H., Mulder, A.A. & Willemze, R. Replacement of animal-derived collagen matrix by human fibroblast-derived dermal matrix for human skin equivalent products. *Biomaterials* 30, 71-78 (2009).
32. Boyd, S. et al. MMP-10 (Stromelysin-2) and MMP-21 in human and murine squamous cell cancer. *Exp.Dermatol.* 18, 1044-1052 (2009).
33. Costea, D.E., Kulasekara, K., Neppelberg, E., Johannessen, A.C. & Vintermyr, O.K. Species-specific fibroblasts required for triggering invasiveness of partially transformed oral keratinocytes. *Am.J.Pathol.* 168, 1889-1897 (2006).
34. Okawa, T. et al. The functional interplay between EGFR overexpression, hTERT activation, and p53 mutation in esophageal epithelial cells with activation of stromal fibroblasts induces tumor development, invasion, and differentiation. *Genes Dev.* 21, 2788-2803 (2007).
35. Cassarino, D.S., Derienzo, D.P. & Barr, R.J. Cutaneous squamous cell carcinoma: a comprehensive clinicopathologic classification. Part one. *J.Cutan.Pathol.* 33, 191-206 (2006).
36. Parkinson, E.K. Senescence as a modulator of oral squamous cell carcinoma development. *Oral Oncol.* 46, 840-853 (2010).

4

Replacement of animal-derived collagen matrix by human fibroblast-derived dermal matrix for human skin equivalent products

Abdoelwaheb El Ghalbzouri, Suzan Commandeur, Marion H. Rietveld, Aat A. Mulder and Rein Willemze

Department of Dermatology, Leiden University Medical Center, Leiden, the Netherlands

Biomaterials 2009;30(1):71-78

Abstract

Reconstructed human skin equivalents (HSEs) are representative models of human skin and widely used for research purposes and clinical applications. Traditional methods to generate HSEs are based on the seeding of human keratinocytes onto three-dimensional human fibroblast-populated non-human collagen matrices. Current HSEs have a limited lifespan of approximately 8 weeks, rendering them unsuitable for long-term studies. Here we present a new generation of HSEs being fully composed of human components and which can be cultured up to 20 weeks. This model is generated on a primary human fibroblast-derived dermal matrix. Pro-collagen type I secretion by human fibroblasts stabilized during long-term culture, providing a continuous and functional human dermal matrix. In contrast to rat-tail collagen-based HSEs, the present fibroblast-derived matrix-based HSEs contain more continuity in the number of viable cell layers in long-term cultures. In addition, these new skin models exhibit normal differentiation and proliferation, based on expression of keratins K10/K15, and K16/K17, respectively. Detection of collagen types IV and VII and laminin 332 was confined to the epidermal–dermal junction, as in native skin. The presence of hemidesmosomes and anchoring fibrils was demonstrated by electron microscopy. Finally, we show that the presented HSE contained a higher concentration of the normal moisturizing factor compared to rat-tail collagen-based skin models, providing a further representation of functional normal human skin *in vitro*. This study, therefore, demonstrates the role of the dermal microenvironment on epidermal regeneration and lifespan *in vitro*.

Introduction

Human skin equivalents (HSEs), also designated as organotypic co-cultures, are three-dimensional culture systems that are generated by seeding human keratinocytes onto a dermal equivalent that is usually seeded with human fibroblasts. Under specific culture conditions, a HSE is formed that shows high similarity with the native tissue from which it was derived.[1-6] HSEs have the advantage that they can harbor different cell types (keratinocytes, melanocytes, fibroblasts, etcetera) that are surrounded by a local microenvironment resembling the *in vivo* situation, and in which cellular processes are normalized compared to conventional monolayer cultures. HSEs are an attractive tool for pharmacotoxicological testing and to study cell–cell, cell–matrix and dermal–epidermal interactions. However, current HSEs have a limited lifespan of approximately 8 weeks due to high contractility of the dermal matrix and resulting poor epidermal homeostasis, rendering them unsuitable for long-term studies. Long-lived HSEs that can be cultured beyond 8 weeks would allow for studies focusing on the effects of long-term exposition to various exogenous stressors. Also, the effects on skin homeostasis and skin cancer by application of physiologically low doses of chemicals or substances can be studied in long-lived skin models in contrast to skin models with a limited lifespan of 8 weeks.

Furthermore, the quality of current HSEs may be compromised by the fact that they are largely based on non-human dermal equivalents e.g. collagen originating from rat or bovine tendon, and bovine fibrin. These non-human biopolymers allow for successful HSE formation, but they still render the dermal compartment an incomplete approach to human extracellular matrix (ECM) *in vivo*, which contains lipids, fibrin, glycosaminoglycans and proteoglycans in addition to collagen as its main substituent. Although the use of human de-epidermized dermis (DED) may offer a human alternative to these animal-derived dermal equivalents, the application of this method is limited by uncontrollable variation in DED thickness and low availability of the native tissue. In addition, all dermal equivalents mentioned serve as exogenous scaffolds that need to be seeded with fibroblasts in order to provide a microenvironment permissive of HSE formation, thereby increasing their artificial character. In contrast, the generation of long-lived HSEs presented here is based on human fibroblast-derived matrices (FDMs) as dermal equivalents.

During tissue homeostasis and repair, fibroblasts synthesize, organize and maintain connective tissue through ECM production and remodeling. This essential function of fibroblasts can be utilized *in vitro* to produce solely cell-based dermal equivalents. *In vitro* modulation of various culture conditions resulted in a microenvironment enabling the

production of FDMs.[7-9] In these cultures, multilayered human fibroblasts are stimulated towards high ECM accumulation, fibrillar fibronectin organization, and the formation of actin stress fibers.[10] The main stimulating additive in these cultures is ascorbic acid, which promotes the *in vitro* processing of pro-collagen to collagen a-chains. The morphological, biochemical and physical characteristics of the resulting FDMs are superior to those of fibroblast-populated reconstituted ECMs.[7, 9] This is supported by the fact that collagen fibril bundle assembly is featured by ECM biosynthesis, since fibroblasts seeded in isolated biopolymers do not form collagen fibril bundles whereas fibroblasts producing their own matrix do form these important structural elements of a fully functional ECM.[8] Although the development of isolated FDMs was established in earlier research as mentioned above, by seeding keratinocytes on these FDMs, a new generation of long-lived HSEs is established, harboring only human cell-derived components. This change in the local microenvironment of these FDM-based HSEs has the potential to improve cell–matrix interactions and maintenance of a functional stem cell compartment, rendering the full human HSEs suitable for long-term studies *in vitro*. We here present a comparison between the newly developed long-lived FDM-based HSEs and established HSEs, focusing on their morphology, ECM production, differentiation and proliferation, ultrastructural basement membrane formation, barrier function and lifespan.

Methods

Cell culture

For isolation of normal human epidermal keratinocytes (NHEKs), epidermis was obtained through overnight incubation of fresh mamma reduction surplus skin with dispase II (Roche Diagnostics, Almere, the Netherlands). NHEKs were isolated from the epidermis through incubation with trypsin at 37°C for 15 min. After trypsin inactivation, the cells were filtered using a 70 µm cell strainer (BD Biosciences, Breda, the Netherlands), and cultured in keratinocyte medium at 37°C and 7.3% CO_2 until subconfluency. Keratinocyte medium consisted of 3 parts Dulbecco's modified Eagle's medium (DMEM, Gibco/Invitrogen, Breda, the Netherlands) and 1 part Ham's F12 medium supplemented with 5% fetal bovine serum (FBS, HyClone/Greiner, Nürtingen, Germany), 0.5 µM hydrocortisone, 1 µM isoproterenol, 0.1 µM insulin (Sigma–Aldrich, Zwijndrecht, the Netherlands), 100 U/ml penicillin and 100 mg/ml streptomycin (Invitrogen, Breda, the Netherlands). In all experiments, secondary cultures were used. For isolation of normal human dermal fibroblasts (NHDFs), human dermis was obtained through overnight incubation of fresh mamma reduction surplus skin with dispase II. NHDFs were isolated from the dermis by incubation with a solution consisting of collagenase II (Invitrogen) and dispase II (ratio 1:3 and 3 ml/g dermis) at 37°C for 2h. The cells were filtered using a 70 µm

cell strainer, and cultured in fibroblast medium at 37°C and 5% CO_2 until subconfluency. Fibroblast medium consisted of DMEM supplemented with 5% FBS, 100 U/ml penicillin and 100 mg/ml streptomycin. Culture medium was refreshed every 3 days. In all experiments, secondary or tertiary cultures were used.

Dermal equivalents

Fibroblast-derived matrices (FDMs) were generated by seeding $6x10^5$ NHDFs into polyester permeable supports (6 well plates with 0.4 µm pore size Transwell inserts, Corning Incorporated, Schiphol-Rijk, the Netherlands). The FDMs were cultured for 3 weeks in fibroblast medium supplemented with 100 mg/ml ascorbic acid phosphate (Sigma–Aldrich) under submerged conditions and the culture medium was refreshed every 2 days. Rat-tail collagen matrices were constructed as described earlier [3]. In brief, acetic acid extracted rattail collagen was seeded with $1.2x10^5$ NHDFs on the same polyester permeable supports as the FDMs and incubated for a period of 1 week with unsupplemented fibroblast medium under submerged conditions.

Human skin equivalents

Human skin equivalents were generated by seeding $4x10^5$ NHEKs onto the FDMs and NHDF-seeded rat-tail collagen matrices that were prepared in advance. Cultures were incubated overnight in keratinocyte medium as described above, supplemented with 1% FBS, 53 µM selenious acid, 10 µM L-serine, 10 µM L-carnitine, 1 µM DL-α-tocopherol-acetate, 100 mg/ml ascorbic acid phosphate, $2.4x10^5$ M bovine serum albumin and a lipid supplement containing 25 µM palmitic acid, 15 µM linoleic acid and 7 µM arachidonic acid (Sigma–Aldrich). The cultures were then lifted to the air–liquid interface in supplemented keratinocyte medium as described above, except for the fact that FBS was omitted, the concentration of linoleic acid was increased to 30 µM and ascorbic acid phosphate was halved to 50 mg/ml. Medium was refreshed every 2 days. FDM-based HSEs were processed for analysis after 1, 2, 3, 4, 6, 8, 13, 18 and 20 weeks of air-exposed culture. Rat-tail collagen-based HSEs were processed for analysis after 2 and 8 weeks of air-exposed culture.

Protein determination by enzyme-linked immunosorbent assay

Quantification of human pro-collagen type I in the culture medium of FDM-based HSEs was performed by enzyme-linked immunosorbent assay (MetraCICP ELISA kit; Quidel Corporations, CA, USA). Culture medium of FDM-based HSEs was collected at each refreshment throughout the entire culture period, starting at the moment of fibroblast seeding, 3 weeks prior to seeding of keratinocytes. Measurements and data analysis were performed according to the manufacturer's procedure. The data are expressed as ng/ml

culture medium with standard deviations resulting from triplicate measurements of specimens originating from three independent cultures.

Morphological and immunohistochemical analyses

All cultures were washed in PBS. One half of each culture was snap-frozen in liquid nitrogen while the other half was fixed in 4% paraformaldehyde, dehydrated and paraffin embedded. Global morphological analysis was performed on 5 µm formalin-fixed paraffin-embedded sections through staining with haematoxylin and eosin (HE). Immunohistochemical analysis of keratins 10, 15, 16 and 17, involucrin, Ki67, laminin 332 and collagen types IV and VII, was performed on 5 µm frozen sections of the FDM-based HSEs, which were air dried overnight and fixed in acetone for 10 min. Specifications of the primary antibodies used in this study are listed in Table 1. After incubation with primary antibodies, sections were processed as previously described using the biotin–streptavidin system.[11] Secondary antibodies included FITC-conjugated goat anti-mouse IgG (Dako Cytomation, Glostrup, Denmark) and Cy3-conjugated goat anti-mouse IgG (Jackson ImmunoResearch Laboratories, Cambridgeshire, UK). All sections were counterstained with 40,6-diamidino-2-phenylindole, dihydrochloride (DAPI; Molecular Probes, Invitrogen). Sections were mounted with Vectashield (Brunschwig chemie, Amsterdam, the Netherlands) and coverslipped.

Estimation of proliferation index

The proliferation index was determined by counting the number of Ki67-positive nuclei among the total number of basal cells. A minimum of 100 cells were counted at immunofluoresence level (magnification 200×) at three different regions in each section. The resulting data are expressed as the mean of two independent experiments ±SD.

Table 1 | Primary anitbodies used for immunohistochemical staining of tissue sections.

Antigen (clone)	Source*
K10 (DE-K10)	ICN Biomedicals Inc., Ohio, USA
K15 (LHK 15)	Neomarkers, Fremont, USA
K16 (LLOO25)	Dr. I.M. Leigh, London, England
K17 (CK-E3)	Sigma, Saint Louis, Missouri, USA
Involucrin (SY5)	Sanbio B.V. Uden, The Netherlands
Ki67 AB-2 (Mb67)	Neomarkers, Union, CA, USA
laminin 332 (MB165)	Dr. M. Aumailley, Cologne, Germany
Type IV collagen (PHM12)	Chemicon, Temecula, USA
Type VII collagen (LH7.2)	Dr. I.M. Leigh, London, England

* Antibodies not purchased from indicated sources were personal gifts from the investigator named.

Electron microscopy

Cultures were cut into small blocks of 1 mm^3 and fixed in 2% paraformaldehyde/2.5% glutaraldehyde in 0.1M sodium cacodylate buffer with pH 7.4. After fixation for 1h at room temperature, specimens were rinsed in PBS 3 times, and post-fixed in 1% osmiumtetroxide in cacodylate buffer, pH 7.4 for 1h at 4 °C. After rinsing 3 times in PBS specimens were dehydrated in an ethanol series up to 100% and embedded in epoxy resin LX-112. Ultrathin sections were prepared, and after staining with uranylacetate and lead hydroxide, sections were observed and recorded using a Philips CEM10 electron microscope (Philips, Eindhoven, the Netherlands).

Semi-quantitative measurement of natural moisturizing factor in the stratum corneum

Using confocal Raman spectroscopy, the molecular concentration profile of natural moisturizing factor (NMF) in the stratum corneum of the HSEs was measured semi-quantitatively. All experiments have been performed by RiverDiagnostics (Rotterdam, the Netherlands). In brief, 1 cm^2 fragments of both HSEs cultured for 8 weeks and normal human skin samples were placed with their stratum corneum touching the surface of the measurement window of the skin analyzer. Optimal spectral acquisition times and depth ranges were determined carefully. Per skin sample, a minimum of 10 Raman depth profiles were measured. Per volunteer or skin model (n=2) a minimum of ten profiles were measured per location. Data analysis was performed by RiverDiagnosts and discussed with our laboratory. Analyses were focused on extracting information regarding molecular NMF concentration profiles in the stratum corneum. The profile was represented in ASCII tables containing a depth axis and relative molecular concentrations. The profile data were represented in Microsoft Excel graphs to compare the relative composition at various depths between cultured HSEs and native human skin. The Raman spectrophotometer had a spectral range of 400–4500 cm^{-1} and a spectral resolution <5 cm^{-1}. The depth resolution was <5 µm and the sensitivity signal throughput from skin to detector was >50% over the entire spectral range.

Statistics

Statistical significance was determined using two-tailed Student's *t* test.

Results

Microenvironment in the dermal matrix

In HSEs generated with rat-tail collagen as the main constituent of the dermal compartment, NHDFs are surrounded by a high concentration (3.2 mg/ml) of collagen type I and collagen fibers, while in HSEs generated with fibroblast-derived matrix (FDM), NHDFs are surrounded by their own secreted ECM (Figure 1). To evaluate the effect of the altered microenvironment, different aspects of these skin models were compared. First, we have evaluated the number of viable cell layers during the culture period. After 2 weeks of culture, differences were observed in the number of viable cell layers, as FDM-based HSEs consisted of 4–5 viable cell layers (Figure 2a), while rat-tail collagen-based HSEs consisted of 7–8 viable cell layers (Figure 2d). In both skin models the stratum basale, stratum granulosum, stratum spinosum and the stratum corneum were present. A remarkable observation was done in long-term cultures of these models. After 13 weeks of culture, the number of viable cell layers in human FDM-based HSEs remained constant at the initial level (3–5 cell layers, Figure 2b) and decreased to approximately 3 cell layers after

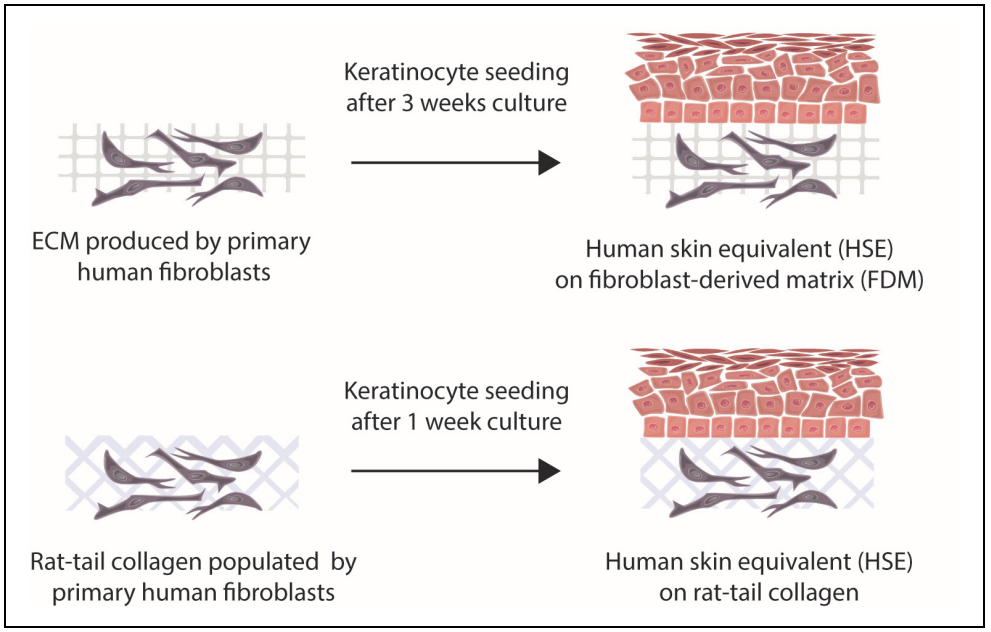

Figure 1 | Schematic representation of the two human skin equivalents (HSEs) investigated in this study. HSEs based on human fibroblast-derived extracellular matrix (ECM) are cultured 3 weeks prior to seeding the keratinocytes, while HSEs based on rat-tail collagen are seeded only 1 week prior to seeding the keratinocytes. After culturing the HSEs at the air–liquid interface, a fully stratified epidermis is formed irrespective of the dermal matrix.

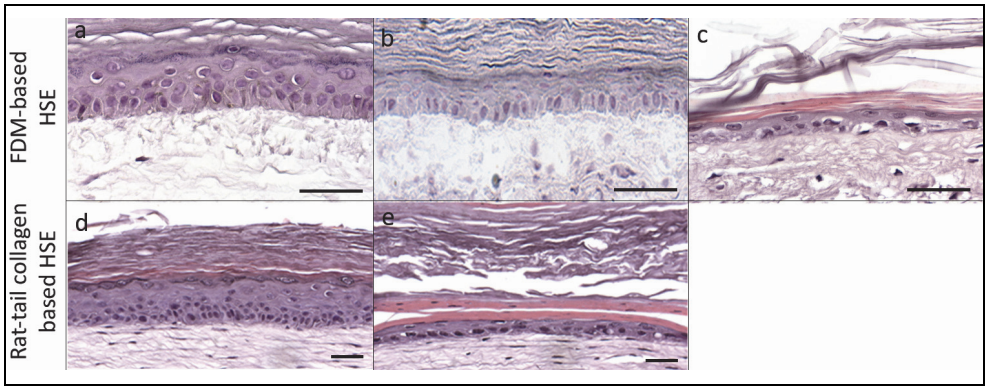

Figure 2 | Epidermal lifespan is modulated by the microenvironment in the dermal matrix. Human keratinocytes were cultured at the air–liquid interface on fibroblast-derived matrices (a–c) or rat-tail collagen matrices populated with fibroblasts (d, e) for 2 weeks (a, d), 8 weeks (e), 13 weeks (b) or 20 weeks (c). Haematoxylin–eosin (HE) stained cross-sections demonstrate the differences in epidermal thickness in culture time. Scale bar: 25 µm.

20 weeks of culture (Figure 2c). Rat-tail collagen-based HSEs cultured for 8 weeks showed a decrease in the number of viable cell layers (4–5 cell layers, Figure 2e) but could not be cultured beyond 8 weeks. These observations indicate that the dermal microenvironment influences epidermal lifespan *in vitro*.

Pro-collagen type I excretion in fibroblast-derived matrix-based HSEs

Pro-collagen type I was measured in culture medium collected during the first 8 weeks of FDM-based HSEs in the absence of growth factors. NHEKs were added after 3 weeks. Measurements were performed 2 weeks prior to NHEK seeding, at the moment of NHEK seeding and 2, 4, 6 and 8 weeks after NHEK seeding. A significant increase in pro-collagen type I secretion was measured during the culture period up to the fourth week (945 ±72 ng/ml), after which the production decreased to the level prior to seeding the keratinocytes (week 0) (284 ±32 ng/ml) (Figure 3). From this experiment we concluded that after three weeks of FDM preparation sufficient pro-collagen (233 ±7 ng/ml) has been secreted by the NHDFs to form a dermal equivalent on which NHEKs could be successfully seeded.

Keratinocyte proliferation in fibroblast-derived matrix-based HSEs

The expression of hyperproliferation-associated protein keratins 16 and 17 (K16, K17) was assessed to evaluate the activation status of the epidermis generated on fibroblast-derived matrices. These proteins were not detected in FDM-based HSEs irrespective of the

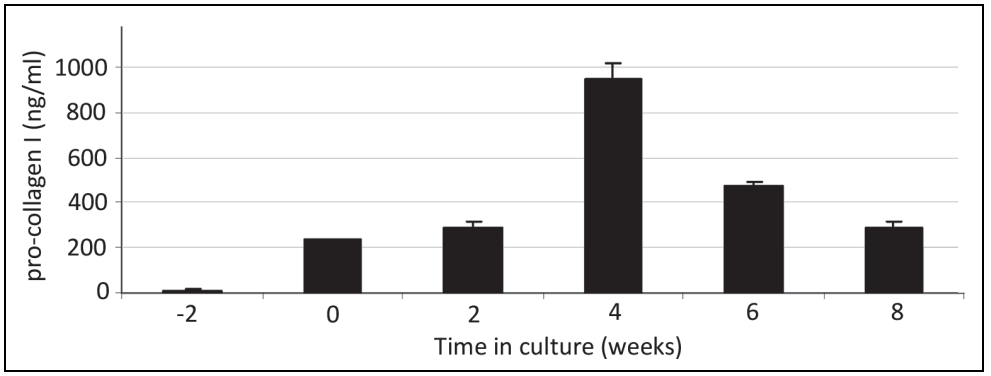

Figure 3 | Quantification of pro-collagen type I secretion into the culture medium of fibroblast-derived matrix (FDM)-based human skin equivalents (HSEs). Concentrations of pro-collagen I in the culture medium were determined by ELISA 2 weeks prior to keratinocyte seeding (t=-2), at keratinocyte seeding (t=0) and 2, 4 6 and 8 weeks after keratinocyte seeding. Bars represent means with standard deviations of triplicate measurements performed in three independent cultures.

culture period (Figure 4a). However, at the periphery of these cultures, K16 and K17 are expressed irrespective of the culture period, indicating cellular activity in migrating keratinocytes (Figure 4b). In previous studies we have shown that the abovementioned proteins K16 and K17 are similarly expressed in rat-tail collagen-based HSEs when they are cultured up to 4 weeks.[12] In addition, we have shown that the expression of these markers was modulated by the number of NHDFs incorporated in the rat-tail collagen matrix.[3] In order to further monitor the proliferation status of the NHEKs cultured on FDMs, we evaluated the proliferation index, expressed as the number of Ki67-positive cells in the basal cell layer of FDM-based HSEs. After 1 week of culture, the proliferation index was 15 ±7%, which decreased to 12±4% in the fourth week of culture, which is similar as in native tissue (12 ±3%) (Fig. 5) and rat-tail collagen-based HSEs.[12] After the fourth week, the proliferation index further decreased and remained stable around 5 ±3% in weeks 6, 8 and 13, to decrease to 3 ±1% after 18 weeks (Fig. 5).

Differentiation in fibroblast-derived matrix-based HSEs

To examine whether epidermal differentiation is affected by the dermal microenvironment, the presence of various protein markers specific for keratinocyte differentiation has been monitored by immunohistochemistry throughout the culture period of the FDMbased HSEs. Expression of the early differentiation marker keratin 10

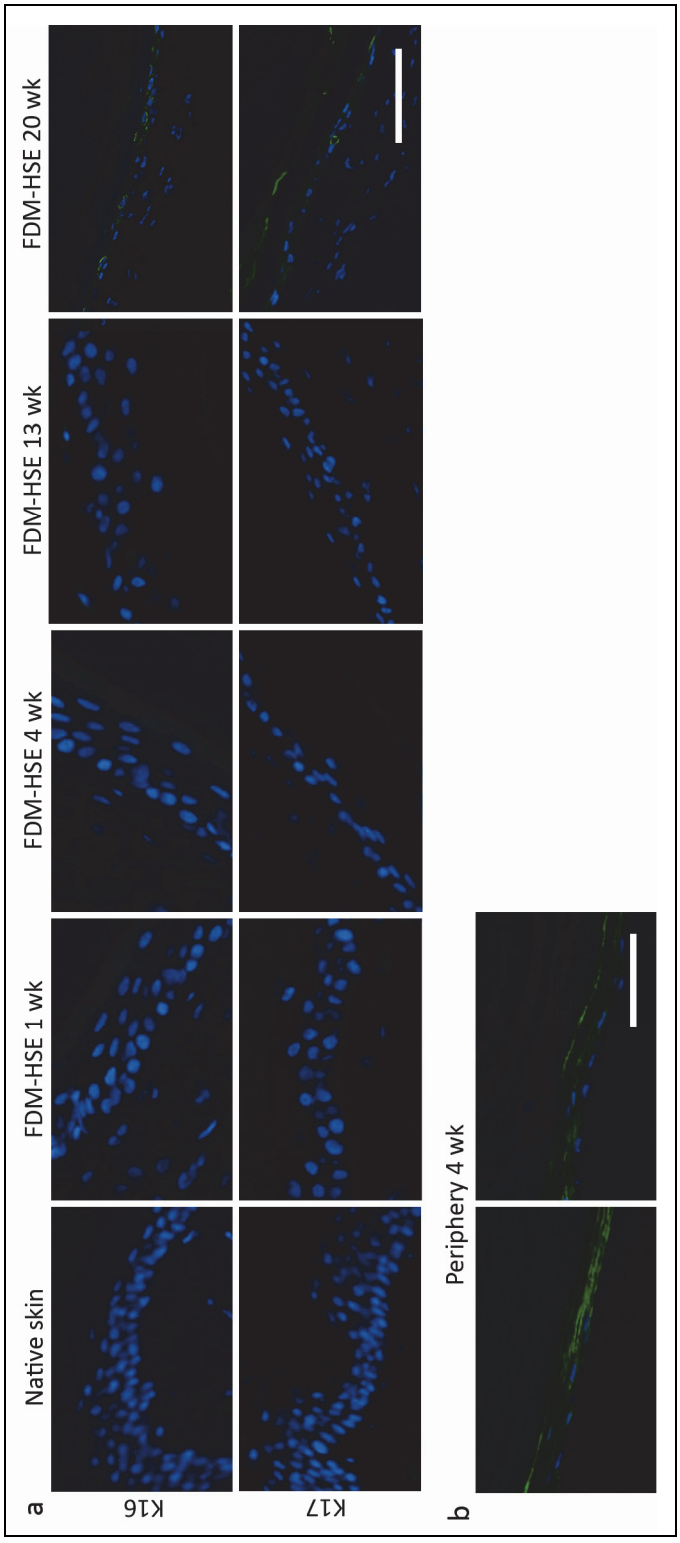

Figure 4 | Immunohistochemical detection of hyperproliferation-associated markers in fibroblast-derived matrix (FDM) based human skin equivalents (HSEs) cultured for longer periods. Human keratinocytes were cultured for 1, 4, 13 and 20 weeks at the air–liquid interface on FDMs. Immunofluorescence staining on cross-sections demonstrate that K16 and K17 are virtually absent in native skin and in FDM-based HSEs cultured for longer periods up to 20 weeks (a). At the periphery of the cultures these keratins are expressed irrespective of culture period, as shown in the periphery of 4-week old cultures (b). Scale bars: 25 µm.

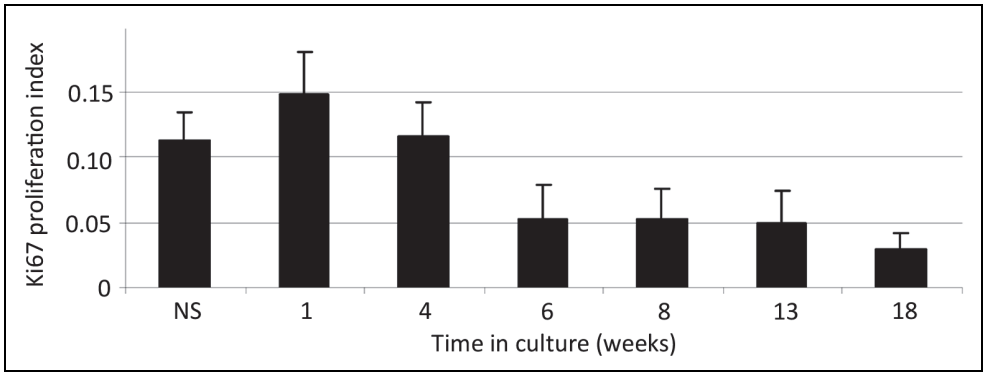

Figure 5 | Detection of proliferation-specific marker Ki67 in human fibroblast-derived matrix (FDM) based human skin equivalents (HSEs). Human keratinocytes were cultured for 1, 4, 6, 8, 13 and 18 weeks at the air–liquid interface on FDMs. The percentage of Ki67-positive cells in these cultures was determined by counting the number of Ki67-positive cells among the total number of basal cells. The resulting data are expressed as the mean of two independent cultures (±SD).

(K10) was only observed in the suprabasal cell layers throughout the entire culture period up to 13 weeks, similar to the native situation (Figure 6) and rat-tail collagen-based HSEs.[3] The basal epithelial marker keratin 15 (K15) was expressed in all basal cell layers as found in native tissue and rat-tail collagen-based HSEs,[13] while the expression of the terminal differentiation marker involucrin changed during culture (Figure 6). Involucrin is normally expressed in the stratum granulosum of native skin and rat-tail collagen-based HSEs,[3] as observed in FDM-based HSEs cultured for 1 week. However, involucrin expression shifted also to the stratum spinosum when FDM-based HSEs were cultured up to 13 weeks or longer (Figure 6).

Basement membrane composition in fibroblast-derived matrix-based HSEs

To evaluate to what extent the basement membrane is formed in FDM-based HSEs, we performed transmission electron microscopy of FDM-based HSEs that were cultured for 13 weeks and performed protein staining of collagen types IV and VII and laminin 332. The transmission electron microscopy recording revealed that the human fibroblasts synthesized new collagen fibers and that the dermal–epidermal junctions exhibit a continuous basement membrane with lamina lucida, lamina densa, regular hemidesmosomes and anchoring fibers (Figure 7). Immunoflurescence analysis showed

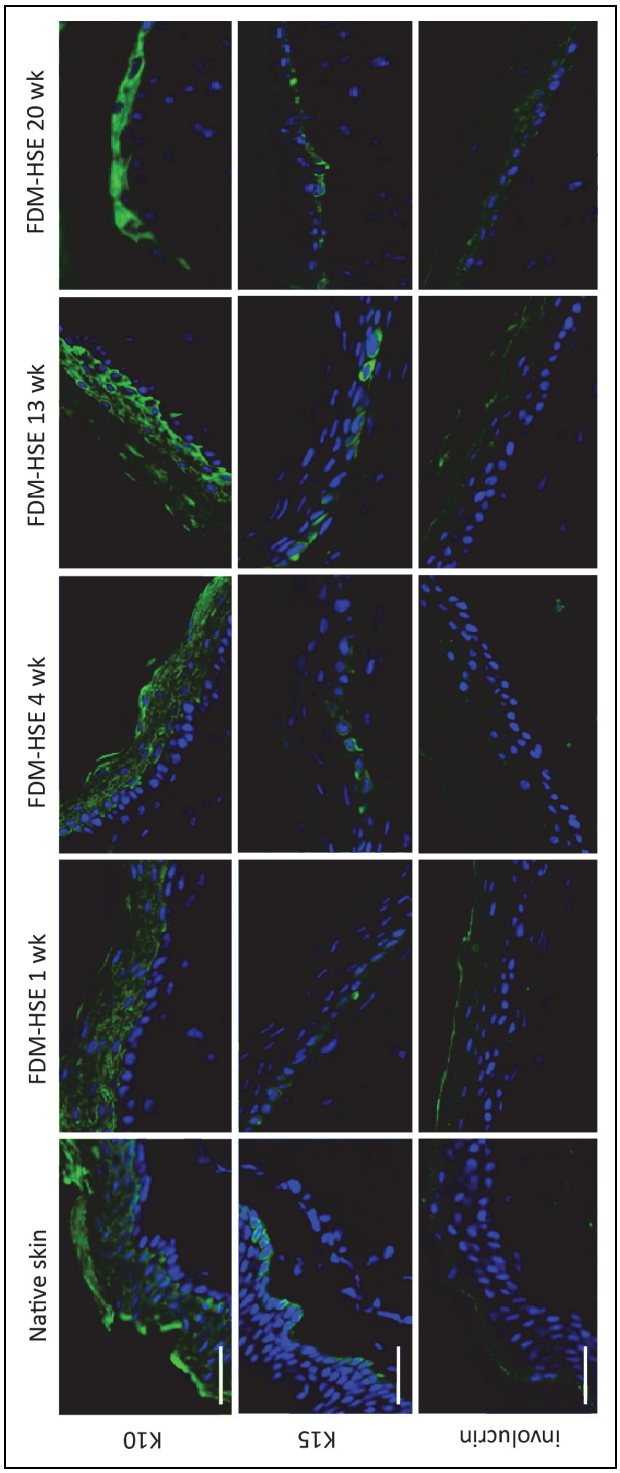

Figure 6 | Expression of differentiation-specific markers in fibroblast-derived matrix (FDM) based human skin equivalents (HSEs) cultured for longer periods. Human keratinocytes were cultured for 1, 4, 13 and 20 weeks at the air–liquid interface on FDMs. Immunofluorescence staining on cross-sections demonstrate that K10 and K15 are expressed as in native skin and that involucrin expression is altered in long-term cultures (13 weeks). Scale bars: 25 µm.

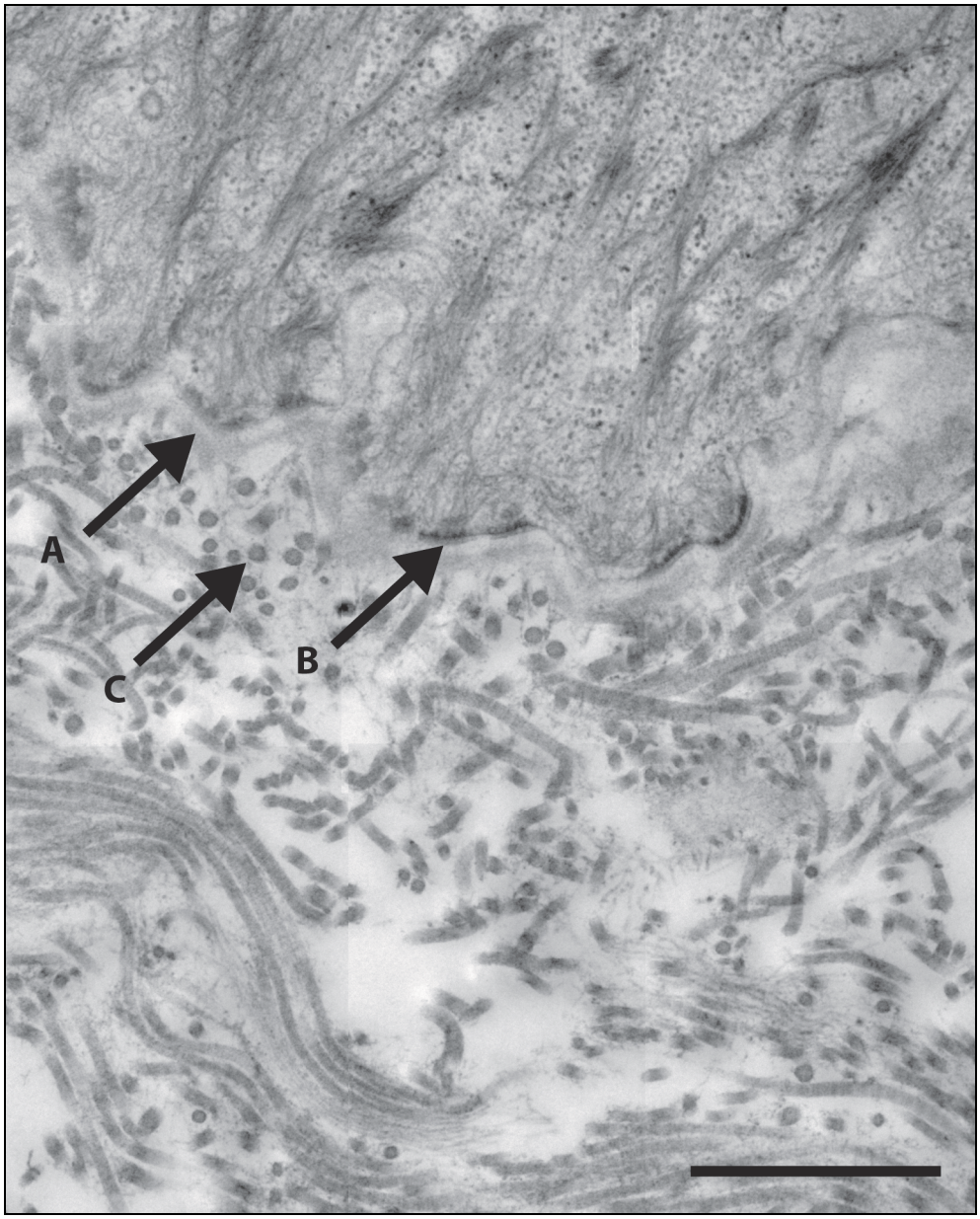

Figure 7 | Ultrastructure of human fibroblast-derived matrix (FDM) based human skin equivalents (HSEs) assessed by transmission electron microscopy. Human keratinocytes were cultured for 13 weeks at the air–liquid interface on FDMs. An overview is shown of the presence of the epidermal and dermal compartment in an FDM-based HSE, containing dermal–epidermal junctions with lamina lucida, laminin densa (A) and regular hemidesmosomes (B). The uniform collagen fibrils indicate their normal processing and proper assembly (C). Scale bar: 1 µm.

irrespective of the culture period, laminin 332 and collagen types IV (data not shown) and VII were all confined to the epidermal–dermal junction, similar to native tissue (Figure 8) and rat-tail collagen-based HSEs.[14] In FDM-based HSEs cultured for 4 weeks similar results were observed (data not shown).

NMF concentration of fibroblast-derived matrix-based HSEs and rat-tail collagen-based HSEs

After evaluation of morphology, proliferation and differentiation status and basement membrane composition in short- and longterm FDM-based HSEs, the concentration of the molecular constituent natural moisturizing factor (NMF), that is essential in skin barrier function, was measured in the stratum corneum of these models in comparison to rat-tail collagen-based HSEs and normal skin. Through this measurement, we assessed the skin barrier function of FDM-based and rat-tail collagen-based HSEs, which depends on proper moisturization, lipid balance, and the presence of humectants, which are the main constituents of NMF. Using confocal Raman spectroscopy the molecular concentration profile for this component was measured in FDM-based HSEs, rattail collagen-based HSEs and normal skin. In normal skin, the NMF reached a relative concentration of 1.2 normalized to keratin, while this constituent was virtually absent in rat-tail collagen-based HSEs (Figure 9). FDM-based HSEs contained an NMF concentration that was 2.5 times lower than in normal skin, but that widely exceeded that of rat-tail collagen-based HSEs (Figure 9).

Discussion

Reconstructed HSEs are widely used by scientists and industry for research purposes and for clinical applications in regenerative medicine. The epithelial–mesenchymal interactions in these skin equivalents are of crucial importance to the quality and functional reliability of the reconstructed epidermis. Therefore, a number of studies focused on the generation and optimization of new threedimensional cell culture matrices to establish better representation of the geometry, chemistry and signalling environment of the native ECM.[15] For dermal scaffold generation, various cellbased approaches have been used to improve epidermal regeneration.[16-18] The dermal matrix presented by Stark et al. consisted of a scaffold consisting of hyaluronic acid fibers and fibrin gel in which fibroblasts were embedded and on which the seeded keratinocytes formed a full epidermal architecture with normalized differentiation status which lasted for a minimum of 12 weeks.[19] Still, the most general used dermal matrix is the collagen matrix, in which the collagen can be of rat or bovine origin. However, the use of fibroblast-populated collagen matrix for long-term studies is hampered by its limited lifespan due to high

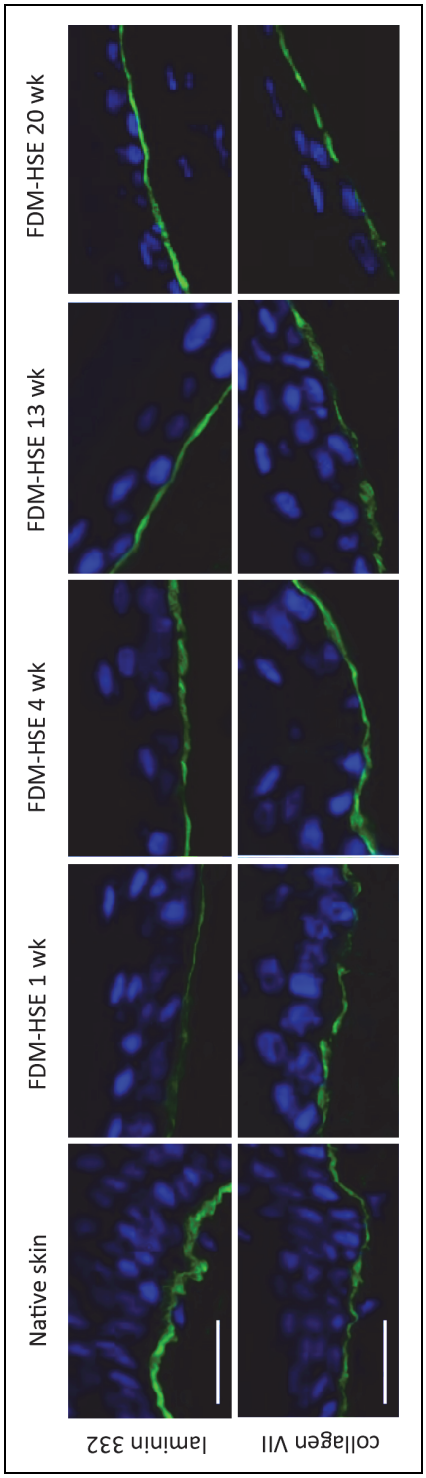

Figure 8 | Detection of basement membrane proteins in human fibroblast-derived matrix (FDM) based human skin equivalents (HSEs) cultured for longer periods. Human keratinocytes were cultured for 1, 4, 13 and 20 weeks at the air–liquid interface on FDMs. Immunofluorescence staining on cross-sections demonstrate that laminin 332 and collagen type VII are expressed at the dermal-epidermal junction, irrespective of the culture period of the FDM-based HSEs. Scale bar: 25 µm.

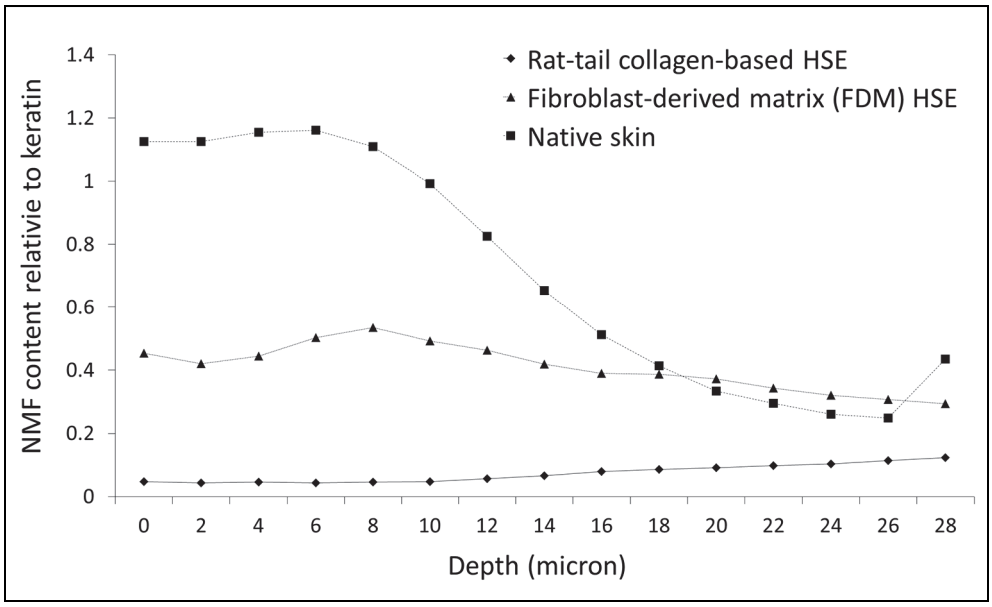

Figure 9 | Semi-quantitative concentration profiles of natural moisturizing factor (NMF) in the stratum corneum of two rat-tail collagen-based human skin equivalents (HSEs) cultured for 8 weeks, two human fibroblast-derived matrix (FDM) based HSEs cultured for 8 weeks, and the forearm of two volunteers (*in vivo* skin) as determined by Raman spectroscopy. NMF was virtually absent in rat-tail collagen-based HSEs (dots), while FDM-based HSEs contained an NMF concentration (triangles) that was 2.5 times lower than in normal skin (squares).

contractibility resulting in poor epidermal homeostasis *in vitro*. The extent of contraction is dependent on the collagen concentration, the number of fibroblasts present in the matrix, and the culture time of the matrices prior to seeding of keratinocytes.[12] To avoid contraction of the dermal compartment, non-contractile matrices can be used such as the natural substrate DED. However, since its uncontrollable variation in thickness, consistent experiments are hard to realize with this substrate. Another impediment is the short lifespan of DED-based skin models. After 8–10 weeks of culture, these skin models have an epidermis harboring only one or two viable cell layers, rendering them unsuitable for long-term studies pertaining to e.g. skin aging and UV carcinogenesis.

In this study we presented a fully human fibroblast-derived matrix (FDM), consisting of human ECM secreted *in vitro* by primary normal human dermal fibroblasts. Using this approach we observed that under specialized circumstances primary human fibroblasts secreted ECM components during the whole culture period with a maximum production of pro-collagen type I in the seventh culture week, being the fourth week after seeding of

normal human epidermal keratinocytes, after which the secretion remains steady up to the eleventh week. This observation indicates that the maximum production of pro-collagen I is linked to maximum cell confluency on the filter insert. An eventual proliferation stop results in stagnation of collagen production starting from week 11. Cross-sections of FDM-based HSEs also revealed epidermal differences when compared to rat-tail collagen-based HSEs. After 2 weeks culture, the epidermis generated on rat-tail collagen-based HSEswas reduced very fast until only 3–4 cell layers were left in the eighth week, while the epidermis generated on FDM-based HSEs maintained its 4–5 viable cell layers up to 13 weeks of culture and slightly decreases to approximately 3 viable cell layers after 20 weeks of culture. These observations emphasize the importance of the microenvironment surrounding the fibroblasts. One could speculate that the keratinocytes cultured on animal-derived collagen may loose their self-renewal capacity due to improper maintenance of the interfollicular stem cell compartment. The proliferative and tissue renewal characteristics of epidermal stem cells (ESCs) of the skin have been clearly demonstrated.[20] Rarely dividing ESC and proliferative progenitor cells play a central role in tissue renewal and repair.[21] Progenitor cells and ESC adhere differentially to ECM components such as collagen type IV and fibronectin, suggesting a stem cells niche with tight adherence to the ECM-rich basement membrane.[22, 23] Among different stem cell markers, cytokeratin 15 (K15) was found to mark putative stem and progenitor cells in the tip of the rete ridges of human skin.[24] Although no rete ridges are present in any of the HSEs presented here, K15 was expressed during the entire culture period irrespective of the dermal matrix used. In another study performed in HSEs, Kaur and her group demonstrated the extensive tissue-regenerative capacity of neonatal human ESCs.[25] However, the questions still remain whether interfollicular ESCs can increase the lifespan of HSEs and why these HSEs lose their self-renewal capacity *in vitro* but not *in vivo* as a graft.[26, 27]

It has been shown that keratinocytes in culture often represent a certain pathologic condition, such as epidermal injury or psoriasis. Under such conditions, the keratinocytes are in an activated state, expressing activation- and hyperproliferation-specific proteins K16 and K17. Having responded to injury, keratinocytes receive a deactivation signal and revert to their normal differentiation program. Based on the results obtained in the present study, it became clear that fibroblasts can produce such signals, since in FDM-based HSEs the expression of K16 and K17 was fully downregulated during the whole culture period up to 20 weeks. In a previous study we demonstrated that a full fibroblast-induced downregulation of K16 expression in keratinocytes occurs on fibroblast-populated collagen matrices already at an earlier time point,[3] indicating that in addition to cell–cell interaction also cell–matrix interaction may be involved in the normalization of epidermal

differentiation *in vitro*. It should be noted that K16 and K17 reappeared at the periphery of FDM-based HSEs (Fig. 5b). These keratins are thought to promote reorganization of the cytoplasmic array of keratin filaments, an event that precedes the onset of keratinocyte migration into the wound site, with K16 induction occurring prior to K17 induction.[28, 29]

As human fibroblasts were directly surrounded by their own secreted microenvironment in FDM-based HSEs, they influenced epidermal proliferation. This growth-promoting effect of fibroblasts is induced by soluble factors released from fibroblasts.[30] In spite of a decreasing proliferation index seen after 6 weeks of FDMbased HSE culture, the localization of the terminal differentiation marker involucrin shifted towards the granulous layer in FDM-based HSEs cultured for 13 weeks or longer. The early differentiation marker K10 was observed in all suprabasal cell layers during the entire culture period, indicating normal differentiation. The microenvironment of FDM-based HSEs did not alter the basement membrane formation as judged by the expression of laminin 332 and collagen types IV and VII when compared to rat-tail collagenbased HSEs.[30] Both proteins were expressed along the epidermal–dermal junction during the entire culture period indicating a proper basement membrane on which keratinocytes can migrate and differentiate. In addition, electron microscopy analyses revealed the presence of essential components of the basement membrane, including dermal–epidermal junctions, hemidesmosomes and anchoring fibers.

It is clear that HSEs generated on different dermal matrices show great similarities to normal human skin. However, one of the key processes impaired under *in vitro* conditions is desquamation as the ultimate representation of terminal differentiation. Desquamation involves the degradation of corneodesmosomes, in which various enzymes participate. Activation of these enzymes is affected by several microenvironmental factors such as pH and water content. The generation of NMF by HSEs is also dependent on the water content in its microenvironment. A water content that is either too low or too high will impair the activity of the enzymes involved in the production of NMF components.[31] A high relative humidity in the microenvironment is, therefore, expected to reduce the formation of NMF, as demonstrated by de Declercq et al.[32] Using Raman spectroscopy we compared both FDM-based HSEs and rat-tail collagen-based HSEs in the presence of NMF.[33] The resulting data indicate that FDM-based HSEs contain higher levels of NMF than the rat-tail collagen-based HSEs, providing grounds to assume that the water and humidity levels are more normalized in FDM-based HSEs than in rat-tail collagen-based HSEs.

The results of the present study indicate that the microenvironment generated by primary human fibroblasts themselves is very suitable to use as a dermal matrix for the generation

of long-lived HSEs. The generated epidermis of resulting HSEs could be maintained up to 20 weeks in culture without the expression of the hyperproliferation markers K16 and K17. In addition, the number of viable cell layers remained constant up to 13 weeks of culture and decreased slightly after 20 weeks of culture. Finally, we have shown that this new generation of HSEs contains a much higher NMF concentration compared to rat-tail collagen-based HSEs. These findings provide a further physiological resemblance to normal human skin and allow for functional studies focused on the effects of long-term exposure to exogenous stressors on epidermal homeostasis and skin cancer.

Acknowledgements

The authors thank Dr. Maria Ponec for critically reviewing the manuscript.

References

1. Bell, E., Ehrlich, H.P., Buttle, D.J. & Nakatsuji, T. Living tissue formed in vitro and accepted as skin-equivalent tissue of full thickness. *Science* 211, 1052-1054 (1981).
2. Boyce, S.T., Christianson, D.J. & Hansbrough, J.F. Structure of a collagen-GAG dermal skin substitute optimized for cultured human epidermal keratinocytes. *J.Biomed.Mater.Res.* 22, 939-957 (1988).
3. El Ghalbzouri, A., Lamme, E. & Ponec, M. Crucial role of fibroblasts in regulating epidermal morphogenesis. *Cell Tissue Res.* 310, 189-199 (2002).
4. Parenteau, N.L. et al. Epidermis generated in vitro: practical considerations and applications. *J.Cell Biochem.* 45, 245-251 (1991).
5. Ponec, M. et al. The formation of competent barrier lipids in reconstructed human epidermis requires the presence of vitamin C. *J.Invest Dermatol.* 109, 348-355 (1997).
6. Stark, H.J., Baur, M., Breitkreutz, D., Mirancea, N. & Fusenig, N.E. Organotypic keratinocyte cocultures in defined medium with regular epidermal morphogenesis and differentiation. *J.Invest Dermatol.* 112, 681-691 (1999).
7. Ahlfors, J.E. & Billiar, K.L. Biomechanical and biochemical characteristics of a human fibroblast-produced and remodeled matrix. *Biomaterials* 28, 2183-2191 (2007).
8. Grinnell, F., Fukamizu, H., Pawelek, P. & Nakagawa, S. Collagen processing, crosslinking, and fibril bundle assembly in matrix produced by fibroblasts in long-term cultures supplemented with ascorbic acid. *Exp.Cell Res.* 181, 483-491 (1989).
9. Ishikawa, O., Kondo, A., Okada, K., Miyachi, Y. & Furumura, M. Morphological and biochemical analyses on fibroblasts and self-produced collagens in a novel three-dimensional culture. *Br.J.Dermatol.* 136, 6-11 (1997).
10. Kessler, D. et al. Fibroblasts in mechanically stressed collagen lattices assume a "synthetic" phenotype. *J.Biol.Chem.* 276, 36575-36585 (2001).
11. Nijhof, J.G. et al. Epidermal stem and progenitor cells in murine epidermis accumulate UV damage despite NER proficiency. *Carcinogenesis* 28, 792-800 (2007).
12. El Ghalbzouri, A., Gibbs, S., Lamme, E., Van Blitterswijk, C.A. & Ponec, M. Effect of fibroblasts on epidermal regeneration. *Br.J.Dermatol.* 147, 230-243 (2002).
13. El Ghalbzouri, A., Jonkman, M., Kempenaar, J. & Ponec, M. Recessive epidermolysis bullosa simplex phenotype reproduced in vitro: ablation of keratin 14 is partially compensated by keratin 17. *Am.J.Pathol.* 163, 1771-1779 (2003).
14. El Ghalbzouri, A., Jonkman, M.F., Dijkman, R. & Ponec, M. Basement membrane reconstruction in human skin equivalents is regulated by fibroblasts and/or exogenously activated keratinocytes. *J.Invest Dermatol.* 124, 79-86 (2005).
15. Lee, J., Cuddihy, M.J. & Kotov, N.A. Three-Dimensional Cell Culture Matrices: State of the Art. *Tissue Engineering* 14 61-85 (2008).
16. Boehnke, K. et al. Effects of fibroblasts and microenvironment on epidermal regeneration and tissue function in long-term skin equivalents. *Eur.J.Cell Biol.* 86, 731-746 (2007).
17. Riva, F. et al. Generation of human epidermal constructs on a collagen layer alone. *Tissue Eng* 13, 2769-2779 (2007).
18. Stark, H.J. et al. Authentic fibroblast matrix in dermal equivalents normalises epidermal histogenesis and dermoepidermal junction in organotypic co-culture. *Eur.J.Cell Biol.* 83, 631-645 (2004).
19. Stark, H.J. et al. Epidermal homeostasis in long-term scaffold-enforced skin equivalents. *J.Investig.Dermatol.Symp.Proc.* 11, 93-105 (2006).
20. Barthel, R. & Aberdam, D. Epidermal stem cells. *J.Eur.Acad.Dermatol.Venereol.* 19, 405-413 (2005).
21. Kaur, P. Interfollicular epidermal stem cells: identification, challenges, potential. *J.Invest Dermatol.* 126, 1450-1458 (2006).
22. Segre, J.A., Bauer, C. & Fuchs, E. Klf4 is a transcription factor required for establishing the barrier function of the skin. *Nat.Genet.* 22, 356-360 (1999).
23. Watt, F.M. Epidermal stem cells: markers, patterning and the control of stem cell fate. *Philos.Trans.R.Soc.Lond B Biol.Sci.* 353, 831-837 (1998).
24. Wan, H. et al. Desmosomal proteins, including desmoglein 3, serve as novel negative markers for epidermal stem cell-containing population of keratinocytes. *J.Cell Sci.* 116, 4239-4248 (2003).
25. Li, A., Pouliot, N., Redvers, R. & Kaur, P. Extensive tissue-regenerative capacity of neonatal human keratinocyte stem cells and their progeny. *J.Clin.Invest* 113, 390-400 (2004).

26. Berking, C. et al. Photocarcinogenesis in human adult skin grafts. *Carcinogenesis* 23, 181-187 (2002).
27. Guerret, S., Govignon, E., Hartmann, D.J. & Ronfard, V. Long-term remodeling of a bilayered living human skin equivalent (Apligraf) grafted onto nude mice: immunolocalization of human cells and characterization of extracellular matrix. *Wound.Repair Regen.* 11, 35-45 (2003).
28. McGowan, K.M. & Coulombe, P.A. Onset of keratin 17 expression coincides with the definition of major epithelial lineages during skin development. *J.Cell Biol.* 143, 469-486 (1998).
29. Paladini, R.D. & Coulombe, P.A. Directed expression of keratin 16 to the progenitor basal cells of transgenic mouse skin delays skin maturation. *J.Cell Biol.* 142, 1035-1051 (1998).
30. El Ghalbzouri, A. & Ponec, M. Diffusible factors released by fibroblasts support epidermal morphogenesis and deposition of basement membrane components. *Wound.Repair Regen.* 12, 359-367 (2004).
31. Rawlings, A.V. & Harding, C.R. Moisturization and skin barrier function. *Dermatol.Ther.* 17 Suppl 1, 43-48 (2004).
32. DeClerqc, L. et al. Adaptation response in human skin barrier to a hot & dry environment. *J Invest Dermatol* 119 716 (2002).
33. Caspers, P.J., Lucassen, G.W. & Puppels, G.J. Combined in vivo confocal Raman spectroscopy and confocal microscopy of human skin. *Biophys.J.* 85, 572-580 (2003).

5

Molecular profiling of cutaneous squamous cell carcinomas and actinic keratoses from organ transplant recipients

Liesbeth Hameetman[1], Suzan Commandeur[2], Jan Nico Bouwes Bavinck[2], Hermina C. Wisgerhof[2], Frank R. de Gruijl[2], Rein Willemze[2], Leon Mullenders[1], Cornelis P. Tensen[2]* and Harry Vrieling[1]*

Departments of [1]Toxicogenetics and [2]Dermatology, Leiden University Medical Center, Leiden, the Netherlands.

* Shared senior authorship

Submitted

Abstract

The risk of developing cutaneous squamous cell carcinoma (SCC) is markedly increased in organ transplant recipients (OTRs) compared to the normal population. Next to sun exposure, the immunosuppressive regimen is an important risk factor for the development of SCC in OTRs. Various gene mutations (e.g. p53) and genetic alterations (e.g. loss of CDKN2A, amplification of RAS) have been found in SCCs. The aim of this genome-wide study was to identify pathways and genomic alterations that are consistently involved in the formation of SCCs and their precursor lesions, actinic keratoses (AKs). To perform the analysis in an isogenic background, RNA and DNA were isolated from SCC, AK and normal (unexposed) epidermis (NS) from each of 13 OTRs. Hierarchical cluster analysis of mRNA expression profiles showed SCC, AK and NS samples to separate into three distinct groups. Several thousand genes were differentially expressed between epidermis, AK and SCC; most upregulated in SCCs were hyperproliferation related genes and stress markers, such as keratin 6 (K6), K16 and K17. Matching to oncogenic pathways revealed activation of downstream targets of RAS and cMYC in SCCs and of NFκB and TNF already in AKs. In contrast to what has been reported previously, genome-wide SNP analysis showed very few copy number variations in AKs and SCCs, and these variations had no apparent relationship with observed changes in mRNA expression profiles. Vast differences in gene expression profiles exist between SCC, AK and NS from immunosuppressed OTRs. Moreover, several pathways activated in SCCs were already activated in AKs, confirming the assumption that AKs are the precursor lesions of SCCs. Since the drastic changes in gene expression appeared unlinked to specific genomic gains or losses, the causal events driving SCC development require further investigation. Other molecular mechanisms, such as DNA methylation or miRNA alterations, may affect gene expression in SCCs of OTRs. Further study is required to identify the mechanisms of early activation of NFκB and TNF, and to establish whether these pathways offer a feasible target for preventive intervention among OTRs.

Introduction

Non-melanoma skin carcinomas, comprising cutaneous squamous cell carcinoma (SCC) and basal cell carcinoma (BCC), are the most common malignancies in fair-skinned Caucasians. The risk of developing cutaneous SCC is markedly increased (100-fold) in organ transplant recipients (OTRs) compared to the normal population and is associated with the immunosuppressive therapy needed to prevent graft rejection.[1-3] Moreover, some studies have suggested that SCCs from OTRs display a more aggressive behavior.[4]

Like other cancers, the development of cutaneous SCC is thought to be a multi-step process, involving sequential acquisition of genetic changes. Sun (UVR) exposure is the principal carcinogen inducing both immunologic tumor-tolerance and DNA damage that can lead to mutations in oncogenes and tumor suppressor genes (TSGs).[5, 6] Other risk factors include impaired immune surveillance, as seen in OTRs, and human papillomavirus (HPV) infections.[7] However, the oncogenic potential of HPV in cutaneous SCCs remains unclear.[8] In a recent transcriptome sequencing study no evidence of active viral gene expression was found in large group of SCCs.[9]

Cutaneous SCCs are thought to develop from precursor lesions, actinic keratoses (AKs). Even though most AKs (80-99%) do not progress to SCC, there is still both histological and molecular evidence to support this hypothesis.[10] UVR-related mutations inactivating the p53 tumor suppressor gene are very common in SCCs and AKs, both in immunocompetent patients and OTRs.[5, 11] p53 mutations are thought to occur very early in the development of skin cancer, since they are already present in microscopic clusters of keratinocytes in sun-exposed human skin.[12] These clusters are thought to precede tumor formation and are more frequent in OTR compared to immunocompetent patients.[13, 14] However, not every SCC contains a mutated p53 gene.[5]

Other common genetic changes found in cutaneous SCC development are the inactivation of the CDKN2A tumor suppressor gene (via mutation, promoter methylation and/or chromosomal loss) and mutation and/or amplification of RAS genes.[15] Both oncogenic changes are associated with the progression of AK to SCC. Also, (over-) expression of RAS downstream proteins (MAPKs and cyclins) has been reported in a subset of SCCs.[16]

At the chromosomal level, several studies have shown that cutaneous SCCs can display complex karyotypes with large numbers of allelic imbalances.[17-19] Moreover, widespread gains and losses of chromosomal fragments have been reported to be already present in AKs.[17, 20]

The aim of our study was to identify genes and/or pathways that are consistently involved in the development of cutaneous SCC and their precursor lesions, AKs in OTRs. Thus far, the genome-wide transcriptional profiling studies on SCCs are diverse in nature, show little overlap in differentially expressed genes (DEGs), have limited sample size, use cell lines and do not integrate genomic and expression data.[21-24] This genome-wide study assesses in parallel both RNA and DNA alterations in a sizeable well-defined group of OTRs presenting with both AKs and SCCs. A better understanding of the pathological mechanisms leading to skin carcinomas in these patients could lead to novel molecular targets for effective intervention.

Methods

Patient material

Approval for the present studies was granted by the Leiden University Medical Center institutional review board. Patients were selected from the group of OTRs that are regularly seen at the dermatology clinic of the Leiden University Medical Center.[25] Patients with clinically suspected SCC were informed on the study and after informed consent was obtained, fresh frozen samples were obtained from the SCC. An AK on the forearm and unexposed normal skin (NS) from the buttock were taken and peripheral blood was drawn to serve as normal internal control in genome-wide SNP analysis. All clinical diagnoses were histologically confirmed. SCCs can be histologically categorized as *well differentiated*, *moderately differentiated* or *poorly differentiated* tumors, based on the degree of keratinization and cellular atypia.[26] All SCCs included in this study were classified as well-differentiated. Most AKs showed mild dysplasia, with the exception of AK_P-11 and AK_P-18, both demonstrating mild to severe dysplasia and AK_P-42 with severe dysplasia. All samples were further handled in an anonymously coded fashion, following the medical ethical guidelines described in the Code 'Proper Secondary Use of Human Tissue' established by the Dutch Federation of Medical Sciences.

RNA and DNA isolation

RNA and DNA were isolated from SCC and AK biopsy samples that contained at least 70% tumor cells, as determined by haematoxylin and eosin stained frozen sections. To ensure that the RNA and DNA represent the same tumor cells/biopsy, the various cut sections were alternately used for RNA and DNA isolation, respectively. From the sample of unexposed NS the epidermis was removed for further processing by cryosectioning parallel to the outer surface of the skin biopsy (cut to a depth where opaque whiting of the remaining dermal surface was observed). RNA was extracted from frozen material

using the RNeasy Fibrous Tissue kit (Qiagen, Hilden, Germany), which included proteinase K treatment (10 min at 55˚C) of the lysed sample in RLT-buffer and on-column DNase treatment. DNA from the tumor and skin samples was isolated using the Genomic-tips 20/G kit (Qiagen). A salting-out procedure was used to isolate genomic DNA from the peripheral blood samples.[27] Both RNA and DNA were quantified using a Nanodrop (NanoDrop technologies, Wilmington, CA) and RNA was further evaluated for degradation with the Lab-on-a-chip assay on the 2100 Bioanalyzer (Agilent Technologies, Santa Clara, CA, USA).

Genome-wide SNP analysis

Genomic DNA from AKs, SCCs and their corresponding normal controls (peripheral blood) were subjected to genome-wide single nucleotide polymorphism (SNP) analysis. 400 ng of DNA was assayed with the Infinium II Sentrix HumanHap550v3 duo Genotyping BeadChip (Illumina, San Diego, CA, USA), containing over 550,000 unique tag SNP markers. Hybridizations were performed at the Leiden Genome Technology Center according to the manufacturer's instructions. Image analysis and quality control (call rate >98%) was performed in Illumina's BeadStudio Version 3.2 software using the genotyping module. Each BeadChip was self-normalized using information contained within the array. Further analysis and visualization was performed with the Illumina Genome Viewer in Beadstudio. First, tumor data was paired with data from their corresponding normal control. Subsequently, examination of the log R ratio (signal intensity tumor/signal intensity normal control) and B allele frequency (BAF) was analyzed for the presence of copy number variations (CNVs) and/or loss of heterozygosity (LOH) in the tumor samples. By plotting the log R ratio across a chromosome, CNVs could be visualized by an increase or decrease in baseline signal. Secondly, the BAF was plotted across each chromosome to detect regions of LOH in tumor cells. A region with LOH was defined as a stretch of heterozygous SNPs in normal DNA but homozygous in the matched tumor DNA.

Genome-wide expression analysis (GWEA)

Gene expression profiles were obtained using HumanWG-6 v2 Expression BeadChips (Illumina). In brief, 100 ng of total RNA was converted to cDNA and subsequently labeled cRNA using the Ambion Illumina TotalPrep RNA Amplification kit (Ambion, Austin TX, USA) according to manufacturer's instructions. The labeled cRNAs were hybridized overnight to the HumanWG-6 v2 BeadChips. After washing, the BeadChips were scanned using the Illumina BeadArray Reader to measure the fluorescence intensity of each probe. Raw data was extracted from the BeadChip data files in Illumina's BeadStudio Version 3.2 software using the gene expression module. Background subtracted data was further analyzed in R-based Bioconductor package, lumi (version 1.12.4).[28] In lumi, the data was transformed

(variance-stabilizing transformation (VST)) and normalized (robust spline normalization (RSN)), resulting in log-transformed normalized data. Several quality control plots of both the normalized and unnormalized data were generated in the lumi package.[28, 29] The R-package illuminaHumanv2.db (version 1.4.1) was used for annotation. The data were purged of genes that did not meet the detection limit (expression-detection P-value >0.01) and/or were not annotated. This selection resulted in 15,969 probes, representing 13,848 genes that were subjected to further analysis. Hierarchical clustering and principal component analysis (PCA) were used to cluster the samples based on their expression levels, using the bioDist package (version 1.18.0). The limma package (version 3.2.3) was used to identify differentially expressed genes (DEGs) between SCC, AK and NS.[30] A Benjamini and Hochberg False Discovery Rate (FDR) of 1% was used as cut-off to select significant DEGs and correct for multiple testing. Gene set enrichment analysis (GSEA) for enriched Gene Ontology (GO) terms and KEGG pathways was performed with the significantly DEGs from the limma analysis using DAVID Bioinformatic Resources v6.7 (http://david.abcc.ncifcrf.gov).[31] Secondly, GSEA on the entire data set was performed using the parametric gene set enrichment analysis (PGSEA) and regional expression bias (reb) packages (version 1.14.0).[32] To identify activation of transcription factors (TFs) in AKs and SCCs, the DEGs from the limma analysis were investigated for over-represented TF binding sites (TFBSs) using the online analysis tool oPOSSUM.[33] Only the vertebrate taxonomic supergroup was selected and for each comparison the top 5 TFs were selected. Both the gene expression data and genome-wide SNP analysis have been deposited in the NCBIs Gene Expression Omnibus as a SuperSeries with accession number GSE32979 (http://www.ncbi.nlm.nih.gov/geo/query/acc.cgi?acc=GSE32979).[34]

Quantitative RT-PCR (QPCR)

For 10 NS, 13 AK and 15 SCC samples sufficient amounts of total RNA were available for cDNA synthesis using the iScript™ cDNA Synthesis Kit (Bio-Rad, Veenendaal, the Netherlands) according to manufacturer's instructions. Primers (Invitrogen, Breda, the Netherlands) were designed for nine genes of interest and four reference genes (Table 6). The reference genes were selected based on their stable expression in all samples in the GWEA. QPCR reactions were performed using the SYBR Green Supermix (Bio-Rad) on the CFX384™ real-time PCR detection system (Bio-Rad). The PCR-program included initialization (6 min at 95˚C), 45 cycles of denaturation (15s at 95˚C), annealing (30s at 60˚C) and elongation (30s at 72˚C), final elongation for 1 min at 72˚C and a DNA melting curve (55˚C to 95˚C through 0.2˚C increments every 10s). All samples were tested in duplicate. Specificity of PCR products was evaluated by size in agarose gel electrophoresis followed by DNA sequence analysis. Serial dilutions of cDNA from spontaneously immortalized keratinocytes (own laboratory) and universal human reference RNA

Table 1 | QPCR primers.

Gene	Accession number	Forward primer 5' > 3'	Reverse primer 5' > 3'	Amplicon size (bp)
Genes of interest				
CCL27	NM_006664	GACTGTCACCTCCAGGCTTT	TCTCTTGGTGCTCAAACCAC	100
K17	NM_000422	CTGGAGCAGGAGATTGCCAC	GGGTGGTCACCGGTTCTTTC	88
MMP1	NM_002421	AGGTCTCTGAGGGTCAAGCA	CTGGTTGAAAAGCATGAGCA	111
MMP3	NM_002422	TGCTTTGTCCTTTGATGCTG	GGAAGAGATGGCCAAAATGA	135
MMP9	NM_004994	CCTGGAGACCTGAGAACCAA	ATTTCGACTCTCCACGCATC	103
MMP10	NM_002425	GTGGAGTTCCTGACGTTGGT	TCAATGGCAGAATCAACAGC	130
PI3	NM_002638	GACTGCCCAGGAATCAAGAA	CAGCAGGGACTTAGGACCAG	148
SERPINB4	NM_002974	CAAAGGGCAGTGGGAGAATA	CCTCCAGCAAGGCAAAATTA	131
TUBB3	NM_006086	CTCAGGGGCCTTTGGACATC	CCCTCCGTGTAGTGACCCTT	96
Reference genes				
ARPC2	NM_005731	TCCGGGACTACCTGCACTAC	GGTTCAGCACCTTGAGGAAG	96
BAT3	NM_004639	AAGAGACGCAAGACGATGCAG	TGTAGCTCTCCTGAACCTCTGG	151
RPS29	NM_001032	TATGTGCCGCCAGTGTTTCC	TGCCCCGGATAATCCTCTGA	92
ZNF410	NM_021188	GCTGTGGTAAGCAGTTTACTACAG	CTTGGGCTTCACAAAGGAAAGG	90

(Stratagene, Santa Clara, CA USA) were included to determine PCR-efficiencies. The stable expression of the reference genes was validated by analyzing their QPCR data using the geNORM method (M<1.0, CV<0.5) in the freely available qBase software.[35, 36] QPCR data of the genes of interest were normalized based on the expression of the reference genes using the normalization factor from geNORM. Relative gene expression between the different sample groups was statistically analyzed in Excel, using a two-sided Student's *t*-test assuming unequal variance. P-value ≤0.05 was considered significant.

Results

Patient material

Patients were selected from the large group of OTRs that visit the dermatology clinic of the LUMC at a regular basis to provide a well-documented sample series for our study. Moreover from these OTRs it was possible to select both SCCs and AKs as well as normal skin (NS) to circumvent inter-patient variability. Fifteen OTRs (7 females and 8 males) participated in this study (Table 2). The average age of the patients when the selected SCC was diagnosed was 59 years (range 47-74 years). Side-matched normal skin in OTRs often already contains a fair amount of UV damage, a phenomenon described as 'field cancerisation'.[37, 38] Therefore, (UV-unexposed) skin from the lower back was chosen as normal skin and served as internal negative control. Of patient 42, only SCC and AK samples were available, and for patient 15 only a SCC sample could be obtained. Samples of these two patients were only included in the GWEA. All patients received immunosuppressive drugs (Table 2).

Genome-wide SNP analysis of SCCs and AKs

Thirteen SCC samples and eleven AKs were subjected to genome-wide SNP array analysis together with the corresponding normal DNA from peripheral blood (Table 3, Figure 1). Six of thirteen SCCs showed chromosomal aberrations, ranging from a single loss of 9p to multiple losses and gains (amplification/duplication) (Table 3, Figure 1a). Copy number neutral loss of heterozygosity (LOH) was observed in 3 SCCs. Overall, more LOH than gain was seen (14 vs. 9). Also large deletions of (almost) whole chromosome arms were more frequent than small deletions (<40 Mb; 12 vs. 8). In several tumors the detected aberrations were not consistently present in >70% of the tumor sample (i.e. not a full signal of loss or gain), suggesting tumor heterogeneity (Table 3). Four out of thirteen (30%) SCCs demonstrated loss of 9p21 where CDKN2A is located.

Analysis of AK samples showed chromosomal aberrations in 6 of 11 samples, ranging from a single up to multiple (11) aberrations in an affected sample (Table 3, Figure 1b). Again, more losses and copy number neutral LOH than gains were seen (21 vs. 3). Generally, the aberrations observed in AKs, were less extensive than those in SCCs. No correlation was detected among the AKs regarding the extent of chromosomal damage and the relative level of dysplasia. However, similar to SCCs, several AKs demonstrated genetic heterogeneity. Notably, there was no clear correlation between the number and type of aberrations found in the AK and SCC from the same OTR. However the number of samples in each group was not large enough to perform any statistical analysis.

Cluster and single-gene analyses of expression profiles of SCCs and AKs

Fifteen SCC, fourteen AK and thirteen NS samples were included in the GWEA. Filtering for annotated and expressed genes resulted in 15,969 probes for further analyses. Subsequent hierarchical clustering, based on expression levels, resulted in two very distinct groups (Figure 2a), separating normal and tumor samples. The tumor samples were divided in three sub-clusters in one arm of the dendogram. Principal component analysis also demonstrated good separation of normal and tumor samples, already in the first component (Figure 2b). In the second component, AKs could be separated from SCCs. No correlation was seen with the type of organ transplanted. However, since 13 of 15 patients were kidney recipients, no definite conclusions can be made about this matter. The same could be concluded for the immunosuppressive regimen (data not shown).

Table 2 | Patient and tumor characteristics.

Patient characteristics					SCC	AK[4]	NS[4]	Blood[5]
Patient ID	Gender[1]	Age[2]	Transplanted organ	Drugs[3]	Location	Location	Location	Yes/No
P-3	M	56	Kidney	MMF, P	Upper leg	Forearm	Lower back	Yes
P-5	M	72	Kidney	Aza, P	Lower arm	Forearm	Lower back	Yes
P-11	F	56	Kidney	Aza, P	Tibia	Forearm	Lower back	Yes
P-15	M	62	Kidney	P	Lower arm	n.a.	n.a.	No
P-18	M	51	Kidney-pancreas	Aza, P	Dorsal hand	Forearm	Lower back	Yes
P-24	M	74	Kidney	Aza, P	Lower leg	Forearm	Lower back	Yes
P-27	F	56	Liver	Tacrolimus, P	Shoulder	Forearm	Lower back	Yes
P-33	F	66	Kidney	Aza, P	Shoulder	Forearm	Lower back	Yes
P-38	F	47	Kidney	Aza, P	Shoulder	Forearm	Lower back	Yes
P-39	F	65	Kidney	Aza, P	Lower leg	Upper arm	Lower back	Yes
P-40	M	60	Kidney	MMF, P	Dorsal hand	Forearm	Lower back	Yes
P-41	M	61	Kidney	Aza, P	Dorsal hand	Forearm	Lower back	Yes
P-42	F	48	Kidney	Aza, P	Dorsal hand	Dorsal hand	n.a.	No
P-44	M	62	Kidney	Aza, P	Dorsal hand	Forearm	Lower back	Yes
P-57	F	53	Kidney	Aza, P	Tibia	Forearm	Lower back	Yes

SCC, squamous cell carcinoma; AK, actinic keratosis; NS, normal skin

[1] F, Female; M, Male
[2] Age at diagnosis of SCC used for study
[3] Immunosuppressive drugs at diagnosis of SCC used for study. MMF, mycophenolate mofetil; P, prednisone; Aza, azathioprine
[4] n.a, not available for study
[5] Peripheral blood was collected to serve as a normal control in genome-wide SNP analysis.

Table 3 | Overview of chromosomal abberrations in SCC and AK.

Sample	Type of aberration	Cytoband	Mb location	Size (Mb)	
SCC_P-03	Loss	4q28.3	1:136,448,440 - 136,988,409	0.54	*
	Gain	5p			*
	Gain	14q23.1-32.2	14:57,558,740 - 96,468,442	38.9	*
SCC_P-11	Gain	9q			*
SCC_P-18	Gain	8q24.22-24.23	8:132,122,430 - 139,467,653	7.3	*
	Gain	14q13.3	14:71,054,120 - 73,596,540	2.5	
	Gain	9p23-tel	9:1 - 12,039,121	12	*
	Loss	9p23-cen		~40	*
	Loss	9q			*
	Loss	14q13.3-tel		~70	*
	cnLOH	17			*
SCC_P-27	Loss	3p			
	Gain	3q			
	Loss	4p12-tel	4:1 - 46,377,946	46,4	*
	Gain	5q25.3-tel	5:83,159,010 - 100,338,915	17.1	*
	Loss	6q13-14.1	6:75,600,000 - 76,627,715	1.0	*
	Loss	9p			
	Gain	9q			
	cnLOH	18p			
SCC_P-38	cnLOH	6p21.31-tel	6:1 - 35,593,684	35.5	
	Loss	9p			
	Loss	14q			
SCC_P-41	cnLOH	22q12.1-tel	22:24,348,300 - 49,554,696	25.2	
AK_P-03	Loss	4q			*
	Loss	5q15-31.1	5:96,745,240 - 133,072,806	36.3	*
	cnLOH	5q31.1-tel	5:133,268,490 - 180,857,816	47.2	*
	cnLOH	9q			*
AK_P-05	Loss	5q			*
	Loss	9p21.1-tel	9:1 - 33,109,143		*
AK_P-11	Loss	2p22.2-25.1	2:11,690,000 - 36,950,000	25.3	*
	cnLOH	8p			*
	Loss	13q			*
	Loss	17p			*
	Loss	18q12.1-tel	18:26,013,440 - 76,117,152	50.1	*
AK_P-33	Loss	6q22.31-tel	6:122,757,319 - 170,975,699	48.2	*
AK_P-41	Loss	1p32.3	1:54,783,720 - 55,100,840	0.4	*
	Loss	3p			
	Gain	3q			*
	Loss	4q33-tel	4:171,450,620 - 191,411,215	20.0	
	Gain	5q31.2-tel	5:138,387,890 - 180,857,851	42.5	*
	Loss	8p12-tel	8:1 - 38,377,990	38.4	
	Loss	8q22.1	8:95,250,740 - 96,376,326	1.3	
	Loss	9p22.2-cen	9:17,230,530 - 50,549,240	33.3	
	Gain	10p	10:1 - 40,144,085	40.1	*
	Loss	12q24.23		0.5	
	Loss	14q			
AK_P-44	cnLOH	8q33.3-tel	8:126,444,040 - 137,979,818	11.4	

* Heterogeneous chromosomal aberration, observed in less than 70% of the tumor sample.

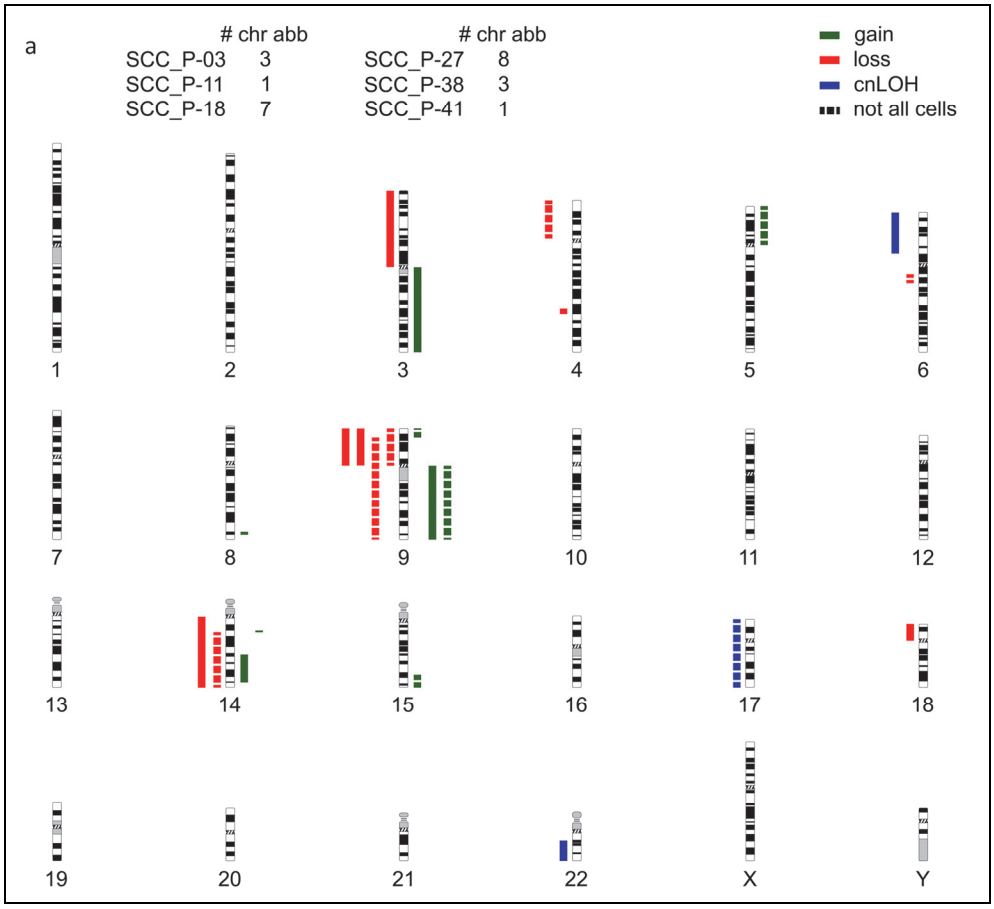

Figure 1a | Graphical overview of chromosomal aberrations in squamous cell carcinomas (SCCs). Idiograms summarizing chromosomal aberrations in SCCs compared to the patient matched normal control. Loss of heterozygosity (LOH) events are shown to the left of the chromosomes in either red (physical loss) or blue (copy-neutral LOH, cnLOH). Gains are indicated on the right of the chromosomes in green. Dotted lines represent aberrations that were not present in all tumor cells of a sample.

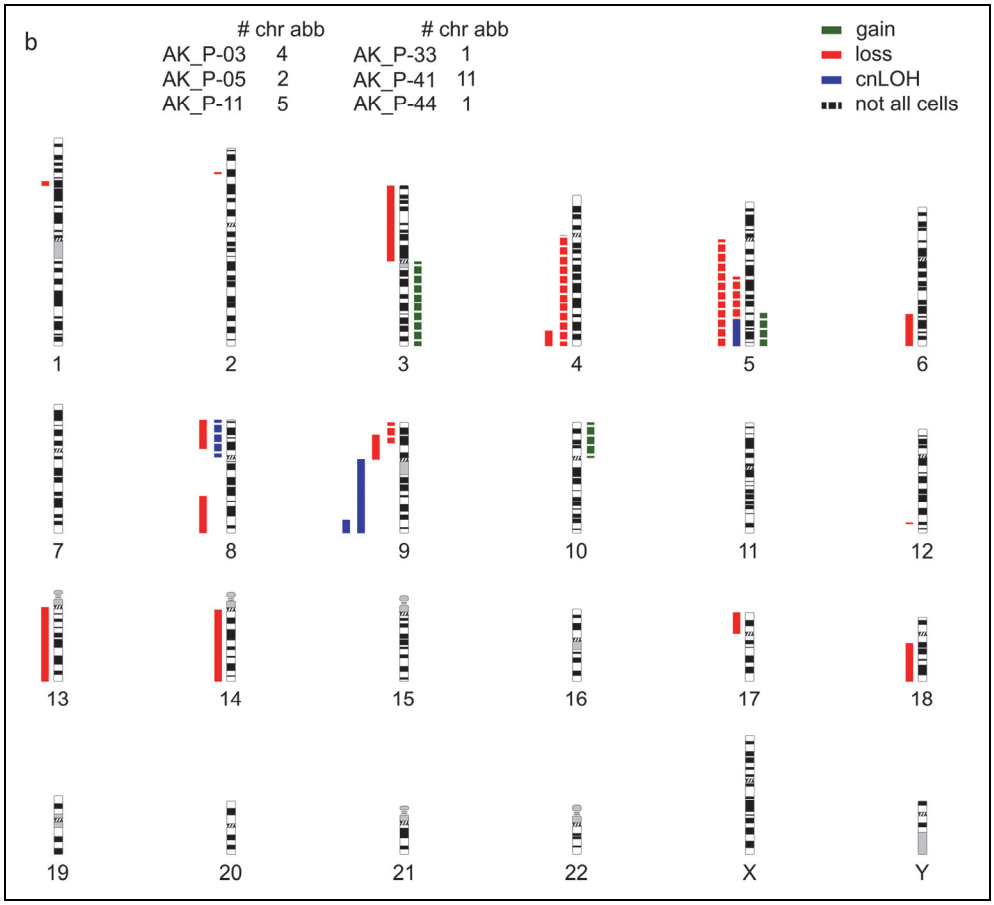

Figure 1b | Graphical overview of chromosomal aberrations in actinic keratoses (AKs). Idiograms summarizing chromosomal aberrations in AKs compared to the patient matched normal control. Loss of heterozygosity (LOH) events are shown to the left of the chromosomes in either red (physical loss) or blue (copy-neutral LOH, cnLOH). Gains are indicated on the right of the chromosomes in green. Dotted lines represent aberrations that were not present in all tumor cells of a sample.

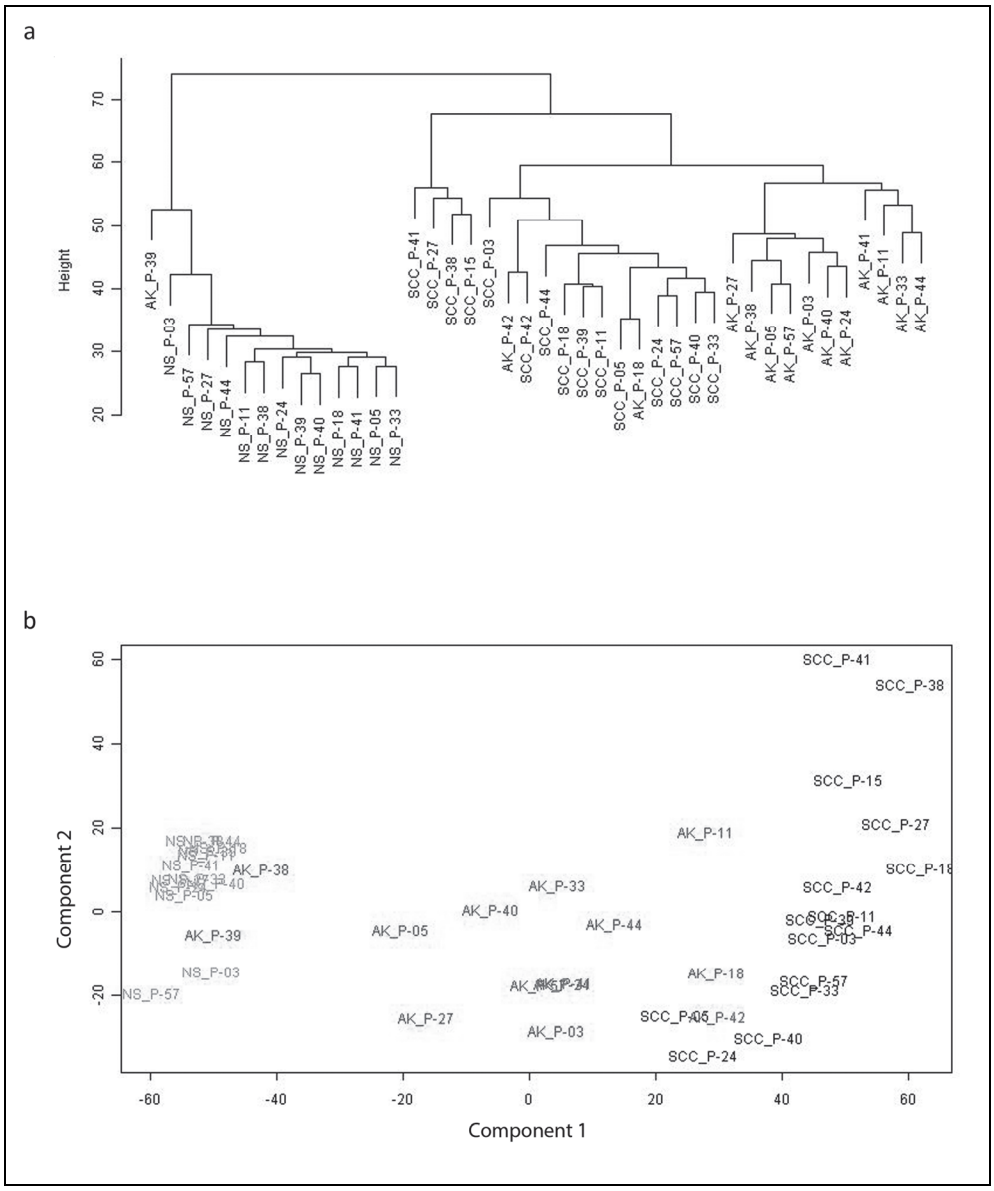

Figure 2 |Dendogram of unsupervised hierarchical cluster analysis of all samples (a). Clustering was based on 10,100 probes for which the average expression among all samples showed a standard deviation ≥ 0.15. Samples are labeled by sample group (normal skin (NS), actinic keratosis (AK), squamous cell carcinoma (SCC) and patient number (P-#). Scatter plot of the first two components from PCA based on 6,104 probes for which the average expression among all samples showed a standard deviation/mean ≥ 0.1 (b). Labels indicate the position for each sample (NS/AK/SCC) of a certain patient (P-#).

Statistical analysis of the expression data was performed using limma. The following comparisons between sample groups were made: SCC vs. NS, SCC vs. AK and AK vs. NS. For each comparison a FDR <1% was used, and the comparisons were made with several $\log_2$ transformed fold change ($\log_2$FC) restrictions, namely $\log_2$FC>0.5, $\log_2$FC>1.0 and no $\log_2$FC-restriction (Table 4). With $\log_2$FC>0.5, 2,087 probes, representing 2,009 genes, were differentially expressed between SCC and NS (Additional file 1)*. Among the upregulated genes in SCC were several genes known to be involved in keratinocyte differentiation and skin cancer, including keratins (e.g. K16, K17 and K6), matrix metalloproteinases (MMPs), S100 molecules and small proline-rich proteins (SPRRs). Most of these genes were highly overexpressed with a $\log_2$FC>2.0. The cutaneous T-cell attracting chemokine, CCL27, was the most downregulated gene in SCCs compared to normal skin ($\log_2$FC=- 4.2). With $\log_2$FC>0.5, 977 probes (947 genes) were differentially expressed between AK and NS samples and expression of 571 probes (547 genes) was significantly different between SCCs and AKs (Additional file 1)*. In total for the $\log_2$FC>0.5 analysis, 180 probes were present in all three comparisons as visualized by a VennDiagram (Figure 3, Additional file 1)*. These probes represented 173 genes that were consistently up- or downregulated during the development of SCC from NS, via AK, and can be considered as genes involved in gradual skin cancer progression. Since SCC, AK and NS samples were available from each patient, we investigated whether the differentially expressed genes between sample groups differed per patient. To this end, a patient factor was included in the design of limma; however this did not change the results (data not shown).

Table 4 | Overview of differentially expressed probes (DEPs) between the different sample groups.

Number of samples	SCC vs. NS 15 vs. 13	AK vs. NS 14 vs. 13	SCC vs. AK 15 vs. 14	'Progression'
# of DEPs with FDR < 0.01	6820[1] (3333/3487)	3734 (1554/2180)	2131 (1088/1043)	658 (262/396)
# of DEPs with FDR < 0.01 and $\log_2$FC >= 0.5	2087 (1087/1009)	977 (526/451)	571 (289/282)	180 (90/90)
# of DEP with FDR < 0.01 and $\log_2$FC>= 1.0	639 (370/269)	219 (167/52)	145 (81/64)	40 (32/8)

SCC, squamous cell carcinoma; AK, actinic keratosis; NS, normal skin; FDR, false discovery rate, FC, fold change.
[1] Total number of DEPs (number of upregulated DEPs/number of downregulated DEPs)

* Additional file 1 can be requested by the author of this thesis and contains results of the toptable from the limma analysis, differentially expressed probes between SCC and NS, between AK and NS, between SCC and AK, and the progression list with FDR < 0.01 and $\log_2$FC >= 0.5, including the VST transformed RSN normalized data.

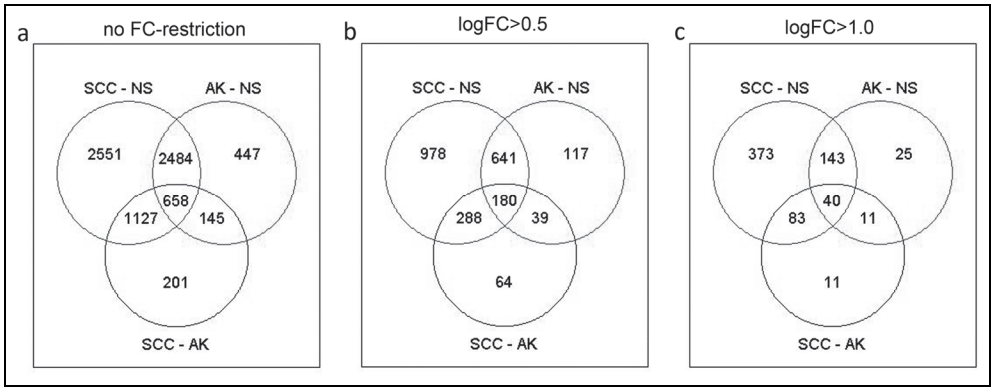

Figure 3 | Venn diagrams of differentially expressed probes (DEPs) from different comparisons within the three sample groups of normal skin (NS), actinic keratosis (AK) and squamous cell carcinoma (SCC). The false discovery rate (FDR) was set at <1%. DEPs with FDR<1% (a). DEPs with $\log_2$FC>0.5 and FDR<1% (b). DEPs with $\log_2$FC>1.0 and FDR<1% (c).

5

Geneset enrichment analyses of expression of SCCs and AKs

In addition to single gene analysis, affected molecular pathways were investigated employing gene set enrichment analysis (GSEA) using two different approaches. Firstly, differentially expressed probes between the sample groups from the limma analysis with $\log_2$FC>0.5 (Additional file 1)* were analyzed for gene set enrichment with DAVID Bioinformatic Resources. All annotated and expressed probes (n=15,969) were used as background list (Additional file 2)*. Genes involved in epidermal development and keratinocytes were among the most enriched GO terms of the biological processes (BP) node in all comparisons. Also KEGG pathways were analyzed by DAVID. When comparing SCC with AK, genes involved in *focal adhesion* and *cancer pathways* in were enriched among the DEGs (Additional file 2)*.

In the second GSEA approach, the entire dataset was analyzed with the PGSEA package (Figure 4). In this analysis expression profiles of AKs and SCCs were compared to those of NS. PGSEA analysis demonstrated that genes upregulated by RAS were enriched in SCC

* Additional files 1 and 2 can be requested by the author of this thesis. Additional file 1 contains results of the toptable from the limma analysis, differentially expressed probes between SCC and NS, between AK and NS, between SCC and AK, and the progression list with FDR < 0.01 and $\log_2$FC >= 0.5, including the VST transformed RSN normalized data. Additional file 2 contains results of the DAVID analysis for the differentially expressed probes between the sample groups from the limma analysis with $\log_2$FC>0.5 and FDR < 0.01.

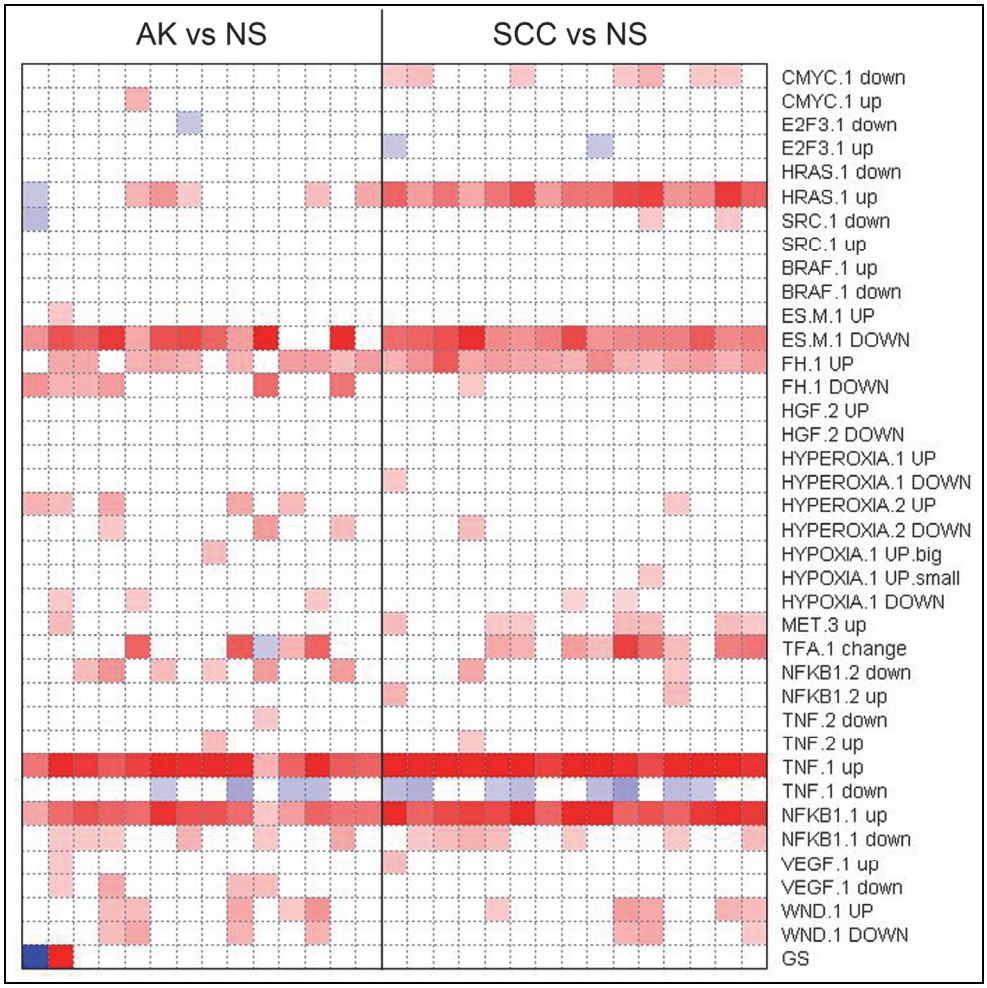

Figure 4 | Results of the Parametric geneset enrichment analysis (PGSEA). Gene expression profiles derived from actinic keratosis (AK, n=14) and squamous cell carcinoma (SCC, n=15) samples were compared with gene expression profiles derived from normal skin (NS, n=13) samples and analyzed using PGSEA for the gene lists that contain genes responsive to oncogenes or for indicated pathways. The genes that show increased expression to NS for each pathway are indicated with 'up'. List of genes that show decreased expression relative to control cells for each pathway are indicated with 'down'.[28] The resulting *t*-statistic for each gene list was plotted (-10<t<10), p<0.005); red squares represent a significant number of genes in the list with increased expression in tumor samples (AK or SCC) relative to NS; blue squares represent a significant number of genes in each list with decreased expression.

compared to NS, whereas this was not seen in AK. For both SCC and AK genes positively regulated by TNF, NFκB and fumarate-hydratase (FH, known to be involved in aggressive renal papillary cancers) were enriched.[39] Genes regulated by the oncogenes BRAF and SRC were not enriched in tumors compared to NS.

In addition to GSEA, the results from the limma analysis ($log_2FC>0.5$, FDR<0.01, additional file 1)* were subjected to oPOSSUM analysis to investigate if the DEGs were controlled by specific transcription factor (TFs). The TFs whose transcription factor binding sites (TFBSs) were found enriched are listed in Table 5. In the list TFs of upregulated genes, the REL transcription factor class (incl. RELA and NFκB1) was overrepresented. These results correspond with the PGSEA, where genes controlled by NFκB1 were upregulated in SCC and AK (Figure 3). The forkhead (incl. FOXF2 and FOXD1) and ZH-finger (incl. SP1 and MZF1) TF classes were overrepresented in the TFBS of downregulated genes.

Comparison of genome-wide SNP analysis and GWEA

Expression levels of both AKs and SCCs were compared to those of NS based on their chromosomal location to identify any regional chromosomal expression bias using the *reb* package.[32] Since at the genomic level only a few, non-recurrent chromosomal alterations were found, we compared the results of the genome-wide SNP analyses with those of the regional expression level results per tumor. However, in only very few regions where at the SNP level alterations were seen the expression level of genes in this region were affected too (data not shown).

Validation of the GWEA with QPCR

To validate microarray results, 9 DEGs were selected based on their high log_2FC, highly significant adjusted p-value, involvement in identified pathways from the GSEA and potential biological relevance for SCC development. Their expression was quantified by QPCR analysis in all patient samples. The expression of these 9 genes was normalized for the expression of 4 reference genes, which were selected based on their stable expression in the GWEA, using geNORM. Relative differences between sample groups were confirmed for all genes (Table 6, Figure 5), although fold changes were often higher in QPCR results compared to those from the gene expression analysis (Table 6). This is probably due to the larger dynamic range of QPCR compared to array-based analysis.

* Additional file 1 can be requested by the author of this thesis and contains results of the toptable from the limma analysis, differentially expressed probes between SCC and NS, between AK and NS, between SCC and AK, and the progression list with FDR < 0.01 and $log_2FC >= 0.5$, including the VST transformed RSN normalized data.

Table 5 |Results of oPOSSUM analysis of overrepresented transcription factors in the differentially expressed genes from limma (logFC>0.5, FDR<0.01).[33]

TF	TF class	Target genes	Z-score [1]	Fisher score [2]
SCC vs NS				
Up- and downregulated genes (1514 of 2036 genes included)[3]				
SRF	MADS	107	12.25	7.38E-05
Hand1-Tcfe2a	bHLH	1148	10.30	3.31E-06
RELA	REL	576	8.01	1.21E-06
SP1	ZN-FINGER, C2H2	1036	7.80	1.34E-09
SPIB	ETS	1374	5.97	4.72E-06
Upregulated genes (736 of 1039 genes included)				
SRF	MADS	62	16.93	5.02E-05
RELA	REL	291	11.68	2.66E-04
Hand1-Tcfe2a	bHLH	565	9.30	1.53E-02
ELF5	ETS	658	9.25	2.38E-05
REL	REL	450	8.40	2.86E-05
Downregulated genes (758 of 1004 genes included)				
FOXF2	FORKHEAD	221	12.93	1.52E-06
SP1	ZN-FINGER, C2H2	536	11.03	1.12E-08
FOXD1	FORKHEAD	459	8.409	2.16E-06
Foxq1	FORKHEAD	349	7.176	1.47E-06
TP53	P53	3	6.687	1.04E-01
AK vs NS				
Up- and downregulated genes (695 of 960 genes included)				
SP1	ZN-FINGER, C2H2	494	16.58	1.32E-08
MZF1_1-4	ZN-FINGER, C2H2	644	14.28	2.43E-07
SRF	MADS	56	13.50	1.32E-04
Cebpa	bZIP	437	10.90	1.99E-05
TEAD1	TEA	217	10.80	8.74E-05
MZF1_5-13	ZN-FINGER, C2H2	527	10.37	1.59E-08
Upregulated genes (364 of 515 genes included)				
SRF	MADS	35	19.82	8.10E-05
ELF5	ETS	319	11.05	2.04E-04
RELA	REL	150	10.03	1.60E-04
SPIB	ETS	338	9.25	2.28E-04
TLX1-NFIC	HOMEO/CAAT	32	9.00	5.07E-03
Downregulated genes (695 of 960 genes included)				
SP1	ZN-FINGER, C2H2	248	17.04	1.63E-07
MZF1_1-4	ZN-FINGER, C2H2	309	11.7	3.74E-04
Arnt-Ahr	bHLH	289	11.49	2.25E-09
Cebpa	bZIP	228	11.18	5.86E-07
Roaz	ZN-FINGER, C2H2	130	10.88	2.11E-05

[1] The Z-score determines whether a transcription factor binding site (TFBS) occurs more frequently in the set of co-expressed genes compared to pre-computed background set provided by the package.

[2] The Fisher score (one-tailed Fisher exact) is calculated to determine the probability of non-random association between the co-expressed genes and the TFBS site of interest.

[3] The number of genes in the differentially expressed gene set that could be aligned to the pre-computed background.

Table 5 (continued) | Results of oPOSSUM analysis of overrepresented transcription factors in the differentially expressed genes from limma (logFC>0.5, FDR<0.01).[33]

TF	TF class	Target genes	Z-score [1]	Fisher score [2]
SCC vs AK				
Up- and downregulated genes (412 of 553 genes included)[3]				
RREB1	ZN-FINGER, C2H2	38	11.29	1.24E-03
FOXF2	FORKHEAD	111	10.99	7.16E-03
SRF	MADS	36	10.01	4.10E-04
RELA	REL	163	9.239	8.26E-04
TEAD1	TEA	120	8.031	2.46E-02
Upregulated genes (209 of 283 genes included)				
SRF	MADS	24	15.39	6.72E-05
RELA	REL	85	11.99	5.32E-03
Fos	bZIP	157	10.98	3.68E-04
NF-kappaB	REL	108	8.39	2.22E-04
REL	REL	129	7.91	1.93E-03
Downregulated genes (204 of 271 genes included)				
FOXF2	FORKHEAD	70	22.37	2.55E-05
FOXI1	FORKHEAD	126	10.74	7.22E-02
RREB1	ZN-FINGER, C2H2	22	9.86	1.81E-03
T	T-BOX	28	8.77	5.00E-03
Foxd3	FORKHEAD	129	7.91	5.37E-02
Progression genes				
Up- and downregulated genes (128 of 172 genes included)				
RELA	REL	54	10.18	1.00E-02
SP1	ZN-FINGER, C2H2	94	9.66	1.76E-03
FOXF2	FORKHEAD	36	7.30	5.18E-02
NFKB1	REL	35	6.21	1.09E-02
MZF1_1-4	ZN-FINGER, C2H2	118	6.11	3.15E-02
Upregulated genes (53 of 85 genes included)				
RELA	REL	23	14.0	5.41E-02
NFKB1	REL	19	9.78	2.48E-03
SRF	MADS	6	8.09	3.82E-02
TLX1-NFIC	HOMEO/CAAT	7	7.65	2.27E-02
MIZF	ZN-FINGER, C2H2	11	7.11	3.21E-02
Downregulated genes (75 of 87 genes included)				
FOXF2	FORKHEAD	29	14.63	6.46E-04
FOXI1	FORKHEAD	48	11.42	1.14E-01
T	T-BOX	13	8.14	7.45E-03
Foxa2	FORKHEAD	50	8.02	4.40E-02
SP1	ZN-FINGER, C2H2	56	7.60	7.94E-03

[1] The Z-score determines whether a transcription factor binding site (TFBS) occurs more frequently in the set of co-expressed genes compared to pre-computed background set provided by the package.

[2] The Fisher score (one-tailed Fisher exact) is calculated to determine the probability of non-random association between the co-expressed genes and the TFBS site of interest.

[3] The number of genes in the differentially expressed gene set that could be aligned to the pre-computed background.

Table 6 | Results of the QPCR validation compared with the results of the genome-wide expression analysis (GWEA).

QPCR validation experiment												
	Normalized relative expression[1]						Fold change and P-value Student's *t*-test[2]					
	NS (n=10)		AK (n=13)		SSC (n=15)		SCC vs NS		AK vs NS		SCC vs AK	
Gene	Median	SE	Median	SE	Median	SE	log_2(FC)	p-value	log_2(FC)	p-value	log_2(FC)	p-value
CCL27	18,45	2,53	2,46	0,91	0,11	0,14	-7,34	**5,48E-05**	-2,91	**1,80E-04**	-4,43	**3,30E-03**
K17	0,12	0,03	1,19	0,41	5,20	0,97	5,39	**7,13E-05**	3,26	**7,07E-03**	2,13	**1,13E-03**
MMP1	0,01	0,01	0,28	1,16	47,19	35,2	12,18	5,68E-02	4,80	**2,32E-01**	7,38	6,14E-02
MMP3	0,01	0,01	0,36	0,37	17,91	4,95	10,99	**3,03E-03**	5,36	4,07E-02	5,63	**4,31E-03**
MMP9	0,07	0,01	1,83	0,74	4,49	4,21	6,07	**1,82E-02**	4,77	**4,42E-03**	1,30	6,07E-02
MMP10	0,02	0,03	0,95	1,17	17,70	8,24	9,59	**2,69E-03**	5,38	4,53E-02	4,21	**5,16E-03**
PI3	0,02	0,01	2,01	1,67	10,62	6,23	8,95	**5,46E-03**	6,55	**7,71E-03**	2,40	**3,25E-02**
S ERPINB4	0,004	0,002	1,99	6,2	18,79	15,7	12,33	**2,35E-02**	9,09	**3,96E-02**	3,24	1,46E-01
TUBB3	0,51	0,08	0,64	0,17	3,68	0,94	2,85	**1,17E-03**	0,32	**3,20E-01**	2,53	**1,78E-03**
Genome-wide expression analysis												
	Normalized expression[3]						Results limma analysis					
	NS (n=13)		AK (n=14)		SSC (n=15)		SCC vs NS		AK vs NS		SCC vs AK	
Gene	Median	SE	Median	SE	Median	SE	log_2FC	Adj. p-val	log_2FC	Adj. p-val	log_2FC	Adj. p-val
CCL27	12,92	0,02	10,74	0,10	8,60	0,03	-4,24	2,03E-15	-2,24	9,64E-08	-2,00	1,65E-06
K17	10,58	0,07	14,43	0,10	15,56	0,01	4,84	1,28E-14	3,16	5,56E-09	1,68	3,66E-04
MMP1	8,32	0,00	8,39	0,05	10,80	0,08	2,41	5,70E-10	0,22	5,65E-01	2,20	1,61E-07
MMP3	8,33	0,01	8,55	0,06	10,59	0,08	2,44	1,16E-09	0,50	1,59E-01	1,84	6,86E-06
MMP9	8,48	0,01	9,29	0,06	10,50	0,09	2,22	1,37E-07	1,05	8,50E-03	1,93	2,02E-06
MMP10	8,31	0,00	8,33	0,02	10,02	0,10	1,93	3,07E-07	0,09	8,41E-01	1,16	4,61E-03
PI3	9,16	0,05	13,60	0,14	15,27	0,04	5,68	1,33E-13	3,96	1,09E-08	1,72	3,44E-03
S ERPINB4	8,34	0,02	10,22	0,13	12,04	0,10	3,81	5,15E-09	2,16	3,64E-04	1,65	6,04E-03
TUBB3	8,84	0,01	8,86	0,05	10,45	0,05	1,91	5,45E-11	0,23	3,66E-01	1,67	5,28E-08

[1] Relative expression normalized to the expression level of four reference genes.
[2] Bold values represent the comparisons that could be statistically confirmed in the QPCR validation experiment.
[3] VST transformed RSN normalized data

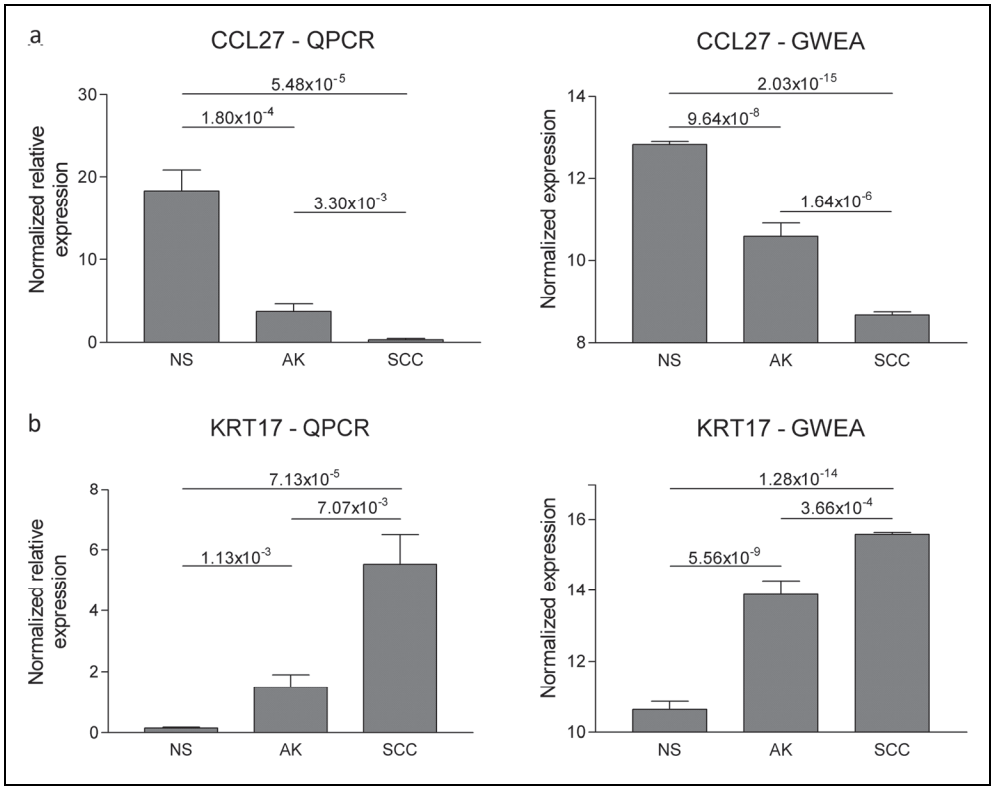

Figure 5 |QPCR and genome-wide expression analysis (GWEA). Histograms show the expression level of CCL27 in normal skin (NS), actinic keratosis (AK) and squamous cell carcinoma (SCC) samples measured by QPCR (a, left) and GWEA (a, right). Histograms show the expression level of keratin 17 (KRT17) in NS, AK and SCC samples measured by QPCR (b, left) and GWEA (b, right). For QPCR, the normalized relative expression level represents the expression of the gene of interest normalized to those of four reference genes. For the GWEA the normalized expression level represents the RSN normalized, VST transformed expression of the gene of interest.

Discussion

In the present study we performed genome-wide expression analysis on SCCs, AKs and NS from OTRs to identify common pathways involved in the cellular transformation from normal skin cells to AKs and eventually SCC. Data analysis disclosed large numbers of DEGs between NS, AKs and tumor samples and identified the activation of several known oncogenic pathways in SCC, some of which were also activated in AKs.

Our unique isogenic approach in this genome-wide profiling study on a well-documented sample series of OTRs, would circumvent the influence of any possible patient-specific

differences on the analysis, including type of immunosuppressive drug used, and would allow identification of genes and pathways specifically involved in progression of skin carcinogenesis. During the last years, several genome-wide expression studies on SCC and AKs have been conducted.[21-24] Most studies focused on genes differentially expressed in SCCs compared to normal skin, although some also included AK samples and cell lines. Since the various studies used different gene expression platforms, tumor selection criteria and isolation and labeling methods, it was impracticable to combine data from these studies with our data into one large dataset and perform a meta-analysis. However, we do see considerable overlap in results obtained, especially after pathway en gene set analyses.

Cluster analysis showed that samples derived from the same patient did not cluster together, indicating that gene expression differences between sample groups (NS, AK and SCC) were larger than differences between patients. So, inter-patient variation did not discernibly influence the results of the expression analysis in our study. Furthermore, gene expression profiles of three AKs demonstrating (mild to) severe dysplasia (AK_P-11, AK_P-18 and AK_P42) showed more similarity to that of SCCs than to the other AKs (Figure 2). Even though the numbers were too small to make any statistically reliable statement, this result suggests that the progression of AK to SCC is a continuous process.

Limma analysis demonstrated that more than 40% of the expressed and annotated probes were differentially expressed between SCC and NS; smaller numbers of DEGs were identified between AK and NS and between SCC and AK. When the analysis was restricted to probes with a $\log_2$FC> 0.5 or $\log_2$FC>1.0 the number of differentially expressed probes reduced dramatically, indicating that it was possible to identify subtle but significant changes in expression level in many genes. However, the large number of DEGs hampered identification of genes crucial to SCC development. Moreover, at least for the comparison of SCC with normal skin, differential gene expression might also be caused by non-specific differences owing to increased proliferation and metabolic rate of fast-growing tumor cells compared to keratinocytes in the epidermis. Similar results were obtained previously, where many transcripts showed relatively small changes in expression level between SCC and sun-exposed skin.[21] Additional gene-targeted, approaches are needed to investigate which genes/pathways are crucial for AK formation and subsequent SCC development.

Next to single gene analysis, GSEA was performed to identify specific gene sets and pathways involved in SCC development. With the online resource tool DAVID both GO terms and KEGG pathways were analyzed. From the GO terms analysis, many gene sets involved in (epidermal) cell proliferation and differentiation were enriched in SCC and AK.

These gene sets include genes encoding keratins, MMPs, S100 molecules and SPRRs, all (highly) upregulated in SCC and AK compared to normal skin. According to the KEGG analysis, several cancer pathways were enriched in SCC vs. AK or SCC vs. NS, and included 'pathways in cancer' and 'small cell lung cancer'. These cancer pathways comprise many genes downstream of known oncogenes, like RAS and MYC.

Upregulation of downstream targets of RAS was also identified by PGSEA when comparing the profiles of SCC to NS, indicating that this pathway is activated in SCC. NFκB1 and TNF pathways were activated in both AKs and SCCs, suggesting that activation of these pathways is an early event in the development of AK and SCC. NFκB1 is part of the REL TF family, which also includes REL and RELA. Gene promoter analysis by oPOSSUM showed that upregulated genes in SCC and AK were enriched for TF binding sites for REL transcription factors. These TFs have shown to be important in both skin development and carcinogenesis.[40, 41] The results from our oPOSSUM analysis concurred with those of a previous study.[21]

Both PSGEA and DAVID demonstrated activated RAS signaling in SCC, but not in AK. Previous studies have suggested that RAS might be activated via amplification of the gene locus or by activating mutations.[15] However, both copy number alterations (SNP analysis) and oncogenic hot-spot mutations in HRAS and KRAS (data not shown) were not found in our SCCs, suggesting other molecular events to be responsible for activating the RAS signaling. These might include overactivation of the epidermal growth factor receptor (EGFR) upstream of RAS, which is known to occur in a subset of cutaneous SCCs.[42, 43]

The accuracy of the GWEA was confirmed by validation experiments using QPCR. Differential expression could be confirmed for all nine genes tested. These genes were selected based on their $\log_2$FC and adjusted p-value, but also for their presumed biological relevance for the development to SCC. One of these genes, the keratinocyte-specific chemokine CCL27 was confirmed to be downregulated progressively in AK and SCC, corresponding to previous findings that CCL27 was downregulated in keratinocyte-derived tumors.[44] As CCL27 is involved in mediating cutaneous homing of T-lymphocytes, its downregulation could signify possible immune evasion by cutaneous SCCs.[45] Furthermore, our GWEA results are in agreement with previous reports that CCL27 is downregulated through activation of the RAS-MAPK-signaling pathway in human skin tumors.[44]

Several DEGs identified by GWEA concerned genes involved in epidermal differentiation. Upregulation of intermediate filament keratins K6, K16 and K17, concurred with our previous work in which we found these proteins abundantly expressed in cutaneous SCCs

of OTRS, in contrast to normal skin.[46] Also a recent study by Hudson *et al*. with samples from immunocompetent patients, showed that genes involved in epidermal differentiation were amongst the most DEGs between SCC and normal skin.[21]

Next to the genes important in epidermal differentiation, genes involved in extracellular matrix (ECM) organization were differentially expressed in SCCs compared to NS. Among others, QPCR confirmed MMP1, MMP3, MMP9 and MMP10 to be highly upregulated in SCC compared to normal skin, sometimes already in AK. Although MMPs are normally induced temporarily in response to exogenous signals, they are known to play a role in tumor progression and metastasis. MMP1, MMP3 and MMP10 are virtually absent in normal skin, but often found upregulated in cutaneous SCC, although not in AK.[47, 48] Moreover, MMP9 has been shown to be involved in the early development of cutaneous SCC in immunosuppressed individuals.[47] Even though it is known that the different MMPs have separate functions, MMPs often cooperate in parallel and are regulated by specific and non-specific inhibitors, such as serine proteases such as chymase, plasmin and kallikrein, to achieve targeted ECM degradation.[48] We were able to identify several kallikrein proteins upregulated in SCC compared to normal skin. Upregulation of plasmin and chymase was not found, however these might be inhibited by serpin peptidase inhibitors, such as SERPINB3 and SERPINB4. These genes, which are known to produce circulating SCC-antigens 1 and 2 respectively, were highly upregulated in SCCs in our study and have previously been reported to promote survival of SCC cells *in vitro*.[49]

The SCCs and AKs from the OTRs investigated in this study displayed very few genomic changes. The careful selection of tumor material and the results of the GWEA and QPCR analyses, make us believe that this lack of observed changes is not caused by interference of tumor material with that of normal cells. Nor do we have any indication that many alterations remained undetected because of the Illumina Genotyping Beadchip platform we used. This platform has been successfully used in various other genomic profiling studies.[50, 51] Our results from the genome-wide SNP analyses contrast reports on previous studies in which SCCs displayed highly complex karyotypes, including many gains and losses of entire chromosome arms.[15, 52] Also in AKs chromosomal aberrations have been reported to occur.[20] However, more recently Purdie *et al*. demonstrated that SCCs could be separated in genetically distinct subpopulations related to the differentiation status of the tumor.[18] Our results coincide with the observation in this study that well-differentiated SCCs possess fewer genomic aberrations compared to moderate and poorly differentiated tumors, albeit that the absolute number of aberrations per SCC in our study was lower. Although no relationship was detected by Purdie *et al.* between the patient's immune status and the number of aberrations observed, eight of nine tumor with 3 or less

alterations originated from transplant patients. This observation and the results of our study suggest that perhaps the suppression of the immune system in OTRs may influence the development of SCCs in these patients. This phenomenon has been reported before by Rehman *et al*., who demonstrated that the LOH rate in SCCs from OTRs was less than half of that in SCCs from immunocompetent patients.[53] Moreover, there could also be a direct effect of the applied immunosuppressive drugs on the molecular pathogenesis of SCCs in OTRs, which has also been suggested before by others.[54] Larger comparative studies with SCCs from both OTRs and immunocompetent patients will be necessary to elucidate this matter further.

The results from our genome-wide SNP analysis are unexpected in view of the many changes in mRNA expression levels found in both SCCs and AKs compared to normal skin. Next to a role for immunosuppression as seen in OTRs, the many differences in gene expression observed might be attributable to epigenetic alterations, such as DNA methylation or changes in miRNA expression. The fact that many genes were differentially expressed between tumors and normal skin may be caused by demethylation of these genes or modulation of their transcription factors (e.g. (de)methylation or (de)phosphorylation or interference from micro-RNA).

With this study we were able to demonstrate vast differences in gene expression profiles to exist between SCC, AK and NS from immunosuppressed OTRs. Moreover, we found that several pathways activated in SCCs were already activated in AKs, confirming the assumption that AKs are the precursor lesions of SCCs. These pathways include the NFκB1 and TNF pathways. RAS and MYC oncogenic pathways on the other hand appear to be specifically activated in SCC. Since the drastic changes in gene expression appeared unlinked to specific genomic gains or losses, the causal events driving SCC development require further investigation. The outcome of the current study also suggests that the early activation of NFκB1 and TNF pathways in the course of SCC development may offer opportunities for targeted preventive intervention in OTRs which may counter act *field cancerisation* by eradicating plaques formed by multiple AKs.

Acknowledgements

The authors thank the patients for the cooperation in this study, Wim Zoutman and Coby Out for their technical assistance, Branco Misovic and Jelle Goeman for their help with the statistical analysis of the GWEA, the Leiden Genome Technology Center for their technical assistance and the pathology department is for the histopathological evaluation of the tumor samples.

References

1. Bordea, C. et al. Skin cancers in renal-transplant recipients occur more frequently than previously recognized in a temperate climate. *Transplantation* **77**, 574-9 (2004).
2. Bouwes Bavinck, J.N. et al. The risk of skin cancer in renal transplant recipients in Queensland, Australia. A follow-up study. *Transplantation* **61**, 715-21 (1996).
3. Fortina, A.B. et al. Immunosuppressive level and other risk factors for basal cell carcinoma and squamous cell carcinoma in heart transplant recipients. *Arch Dermatol* **140**, 1079-85 (2004).
4. Glover, M.T., Deeks, J.J., Raftery, M.J., Cunningham, J. & Leigh, I.M. Immunosuppression and risk of non-melanoma skin cancer in renal transplant recipients. *Lancet* **349**, 398 (1997).
5. Brash, D.E. et al. A role for sunlight in skin cancer: UV-induced p53 mutations in squamous cell carcinoma. *Proc Natl Acad Sci U S A* **88**, 10124-8 (1991).
6. Ullrich, S.E. Mechanisms underlying UV-induced immune suppression. *Mutat Res* **571**, 185-205 (2005).
7. Proby, C.M. et al. A case-control study of betapapillomavirus infection and cutaneous squamous cell carcinoma in organ transplant recipients. *Am J Transplant* **11**, 1498-508 (2011).
8. Nindl, I., Gottschling, M. & Stockfleth, E. Human papillomaviruses and non-melanoma skin cancer: basic virology and clinical manifestations. *Dis Markers* **23**, 247-59 (2007).
9. Arron, S.T., Ruby, J.G., Dybbro, E., Ganem, D. & Derisi, J.L. Transcriptome sequencing demonstrates that human papillomavirus is not active in cutaneous squamous cell carcinoma. *J Invest Dermatol* **131**, 1745-53 (2011).
10. Ko, C.J. Actinic keratosis: facts and controversies. *Clin Dermatol* **28**, 249-53 (2010).
11. McGregor, J.M. et al. p53 mutations implicate sunlight in post-transplant skin cancer irrespective of human papillomavirus status. *Oncogene* **15**, 1737-40 (1997).
12. Jonason, A.S. et al. Frequent clones of p53-mutated keratinocytes in normal human skin. *Proc Natl Acad Sci U S A* **93**, 14025-9 (1996).
13. de Graaf, Y.G. et al. More epidermal p53 patches adjacent to skin carcinomas in renal transplant recipients than in immunocompetent patients: the role of azathioprine. *Exp Dermatol* **17**, 349-55 (2008).
14. Rebel, H. et al. Early p53-positive foci as indicators of tumor risk in ultraviolet-exposed hairless mice: kinetics of induction, effects of DNA repair deficiency, and p53 heterozygosity. *Cancer Res* **61**, 977-83 (2001).
15. Boukamp, P. Non-melanoma skin cancer: what drives tumor development and progression? *Carcinogenesis* **26**, 1657-67 (2005).
16. Tsang, D.K. & Crowe, D.L. The mitogen activated protein kinase pathway is required for proliferation but not invasion of human squamous cell carcinoma lines. *Int J Oncol* **15**, 519-23 (1999).
17. Ashton, K.J., Weinstein, S.R., Maguire, D.J. & Griffiths, L.R. Chromosomal aberrations in squamous cell carcinoma and solar keratoses revealed by comparative genomic hybridization. *Arch Dermatol* **139**, 876-82 (2003).
18. Purdie, K.J. et al. Single nucleotide polymorphism array analysis defines a specific genetic fingerprint for well-differentiated cutaneous SCCs. *J Invest Dermatol* **129**, 1562-8 (2009).
19. Purdie, K.J. et al. Allelic imbalances and microdeletions affecting the PTPRD gene in cutaneous squamous cell carcinomas detected using single nucleotide polymorphism microarray analysis. *Genes Chromosomes Cancer* **46**, 661-9 (2007).
20. Rehman, I., Takata, M., Wu, Y.Y. & Rees, J.L. Genetic change in actinic keratoses. *Oncogene* **12**, 2483-90 (1996).
21. Hudson, L.G. et al. Microarray analysis of cutaneous squamous cell carcinomas reveals enhanced expression of epidermal differentiation complex genes. *Mol Carcinog* **49**, 619-29 (2010).
22. Padilla, R.S., Sebastian, S., Jiang, Z., Nindl, I. & Larson, R. Gene expression patterns of normal human skin, actinic keratosis, and squamous cell carcinoma: a spectrum of disease progression. *Arch Dermatol* **146**, 288-93 (2010).
23. Ra, S.H., Li, X. & Binder, S. Molecular discrimination of cutaneous squamous cell carcinoma from actinic keratosis and normal skin. *Mod Pathol* **24**, 963-73 (2011).
24. Van Haren, R., Feldman, D. & Sinha, A.A. Systematic comparison of nonmelanoma skin cancer microarray datasets reveals lack of consensus genes. *Br J Dermatol* **161**, 1278-87 (2009).

25. Wisgerhof, H.C. et al. Incidence of cancer in kidney-transplant recipients: a long-term cohort study in a single center. *Cancer Epidemiol* **35**, 105-11 (2011).
26. Breuninger, H., Black, B. & Rassner, G. Microstaging of squamous cell carcinomas. *Am J Clin Pathol* **94**, 624-7 (1990).
27. Miller, S.A., Dykes, D.D. & Polesky, H.F. A simple salting out procedure for extracting DNA from human nucleated cells. *Nucleic Acids Res* **16**, 1215 (1988).
28. Du, P., Kibbe, W.A. & Lin, S.M. lumi: a pipeline for processing Illumina microarray. *Bioinformatics* **24**, 1547-8 (2008).
29. Lin, S.M., Du, P., Huber, W. & Kibbe, W.A. Model-based variance-stabilizing transformation for Illumina microarray data. *Nucleic Acids Res* **36**, e11 (2008).
30. Smyth, G.K. Linear models and empirical bayes methods for assessing differential expression in microarray experiments. *Stat Appl Genet Mol Biol* **3**, Article3 (2004).
31. Huang da, W., Sherman, B.T. & Lempicki, R.A. Systematic and integrative analysis of large gene lists using DAVID bioinformatics resources. *Nat Protoc* **4**, 44-57 (2009).
32. Furge, K.A. et al. Detection of DNA copy number changes and oncogenic signaling abnormalities from gene expression data reveals MYC activation in high-grade papillary renal cell carcinoma. *Cancer Res* **67**, 3171-6 (2007).
33. Ho Sui, S.J. et al. oPOSSUM: identification of over-represented transcription factor binding sites in co-expressed genes. *Nucleic Acids Res* **33**, 3154-64 (2005).
34. Edgar, R., Domrachev, M. & Lash, A.E. Gene Expression Omnibus: NCBI gene expression and hybridization array data repository. *Nucleic Acids Res* **30**, 207-10 (2002).
35. Hellemans, J., Mortier, G., De Paepe, A., Speleman, F. & Vandesompele, J. qBase relative quantification framework and software for management and automated analysis of real-time quantitative PCR data. *Genome Biol* **8**, R19 (2007).
36. Vandesompele, J. et al. Accurate normalization of real-time quantitative RT-PCR data by geometric averaging of multiple internal control genes. *Genome Biol* **3**, RESEARCH0034 (2002).
37. Braakhuis, B.J., Tabor, M.P., Kummer, J.A., Leemans, C.R. & Brakenhoff, R.H. A genetic explanation of Slaughter's concept of field cancerization: evidence and clinical implications. *Cancer Res* **63**, 1727-30 (2003).
38. Hofbauer, G.F., Bouwes Bavinck, J.N. & Euvrard, S. Organ transplantation and skin cancer: basic problems and new perspectives. *Exp Dermatol* **19**, 473-82 (2010).
39. Sudarshan, S., Linehan, W.M. & Neckers, L. HIF and fumarate hydratase in renal cancer. *Br J Cancer* **96**, 403-7 (2007).
40. Gugasyan, R. et al. The transcription factors c-rel and RelA control epidermal development and homeostasis in embryonic and adult skin via distinct mechanisms. *Mol Cell Biol* **24**, 5733-45 (2004).
41. Loercher, A. et al. Nuclear factor-kappaB is an important modulator of the altered gene expression profile and malignant phenotype in squamous cell carcinoma. *Cancer Res* **64**, 6511-23 (2004).
42. Commandeur, S., van Drongelen, V., de Gruijl, F.R. & El Ghalbzouri, A. Epidermal growth factor receptor activation and inhibition in 3D *in vitro* models of normal skin and human cutaneous squamous cell carcinoma. *Cancer Sci* (2012).
43. Rittie, L. et al. Differential ErbB1 signaling in squamous cell versus basal cell carcinoma of the skin. *Am.J.Pathol.* **170**, 2089-2099 (2007).
44. Pivarcsi, A. et al. Tumor immune escape by the loss of homeostatic chemokine expression. *Proc.Natl.Acad.Sci.U.S.A* **104**, 19055-19060 (2007).
45. Morales, J. et al. CTACK, a skin-associated chemokine that preferentially attracts skin-homing memory T cells. *Proc.Natl.Acad.Sci.U.S.A* **96**, 14470-14475 (1999).
46. Commandeur, S., de Gruijl, F.R., Willemze, R., Tensen, C.P. & El Ghalbzouri, A. An *in vitro* three-dimensional model of primary human cutaneous squamous cell carcinoma. *Exp.Dermatol.* **18**, 849-856 (2009).
47. Chebassier, N., Leroy, S., Tenaud, I., Knol, A.C. & Dreno, B. Overexpression of MMP-2 and MMP-9 in squamous cell carcinomas of immunosuppressed patients. *Arch.Dermatol.Res.* **294**, 124-126 (2002).
48. Tsukifuji, R., Tagawa, K., Hatamochi, A. & Shinkai, H. Expression of matrix metalloproteinase-1, -2 and -3 in squamous cell carcinoma and actinic keratosis. *Br J Cancer* **80**, 1087-91 (1999).
49. Ahmed, S.T. & Darnell, J.E., Jr. Serpin B3/B4, activated by STAT3, promote survival of squamous carcinoma cells. *Biochem Biophys Res Commun* **378**, 821-5 (2009).
50. Peiffer, D.A. et al. High-resolution genomic profiling of chromosomal aberrations using Infinium whole-genome genotyping. *Genome Res* **16**, 1136-48 (2006).

51. Yachida, S. et al. Distant metastasis occurs late during the genetic evolution of pancreatic cancer. *Nature* **467**, 1114-7 (2010).
52. Ashton, K.J., Carless, M.A. & Griffiths, L.R. Cytogenetic alterations in nonmelanoma skin cancer: a review. *Genes Chromosomes Cancer* **43**, 239-48 (2005).
53. Rehman, I., Quinn, A.G., Takata, M., Taylor, A.E. & Rees, J.L. Low frequency of allelic loss in skin tumours from immunosuppressed individuals. *Br J Cancer* **76**, 757-9 (1997).
54. O'Donovan, P. et al. Azathioprine and UVA light generate mutagenic oxidative DNA damage. *Science* **309**, 1871-4 (2005).

6

Epidermal growth factor receptor activation and inhibition in 3D *in vitro* models of normal skin and human cutaneous squamous cell carcinoma

Suzan Commandeur, Vincent van Drongelen, Frank R. de Gruijl and Abdoelwaheb El Ghalbzouri

Department of Dermatology, Leiden University Medical Center, Leiden, the Netherlands

Cancer Science 2012, doi: 10.1111/cas.12026

Abstract

The transmembrane tyrosine kinase epidermal growth factor receptor (EGFR) is considered a key player in the development of cutaneous squamous cell carcinoma (SCC), which is the second most common malignancy in white populations. Inhibition of EGFR with the small molecule tyrosine kinase inhibitor erlotinib is currently under clinical investigation in cutaneous SCC patients. In this study, we investigated the effects of EGFR activation and inhibition on normal and malignant *in vitro* human skin equivalents (HSEs). In healthy HSEs, increasing EGF concentrations ranging from 5 to 50 ng/ml resulted in a dramatic decrease in epidermal proliferation as immunohistochemically assessed by Ki67 and increased epidermal stress as assessed by keratin 17 after 2 weeks of air-exposed culture. Also, higher concentrations of EGF induced remarkable epidermal disorganization with loss of proper stratification. Similar effects were observed in HSEs generated with cutaneous SCC cell lines SCC-12B2 and SCC-13. Treatment of both healthy and SCC-HSEs with 10 µM erlotinib resulted in efficient reduction of epidermal thickness from 10 to 3 viable cell layers and counteracted EGF-induced epidermal stress. Remarkably, erlotinib treatment caused severe desquamation in healthy HSEs, reminiscent of xerosis as a known side-effect in patients treated with erlotinib. The presented three-dimensional organotypic SCC models appear suitable for further investigations on the morphological and functional impacts of modifying EGFR signaling in cutaneous SCC, without burdening patients or mice. The effective inhibition of epidermal growth by erlotinib in our HSEs confirms the therapeutic potential of this tyrosine kinase inhibitor for cutaneous SCC patients.

Introduction

Cutaneous squamous cell carcinoma (SCC) is one of the most common malignancies in Caucasian populations, causing substantial morbidity and mortality.[1, 2] Cutaneous SCCs originate from epidermal keratinocytes and are histopathologically characterized by uncontrolled advancing and often disorganized sheets of malignant epidermal cells invading the dermis.[3] Squamous cell carcinoma development is driven by a misbalance between proliferation and differentiation of epidermal keratinocytes.[3, 4] As a crucial player in epithelial tissue homeostasis, the transmembrane tyrosine kinase epidermal growth factor receptor (EGFR, also known as ErbB1 and HER1) is of vital importance in SCC development. In healthy epithelial tissue, EGFR signaling is involved in proliferation, differentiation and migration of epithelial cells.[5] Accordingly, overexpression and activation of EGFR is found in many epithelial cancers, including colorectal carcinoma, non small cell lung carcinoma and breast carcinoma.[6] In many carcinomas, EGFR overexpression is associated with more aggressive disease, poor prognosis and difficulties in treatment.[7] In cutaneous SCC, EGFR overexpression, numerical aberrations, genetic amplification and overactivation have been reported in comparison to normal skin.[8-10] In metastatic SCCs of cutaneous origin, EGFR overexpression is common.[11] Epidermal growth factor receptor has been shown to be activated by ligand binding or by ultraviolet radiation.[12] Epidermal growth factor receptor ligands include epidermal growth factor (EGF), heparin-binding EGF (HB-EGF), amphiregulin (AREG), betacellulin (BTC), transforming growth factor-α (TGF-α) and epiregulin.[13] In cutaneous SCCs and surrounding stroma, increased mRNA levels were shown for AREG, HB-EGF and TGF-α compared to adjacent normal skin.[9] Activation of EGFR results in activation of a complex network of signaling pathways, including the phosphoinositide 3 kinase (PI3K) pathway affecting the downstream Akt kinase.[5]

As a tyrosine kinase receptor, EGFR is a known drug target in epithelial cancers. Various small molecule EGFR inhibitors are approved for treatment of several epithelial cancers with EGFR overexpression, including colorectal and non small cell lung carcinoma.[7] Treatment of cancer patients with EGFR inhibitors is often associated with discomforting skin toxicity.[14] The small molecule tyrosine kinase inhibitor erlotinib has been shown to induce partial regression of cutaneous SCCs and its precursor lesion actinic keratosis.[15, 16] This EGFR inhibitor is currently under clinical investigation for treatment of recurrent, late-stage and metastatic cutaneous SCCs (www.clinicaltrials.gov: NCT00369512, NCT01198028, NCT01059305).

In the present study, we aimed to assess the effects of EGFR overactivation and EGFR inhibition on normal and transformed human skin. So far, modulation of EGFR activity in human skin cells *in vitro* is limited to two-dimensional monolayer cell cultures. Here we investigated for the first time the effects of EGFR activation and inhibition on normal and malignant three-dimensional human skin *in vitro*. To this end, we treated human skin equivalents (HSEs) with EGF and erlotinib. These HSEs allow for investigation of the role of EGFR in a relevant cutaneous microenvironment, as they recapitulate most of the *in vivo* characteristics of human skin, including a functional basement membrane and a living fibroblast-seeded dermis harboring extracellular matrix components.[3, 17] These models are therefore an excellent tool to study skin homeostasis, dermal-epidermal interactions or to mimic and study skin diseases.[18-20] In this study, we examined the effects of EGFR stimulation and inhibition in HSEs generated with both healthy and SCC keratinocytes.

Methods

Primary cells and cell lines

Healthy mamma reduction surplus skin of Caucasian women aged 37–41 years was obtained with written informed consent of the donors according to the Dutch law on medical treatment agreement. From this material, primary normal human epidermal keratinocytes (NHEKs) and primary normal human dermal fibroblasts (NHDFs) were isolated as described earlier.[18] Two SCC cell lines representing the tumorigenic populations of cutaneous SCCs (SCC-12B2 and SCC-13) were kindly provided by Dr J.G. Rheinwald.[21] These cell lines have been authenticated by short tandem repeat (STR) analysis no longer than 6 months prior to the experiments described in this work. Keratinocyte culture medium consisted of three parts of DMEM and one part of Ham's F12 (Invitrogen, Breda, the Netherlands) supplemented with 5% fetal bovine serum (FBS, HyClone/Greiner, Nürtingen, Germany), 100 U/ml penicillin, 100 µg/ml streptomycin (Invitrogen), 1 µM hydrocortisone, 1 µM isoproterenol and 0.1 µM insulin (Sigma-Aldrich, Zwijndrecht, the Netherlands). Normal human epidermal keratinocytes were used for experiments in their first passage and cultured at 37°C and 7.3% CO_2. Fibroblast culture medium consisted of DMEM supplemented with 5% FBS and 10 mg/ml penicillin/streptamycin. Normal dermal fibroblasts were used for experiments in their second or third passage and cultured at 37°C and 5% CO_2. For both NHEKs and NHDFs, culture medium was refreshed twice a week.

Human skin equivalents

Human skin equivalents were generated as described earlier.[17] Briefly, dermal equivalents were generated by seeding rat-tail collagen (4 mg/ml, isolated in-house) with $1.25x10^5$

fibroblasts/ml, which were incubated for 1 week under submerged conditions in fibroblast medium at 37°C and 5% CO_2. Subsequently, dermal equivalents were seeded with $5x10^4$ keratinocytes/cm^2 (either NHEKs, SCC-12B2 or SCC-13). Human skin equivalents were incubated overnight under submerged conditions at 37°C and 7.3% CO_2 in standard keratinocyte medium as described above. After 3 days, FBS was reduced to 1%. Two days thereafter, FBS was omitted and HSEs were cultured at the air-liquid interface for 14 days while medium was refreshed every 3 days. Culture medium used during the air-exposed period was keratinocyte medium as described above, but without serum and supplemented with 2 µM L-serine, 10 µM L-carnitine, 1 µM DL-α-tocopherol-acetate, 50 µM ascorbic acid, $2.4x10^{-5}$ µM BSA and a free fatty acid supplement which contained 25 µM palmitic acid, 30 µM linoleic acid and 7 µM arachidonic acid (Sigma-Aldrich). Culture medium was refreshed twice a week.

Epidermal growth factor treatment

Healthy HSEs based on NHEKs and HSEs with SCC-12B2 or SCC-13 were cultured in the presence of either 5 ng/ml, 20 ng/ml or 50 ng/ml EGF (Roche, Basel, Switzerland) during their entire airexposed culture period of 14 days (chronic exposure). After termination, all HSEs were processed for immunohistochemistry.

Erlotinib treatment

Erlotinib (Roche) was dissolved in DMSO to a 10 mM stock solution and kept at room temperature to prevent precipitation. Based on literature and suppliers' instructions for epithelial cells, erlotinib was further diluted in the culture medium to a final concentration of 10 µM.[22, 23] Healthy HSEs based on NHEKs were cultured in the presence of 10 µM erlotinib either during their entire 14-day air-exposed culture period (chronic exposure), or only during the last 4 days of this period (from 10 to 14 days air-exposed). Another set of healthy HSE cultures was supplemented with 5 ng/ml EGF during their entire air-exposed culture period of 14 days and co-supplemented with 10 lM erlotinib either during their entire air-exposed culture period or only during the last 4 days of this period (from 10 to 14 days air-exposed). Furthermore, HSEs based on SCC-12B2 or SCC-13 keratinocytes were cultured in the presence of 10 µM erlotinib during their entire 14-day air-exposed culture period. Afterwards, HSEs were terminated and processed for immunohistochemistry.

Immunohistochemistry

Human skin equivalents processed for immunohistochemistry were cut into two fragments. One part was snap-frozen in liquid nitrogen while the other part was fixed in 4% paraformaldehyde, dehydrated and paraffin embedded. Global histological analysis

was performed on 5 µm sections through staining with H&E. Immunohistochemical analysis of involucrin (1:200, clone SY5, Santa Cruz Biotechnology, Santa Cruz, CA, USA), keratin 10 (1:50, DEK10, Labvision/Neomarkers, Fremont CA, USA), keratin 16 (1:20, clone LL025, AbD Serotec, Düsseldorf, Germany), keratin 17 (1:400, clone CKE3, Sigma, St. Louis, MO, USA) and Ki67 (1:100, clone MIB1, DAKO, Glostrup, Germany) was performed on 5 µm sections that were cut, dried o/n at 60°C, deparaffinized and rehydrated. For antigen retrieval, sections were boiled in citrate buffer (pH 6.0) in an autoclave at 110°C for 5 min. Endogenous peroxidase activity was blocked with methanol and H_2O_2. Sections were blocked with 5% normal goat serum in 1% bovine serum albumin (BSA) in PBS for 10 min at room temperature prior to incubation with the primary antibody overnight at 4°C. Next, sections were incubated with biotinylated goat anti mouse secondary antibody for 1h at room temperature. Sections were labeled with streptavidin-biotin in 1% BSA in PBS for 45 min at room temperature. Deaminobenzidinetetrahydrochloride was used as a chromogen. All sections were counterstained with haematoxylin.

Proliferation index

The proliferation index of HSEs was determined by the number of immunohistochemically stained Ki67 positive nuclei from a total number of 100 epidermal cells (x100%) in three different sections of each sample at a magnification of 200×. The resulting data are expressed as the mean of the three independent counts ± SD (error bars). This is a straightforward and generally accepted scoring method for proliferation determination in sections.[24]

Results

Epidermal growth factor results in decreased proliferation and affects differentiation

To assess the effect of EGF on three-dimensional skin models, we exposed healthy HSEs to EGF throughout their entire air-exposed culture period. Persistent exposure of healthy HSEs to 5 ng/ml, 20 ng/ml or 50 ng/ml EGF strongly influenced epidermal morphology, proliferation, differentiation and activation, as determined by immunohistochemical analyses. Exposure of healthy HSEs to increasing concentrations of EGF for 2 weeks resulted in substantial epidermal disorganization starting at 5 ng/ml EGF and persisting with 20 ng/ml and 50 ng/ml EGF (Figure 1a). The proliferation rate of epidermal keratinocytes after 2 weeks of culturing slightly increased from 0.27 (±0.01) to 0.33 (±0.07, P=0.01) upon chronic exposure to 5 ng/ml EGF, but dramatically decreased to 0.05 (±0.03, P< 0.05) at 20 ng/ml EGF, as quantified by immunohistochemical Ki67 staining (Figure 1b). Virtually no proliferation was observed at 50 ng/ml EGF (Figure 1b). Treatment of HSEs

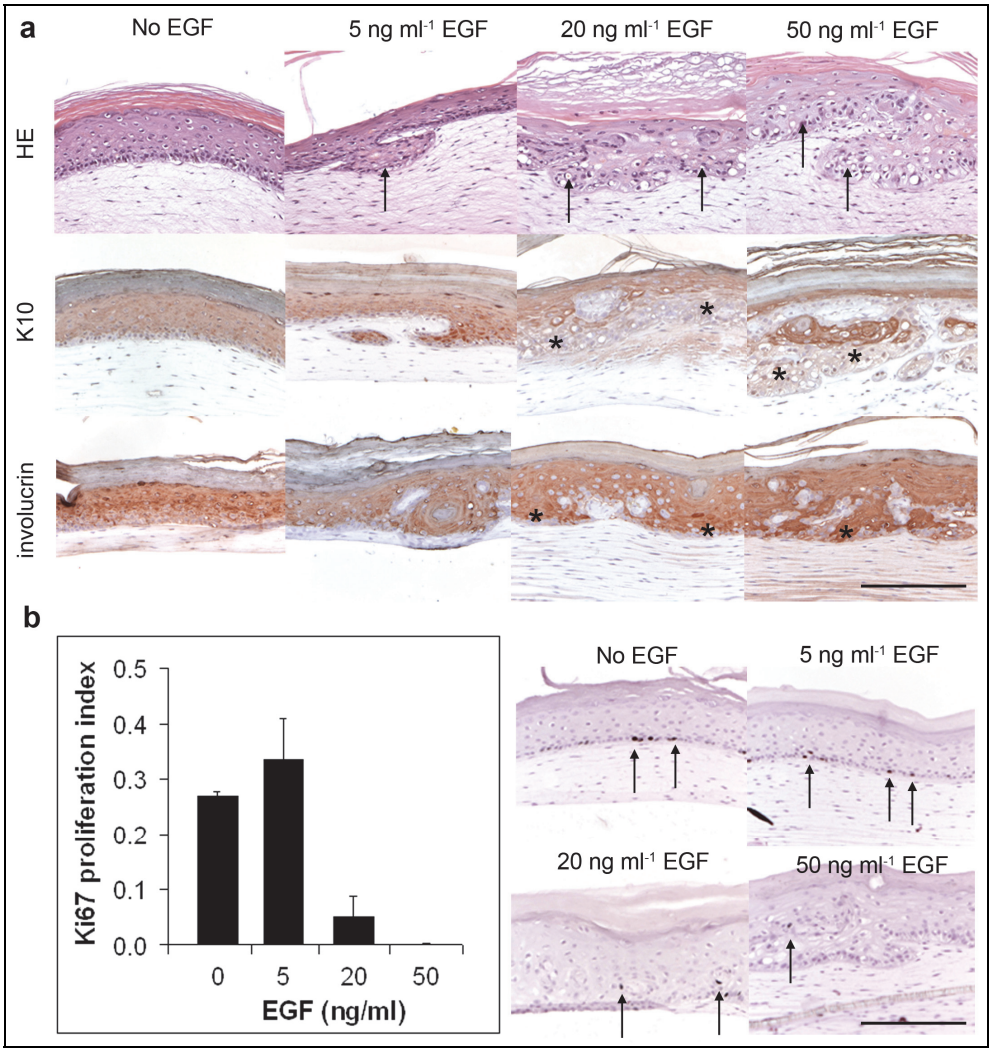

Figure 1 | Epidermal growth factor (EGF) affects epidermal morphology, proliferation and differentiation in human skin equivalents (HSEs). (a) Shown are cross sections of HSEs chronically supplemented with increasing concentrations of EGF. Epidermal growth factor-treated healthy HSEs stained with hematoxylin and eosin (HE) showed global epidermal disorganization increasing with EGF-concentration. Early differentiation of HSEs was disturbed upon exposure to increasing EGF concentrations, as reflected by a disorganized staining pattern of K10 at higher EGF concentrations. Terminal differentiation, as reflected by involucrin staining, slightly expanded over multiple cell layers in HSEs exposed to increasing concentrations of EGF. Arrows and asterisks indicate examples of significant staining patterns. Scale bar holds for all panels and indicates 200 µm. (b) Proliferation of HSEs first increased and then significantly decreased upon chronic exposure to increasing concentrations of EGF, as quantified after Ki67 staining. Representative Ki67 stainings are shown for all conditions. Arrows indicate examples of significantly stained nuclei.

with increasing concentrations of EGF resulted in a disturbed early differentiation pattern, as demonstrated by immunohistochemical staining of the early differentiation marker keratin 10 (K10). This protein is normally expressed in all suprabasal layers of the epidermis, while in EGF-treated HSEs it was found throughout the epidermis, along with the morphological disorganization at 20 ng/ml and 50 ng/ml (Figure 1a). Terminal differentiation also appeared to be slightly disturbed, as demonstrated by immunohistochemical staining of the late differentiation marker involucrin. Involucrin staining was present in the granular layers in control HSEs and slightly expanded to the lower suprabasal layers in HSEs stimulated with EGF (Figure 1a).

Epidermal growth factor induces epidermal stress in healthy human skin models

Epidermal stress increased upon EGF stimulation, as determined by immunohistochemical staining of stress associated proteins keratin 16 (K16) and keratin 17 (K17). In non-treated HSEs, K16 staining is predominantly observed in the stratum granulosum. Treatment with increasing concentrations of EGF resulted in intensified staining, expanding to the granular epidermal layers (Figure 2). Staining of K17 first appears at EGF levels of 5 ng/ml EGF and dramatically increases with increasing EGF concentrations (Figure 2).

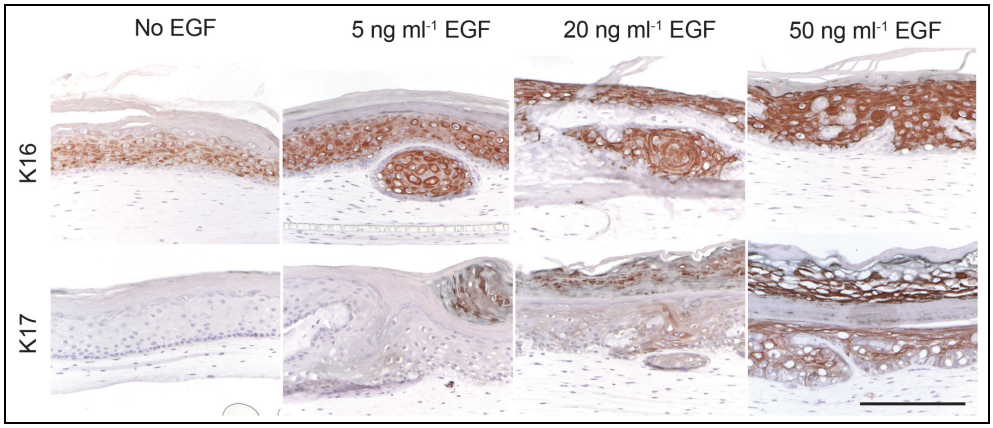

Figure 2 | Epidermal growth factor (EGF) increases epidermal stress in human skin equivalents (HSEs). Shown are cross sections of HSEs chronically supplemented with increasing concentrations of EGF. Epidermal activation and stress in HSEs increased upon chronic exposure to increasing concentrations of EGF, as indicated by immunohistochemical staining of epidermal stress markers keratin 16 (K16) and keratin 17 (K17). Scale bar holds for all panels and indicates 200 µm.

Erlotinib reduces epidermal thickness in healthy human skin models

Upon chronic supplementation with the EGFR-inhibitor erlotinib during the entire air-exposed culture period, the epidermal thickness of healthy HSEs was reduced from 10 to 3 viable cell layers, while lacking a clear stratum corneum (Figure 3a,b). To mimic the native situation, in which erlotinib is used on fully developed human skin, healthy HSEs were treated with 10 lM erlotinib during the last 4 days of their air-exposed culture period (from 10 to 14 days air-exposed). These cultures maintained their epidermal thickness of approximately 10 viable cell layers (Figure 3c). Also in these cultures, the stratum corneum was absent. When the HSEs were simultaneously supplemented with 5 ng/ml EGF and 10 µM erlotinib during the last 4 days of air-exposed culture (from 10 to 14 days airexposed), they showed a slightly reduced epidermal thickness of approximately 6 viable cell layers (Figure 3d). Again, the thickness of the stratum corneum was reduced. Pre-treatment of HSEs with 5 ng/ml EGF during the entire air-exposed period, combined with erlotinib treatment during the last 4 days resulted in a normal epidermis of 10 viable cell layers, topped by a thick stratum corneum (Figure 3e). Proliferation of basal keratinocytes in the epidermis of HSEs significantly decreased upon chronic erlotinib treatment, as assessed by Ki67 staining (Figure 4a). Differentiation of HSEs was unaffected by erlotinib treatment, as indicated by K10 and involucrin (Figure 4b). Erlotinib treatment did not result in epidermal stress, as reflected by the absence of K17 in erlotinib-treated HSEs (Figure 4b).

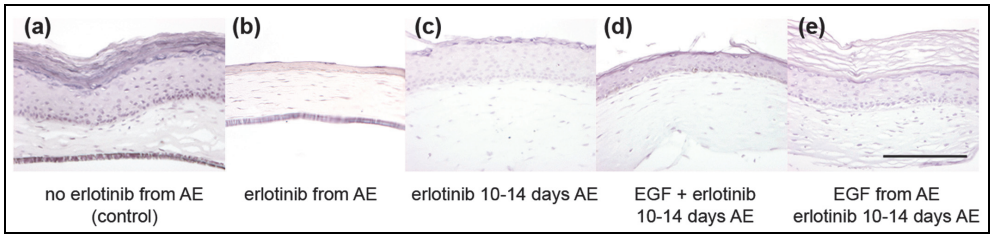

Figure 3 | Erlotinib reduces epidermal thickness and integrity. Shown are hematoxylin and eosin (HE) stained cross sections of healthy human skin equivalents (HSEs) treated with erlotinib during their air-exposed (AE) culture phase, either with or without 5 ng/mL epidermal growth factor (EGF). Treatment of healthy HSEs with erlotinib resulted in a lower number of viable cell layers and an absence of stratum corneum (b–d) when compared to untreated control HSEs (a). This effect was most pronounced upon chronic supplementation of erlotinib (b) and less pronounced when co-treated with EGF (d,e). When treated with erlotinib only in the final stage of the HSE culture (10–14 days AE), epidermal thickness was unaffected (c–e). Chronic supplementation with EGF, combined with erlotinib treatment in the final culture (10–14 days AE) phase affected neither the thickness of the epidermis nor that of the stratum corneum of the HSEs (e). Scale bar holds for all panels and indicates 200 µm.

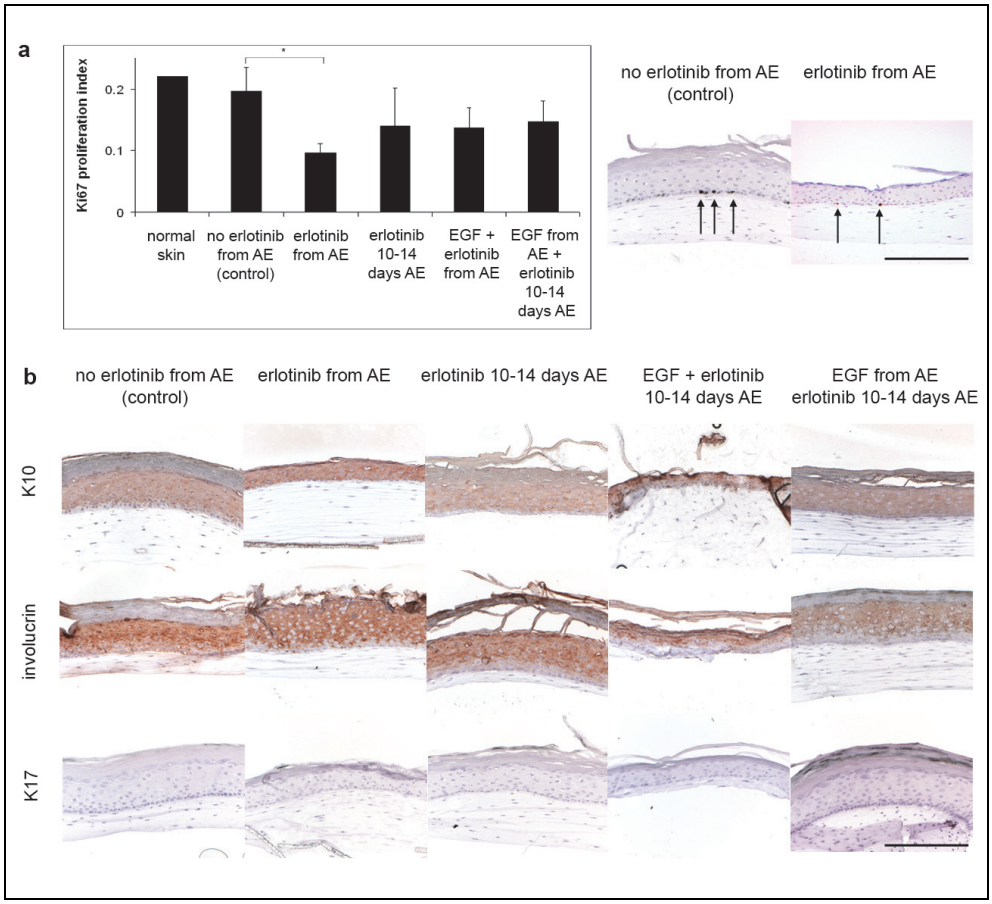

Figure 4 | Erlotinib affects epidermal proliferation, differentiation and activation in healthy human skin equivalents (HSEs). (a) Proliferation of HSEs significantly decreased after chronic erlotinib treatment during the entire air-exposed (AE) culture phase compared to normal skin and untreated HSEs, as quantified after Ki67 staining. Erlotinib treatment only during the last 4 days of AE culture (10–14 days AE) or simultaneous treatment with epidermal growth factor (EGF) did not significantly affect proliferation. Representative Ki67 stainings are shown for the significantly different conditions. Arrows indicate examples of significantly stained nuclei. (b) Shown are cross sections of HSEs supplemented with erlotinib, either with or without EGF. Erlotinib treatment did not affect early and terminal differentiation of HSEs, as reflected by K10 and involucrin staining, respectively. Erlotinib treatment did not result in epidermal stress, as K17 staining remained negative. Scale bar holds for all panels and indicates 200 µm.

Erlotinib efficiently reduces epidermal growth of malignant SCC cell line HSEs

When cultured in a HSE, cell line SCC-12B2 formed a thick, strongly disorganized epidermis with reduced dermis caused by its invasive potential (Figure 5). Upon chronic supplementation with 5 ng/ml EGF, the number of viable cell layers slightly increased while its disorganization was maintained. Higher concentrations of EGF did not result in any further morphological changes (data not shown). Chronic erlotinib supplementation of HSEs with SCC-12B2 cells resulted in a very thin epidermis. Human skin equivalents generated with cell line SCC-13 presented with a poorly attached but thick epidermis that is slightly disorganized, but still has a basal layer. Chronic EGF supplementation resulted in strong epidermal disorganization and reduced thickness. Upon erlotinib supplementation, HSEs generated with SCC-13 cells showed a strong reduction in the number of viable epidermal cell layers. Furthermore, a fraction of SCC-13 cells detached from the epidermis upon erlotinib treatment, resulting in epidermal scaling (Figure 5).

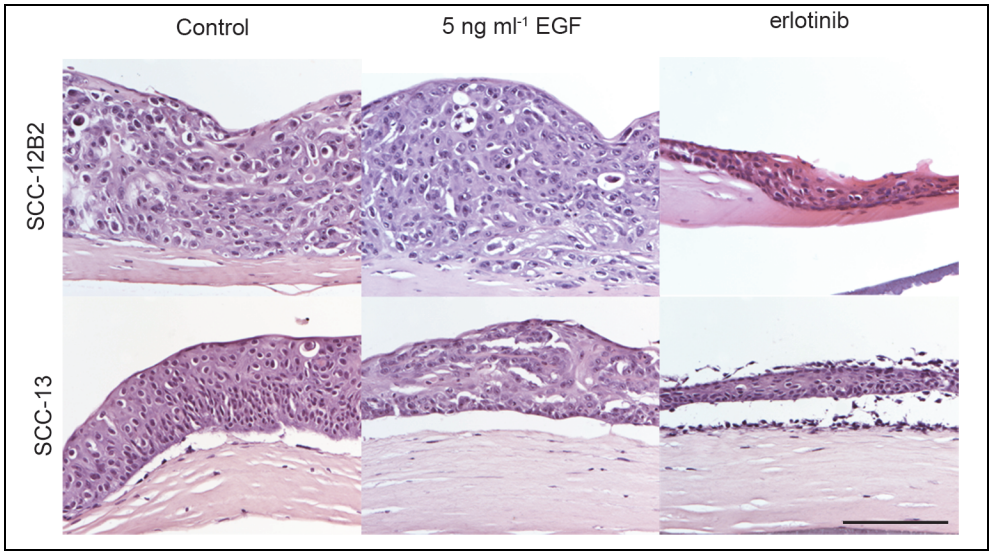

Figure 5 | Erlotinib affects epidermal thickness in human skin equivalents (HSEs) generated with squamous cell carcinoma (SCC) cell lines SCC-12B2 and SCC-13. Shown are hematoxylin and eosin (HE) stained cross sections of HSEs generated with cutaneous SCC cell lines SCC-12B2 and SCC-13 in the presence of epidermal growth factor (EGF) or erlotinib. SCC-12B2 incorporated in HSEs resulted in a thick and disorganized epidermis. Human skin equivalents with SCC-13 showed slight epidermal disorganization and poor dermal-epidermal attachment. Upon EGF supplementation, epidermis generated with SCC-12B2 thickened, whereas epidermis generated with SCC-13 increased in disorganization. Erlotinib treatment resulted in strongly reduced epidermal thickness, leaving a thin disorganized epidermal SCC-12B2 cell layer and a thin and detached but scaly SCC-13 cell layer on top of the dermal equivalent. Scale bar holds for all panels and indicates 200 µm.

Discussion

To investigate the effects of EGFR activation and inhibition on normal and malignant human skin, we generated and exposed three-dimensional *in vitro* human skin models with either NHEKs or SCC cell line keratinocytes to EGF and erlotinib. At a chronic but low concentration of 5 ng/ml, EGF treatment slightly increased epidermal thickness and proliferation in both healthy and malignant HSEs. In contrast, higher chronic EGF concentrations starting at 20 ng/ml resulted in drastically reduced epidermal proliferation in healthy HSEs without significantly affecting epidermal thickness. This is in concordance with earlier findings that EGF causes a dosedependent decrease in cell proliferation in SCC cell lines when cultured in a monolayer.[25] Moreover, EGF-induced EGFR activation resulted in severe epidermal disorganization and invasion, increasing with higher concentrations of EGF. This effect was not limited to healthy HSEs, as increased disorganization was also observed in HSEs generated with SCC-13. In the literature, similar results were reported with immortalized primary esophageal cells overexpressing EGFR, which increased invasion in a three-dimensional organotypic culture model and formed SCC-like tumors *in vivo*.[26] This indicates that EGFR may function as a switch between epidermal proliferation and differentiation *in vitro*, which is emphasized by the disturbance of both early and terminal differentiation patterns in healthy HSEs upon increasing EGF concentrations. Our findings in HSEs parallel those found in monolayer cultures in which mammalian keratinocytes were maintained in a disturbed differentiation state upon EGF stimulation.[27] Furthermore, epidermal stress increased in healthy HSEs upon stimulation with higher concentrations of EGF.[28] As these effects coincide with a decrease in epidermal proliferation, it might be interesting to investigate whether or not part of the epidermal cell population resides in a senescent state.

The small molecule tyrosine kinase inhibitor erlotinib is approved for treatment of several epithelial cancers and currently investigated for treatment of cutaneous SCC.[7, 15] As a proof of principle, we evaluated whether our malignant SCC-HSEs can serve as relevant *in vitro* readout systems to monitor effects of this small molecule tyrosine kinase inhibitor. Inhibition of EGFR by erlotinib resulted in a dramatic and significant reduction of epidermal thickness and proliferation in both healthy and SCC cell line generated HSEs compared to the unexposed controls. This was not observed upon short (4 days) exposure of established, healthy HSEs to erlotinib. So, HSEs treated from their early AE phase still need to form their final epidermal layers, which is efficiently blocked by erlotinib treatment. In established cultures, erlotinib treatment only results in breakdown of the stratum corneum. Longer treatment of these established cultures with erlotinib (beyond 14 days AE) may affect the other cell layers as well. Furthermore, in HSEs supplemented

with erlotinib the epidermal stress marker K17 was absent irrespective of prior EGF stimulation, in contrast to HSEs exposed to EGF alone. The fact that erlotinib efficiently inhibited the growth of two distinct malignant cutaneous SCC cell lines in our HSEs confirms the therapeutic potential of this drug for cutaneous SCC patients.[29] Remarkably, chronic supplementation of erlotinib caused severe desquamation in healthy HSEs. This was not observed upon short (4 days) exposure of HSEs to erlotinib. Desquamation also occurred in the outer cell layers of erlotinib-treated SCC-13 HSEs, but not in SCC-12B2 HSEs. This may be explained by the fact that SCC-12B2 represents poorly differentiated cells and SCC-12B2 HSEs completely lack any stratification or terminal differentiation, whereas SCC-13 HSEs show some stratification. In epithelial cancer patients treated with erlotinib or other EGFR inhibitors (e.g. gefitinib, lapatinib, cetuximab and panitumumab), a wide range of dermatological side-effects is observed, including severely dehydrated, fragile skin caused by abnormal keratinocyte differentiation, resulting in significant reduction of the thickness of the stratum corneum.[14, 30, 31] The loss of terminally differentiated cell layers upon erlotinib treatment in our HSEs appears to be an *in vitro* emulation of xerosis in patients. Future research may be directed at investigating the respective contribution of fibroblasts and keratinocytes to the eventual HSE phenotypes resulting from treatment with EGF and erlotinib. Altogether, these results prove our threedimensional healthy and malignant HSEs to be relevant and valid *in vitro* systems to study the effects of erlotinib and other anti skin cancer drugs.

Acknowledgements

We hereby thank Prof. Dr. R. Willemze and Dr. C.P. Tensen from the Department of Dermatology, Leiden University Medical Center, for critically reviewing the manuscript. Furthermore, we hereby acknowledge F. Hoffmann-La Roche, Basel, Switzerland for providing the erlotinib hydrochloride salt.

References

1. Erb, P. et al. Role of apoptosis in basal cell and squamous cell carcinoma formation. *Immunol.Lett.* 100, 68-72 (2005).
2. Williams, H. et al. Epidemiology of skin diseases in Europe. *Eur.J.Dermatol.* 16, 212-218 (2006).
3. Kane, C.L., Keehn, C.A., Smithberger, E. & Glass, L.F. Histopathology of cutaneous squamous cell carcinoma and its variants. *Semin Cutan Med Surg* 23, 54-61 (2004).
4. Kalluri, R. & Zeisberg, M. Fibroblasts in cancer. *Nat Rev Cancer* 6, 392-401 (2006).
5. Jorissen, R.N. et al. Epidermal growth factor receptor: mechanisms of activation and signalling. *Exp.Cell Res.* 284, 31-53 (2003).
6. Vlahovic, G. & Crawford, J. Activation of tyrosine kinases in cancer. *Oncologist.* 8, 531-538 (2003).
7. Mendelsohn, J. & Baselga, J. Status of epidermal growth factor receptor antagonists in the biology and treatment of cancer. *J.Clin.Oncol.* 21, 2787-2799 (2003).
8. Fogarty, G.B., Conus, N.M., Chu, J. & McArthur, G. Characterization of the expression and activation of the epidermal growth factor receptor in squamous cell carcinoma of the skin. *Br.J.Dermatol.* 156, 92-98 (2007).
9. Rittie, L. et al. Differential ErbB1 signaling in squamous cell versus basal cell carcinoma of the skin. *Am.J.Pathol.* 170, 2089-2099 (2007).
10. Toll, A. et al. Epidermal growth factor receptor gene numerical aberrations are frequent events in actinic keratoses and invasive cutaneous squamous cell carcinomas. *Exp Dermatol* 19, 151-3 (2010).
11. Shimizu, T. et al. Epidermal growth factor receptor overexpression and genetic aberrations in metastatic squamous-cell carcinoma of the skin. *Dermatology* 202, 203-206 (2001).
12. El Abaseri, T.B. & Hansen, L.A. EGFR Activation and Ultraviolet Light-Induced Skin Carcinogenesis. *J.Biomed.Biotechnol.* 2007, 97939 (2007).
13. Citri, A. & Yarden, Y. EGF-ERBB signalling: towards the systems level. *Nat Rev Mol Cell Biol* 7, 505-16 (2006).
14. Li, T. & Perez-Soler, R. Skin toxicities associated with epidermal growth factor receptor inhibitors. *Target Oncol* 4, 107-19 (2009).
15. Amini, S., Viera, M.H., Valins, W. & Berman, B. Nonsurgical innovations in the treatment of nonmelanoma skin cancer. *J Clin Aesthet Dermatol* 3, 20-34 (2010).
16. Hermanns, J.F., Pierard, G.E. & Quatresooz, P. Erlotinib-responsive actinic keratoses. *Oncol Rep* 18, 581-4 (2007).
17. El Ghalbzouri, A., Gibbs, S., Lamme, E., Van Blitterswijk, C.A. & Ponec, M. Effect of fibroblasts on epidermal regeneration. *Br.J.Dermatol.* 147, 230-243 (2002).
18. Commandeur, S., de Gruijl, F.R., Willemze, R., Tensen, C.P. & El Ghalbzouri, A. An in vitro three-dimensional model of primary human cutaneous squamous cell carcinoma. *Exp.Dermatol.* 18, 849-856 (2009).
19. El Ghalbzouri, A. et al. Fibroblasts facilitate re-epithelialization in wounded human skin equivalents. *Lab Invest* 84, 102-112 (2004).
20. El Ghalbzouri, A., Jonkman, M., Kempenaar, J. & Ponec, M. Recessive epidermolysis bullosa simplex phenotype reproduced in vitro: ablation of keratin 14 is partially compensated by keratin 17. *Am.J.Pathol.* 163, 1771-1779 (2003).
21. Rheinwald, J.G. & Beckett, M.A. Tumorigenic keratinocyte lines requiring anchorage and fibroblast support cultures from human squamous cell carcinomas. *Cancer Res.* 41, 1657-1663 (1981).
22. Birle, D.C. & Hedley, D.W. Signaling interactions of rapamycin combined with erlotinib in cervical carcinoma xenografts. *Mol Cancer Ther* 5, 2494-502 (2006).
23. Yamasaki, F. et al. Sensitivity of breast cancer cells to erlotinib depends on cyclin-dependent kinase 2 activity. *Mol Cancer Ther* 6, 2168-77 (2007).
24. Jonat, W. & Arnold, N. Is the Ki-67 labelling index ready for clinical use? *Ann Oncol* 22, 500-2 (2011).
25. Ponec, M., Weerheim, A., Kempenaar, J. & Boonstra, J. Proliferation and differentiation of human squamous carcinoma cell lines and normal keratinocytes: effects of epidermal growth factor, retinoids, and hydrocortisone. *In Vitro Cell Dev Biol* 24, 764-70 (1988).
26. Okawa, T. et al. The functional interplay between EGFR overexpression, hTERT activation, and p53 mutation in esophageal epithelial cells with activation of stromal fibroblasts induces tumor development, invasion, and differentiation. *Genes Dev.* 21, 2788-2803 (2007).
27. Rheinwald, J.G. & Green, H. Epidermal growth factor and the multiplication of cultured

human epidermal keratinocytes. *Nature* 265, 421-4 (1977).
28. El Ghalbzouri, A., Lamme, E. & Ponec, M. Crucial role of fibroblasts in regulating epidermal morphogenesis. *Cell Tissue Res.* 310, 189-199 (2002).
29. Uribe, P. & Gonzalez, S. Epidermal growth factor receptor (EGFR) and squamous cell carcinoma of the skin: molecular bases for EGFR-targeted therapy. *Pathol Res Pract* 207, 337-42 (2011).
30. Tan, W., Dong, Z., Wilkinson, T.A., Barbas, C.F., 3rd & Chow, S.A. Human immunodeficiency virus type 1 incorporated with fusion proteins consisting of integrase and the designed polydactyl zinc finger protein E2C can bias integration of viral DNA into a predetermined chromosomal region in human cells. *J Virol* 80, 1939-48 (2006).
31. Tsimboukis, S., Merikas, I., Karapanagiotou, E.M., Saif, M.W. & Syrigos, K.N. Erlotinib-induced skin rash in patients with non-small-cell lung cancer: pathogenesis, clinical significance, and management. *Clin Lung Cancer* 10, 106-11 (2009).

7

General discussion

Modeling cutaneous squamous cell carcinoma *in vitro*

The aim of the research described in this thesis was to develop a representative *in vitro* model of human cutaneous squamous cell carcinoma (SCC) for screening potential therapeutic compounds, without the unnecessary use of animals. To this end, we generated several three-dimensional *in vitro* SCC models in which the malignant epidermal cancer cells were either represented by intact primary human cutaneous SCCs from immune suppressed organ transplant recipients (OTRs) or by established, spontaneously immortalized human cutaneous SCC cell lines of OTR and non-OTR origin. The dermal microenvironment in our models was either represented by rat-tail collagen type III or by normal human dermal fibroblast-derived matrix (FDM) seeded with either primary normal human dermal fibroblasts (NHDFs) or primary cancer-associated fibroblasts (CAFs) isolated from OTR-SCCs. In verifying human cutaneous SCC representation in these *in vitro* models, we focused on hyperproliferation, cytological and architectural atypia and invasion as three main features of primary SCC. First, epidermal hyperproliferation is characterized by a thickened epidermis and an increased proliferation index, which are quantified by the number of viable cell layers present in the epidermis and by nuclear immunohistochemical staining of cell cycling marker Ki67, respectively. Second, cytologic and architectural atypia is characterized by large, atypic keratinocytes and a lack of organized maturation resulting in disturbed epidermal differentiation and stratification. Third, invasion is defined as the infiltration of epidermal cancer cells expanding through the basement membrane (BM) and populating the underlying dermis. A summary of the extent to which our *in vitro* SCC models as presented in this thesis represent primary human cutaneous SCCs is shown in Table 1.

Primary cutaneous SCC explant models

To study human cutaneous SCC in three-dimensional *in vitro* models, the epidermal compartment of such models should represent primary human SCC. As primary cutaneous SCC single cell cultures are notoriously difficult to establish, we based our *in vitro* SCC models on intact primary human cutaneous SCCs (**Chapter 2**).[1-3] To the best of our knowledge, all *in vitro* SCC models described to date have been generated with immortalized SCC cell lines.[4-8] Therefore, we described for the first time the three-dimensional *in vitro* expansion of primary SCC biopsies. As a reference, we also generated *in vitro* SCC models using established SCC cell lines SCC-12B2 and SCC-13. In all three model types, we used rat-tail collagen matrices seeded with NHDFs as a dermal component.

Table 1 | Comparison of different *in vitro* skin (cancer) models with normal skin and primary squamous cell carcinoma (SCC).

		HYPERPROLIFERATION	ARCHITECTURAL ATYPIA	INVASION
Normal skin	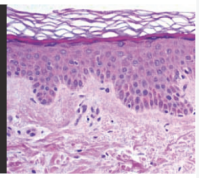	-	-	-
Primary SCC	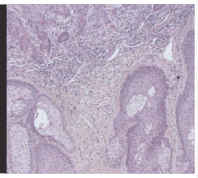	+++	+++	+++
Chapter 2 Primary SCC explant model	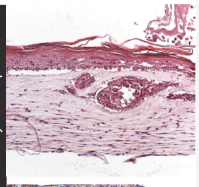	-	+	+
Chapter 2 SCC cell line model	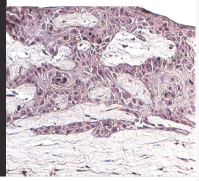	++	++	++
Chapter 3 SCC-CAF model	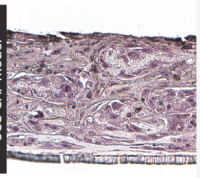	+	++	+++
Chapter 4 FDM model	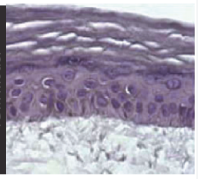	-	-	-
Chapter 6 SCC cell line model + EGF	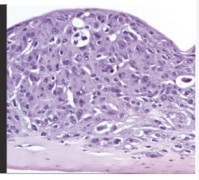	+++	+++	++

LEGEND

- no presence + weak presence ++ presence +++ strong presence

Hyperproliferation

In line with literature findings and based on quantified proliferation indexes, **Chapter 2** of this thesis describes the hyperproliferative state of original biopsies of OTR-SCCs in comparison to normal skin.[9-12] In literature, increased Ki67 gene expression was shown in various cutaneous SCC cell lines cultured in monolayers.[13] Accordingly, our *in vitro* models generated with SCC cell lines SCC-12B2 and SCC-13 presented with a thick epidermis and a high Ki67 proliferation index. Our primary SCC explant models laterally grew a thin epidermis with a proliferation index similar to that observed in normal skin. The limited epidermal thickness and proliferation index of these models suggests that the hyperproliferation present in the primary SCC biopsies is normalized in culture. However, determination of the proliferation index is an endpoint analysis performed after two weeks of air-exposed culture. This possibly obscures periods of hyperproliferation earlier in the culture period. The number of Ki67-positive cells in normal skin is known to progressively decrease after one week of air-exposed organ culture.[14] In contrast, the proliferation index of normal skin biopsies was fully maintained in our culture system after two weeks of culture, whereas dramatic loss of hyperproliferation was observed in primary SCC biopsies after two weeks of culture. This may be explained by the fact that the primary SCC biopsies harbored a heterogenic mixture of malignant SCC cells and associated skin and appendage cells, none of which had an apparent growth advantage in our culture system. Moreover, malignant cells present in the primary SCC biopsies may have lost too much cell-cell and cell-matrix contacts to maintain their hyperproliferative state.

Cytological and architectural atypia

All models described in **Chapter 2** of this thesis lacked proper epidermal stratification and showed aberrant early and late differentiation patterns. In terms of cytologic and architectural atypia, SCC cell line SCC-12B2 based models exhibited the best representation of primary SCC, with large fields of unstratified keratinocytes greatly varying in size and shape, accompanied by a distorted differentiation pattern. Without exception, cutaneous SCC cell line based three-dimensional *in vitro* models described in literature also show cytological and architectural atypia.[4-8] The epidermal compartments of our SCC cell line based models consisted of a single malignant cellular clone per model, whereas our primary SCC explant models harbored a heterogenic mixture of SCC cells and associated cells, also including healthy epidermal keratinocytes that generated a thin but stratified epidermis *in vitro*. Epidermal differentiation was however altered in our primary SCC explant models, showing aberrant expression of early differentiation-specific keratins K1 and K10 and consistent expression of K4 and K13, which are present in primary SCC and not in normal skin.[15] Furthermore, epidermal keratinocytes in all SCC models were in an

activated state, indicated by abundant expression of intermediate filament keratins K16 and K17. These keratins are only expressed in epithelial cells in pathologic conditions, including (chronic) wounds, psoriasis and cutaneous SCC.[16-18]

Invasion

The three-dimensional *in vitro* expansion and invasion of primary SCCs as described in this thesis are unique to the field. Our findings with SCC cell lines are in line with literature, showing extensive invasion of malignant cutaneous SCC cell lines in dermal rat-tail collagen matrices of three-dimensional *in vitro* models.[4-8] In our primary SCC explant model described in **Chapter 2**, a subpopulation of expanded SCC-associated keratinocytes formed squamous cell nests in the dermal matrix, resembling those of invasive well-differentiated primary SCC.[19] However, extensive invasive areas as seen in primary SCC and in invasive SCC cell line models based on SCC-12B2 were not observed in these primary SCC explant models. This may be explained by the fact that our culture conditions were not specifically selective for SCC cells heterogeneously residing in the primary SCC biopsy. The dermal matrix in these models was composed of non-human collagen type III seeded with healthy human fibroblasts, providing a normalized microenvironment that may offer limited tumor support. Therefore, the squamous cell nests observed in our primary SCC model may reflect the invasive capacity of lesional keratinocytes in concert with the healthy fibroblasts seeded in their dermal equivalent, possibly supported by few SCC-associated fibroblasts present in the primary biopsy as well.

A functional basement membrane (BM), which is formed upon interaction between epidermal keratinocytes and dermal fibroblasts, is the main physical barrier to invasion. In all invasive *in vitro* SCC models presented in **Chapter 2**, a continuous BM containing at least collagen type IV, laminin 332 and integrinβ4, was lining the dermal-epidermal junctions and all invasive squamous cell areas. This is in contrast with primary SCC, which is known to lack functional BM components.[20] Although great variability in BM aberrations is observed between tumors, well-differentiated and highly keratinized SCCs generally have a more continuous and functional BM than poorly differentiated and poorly keratinized SCCs, which combine a degraded BM with high protease activity.[20, 21] Like the majority of lesions available from OTRs, the SCC biopsies used to generate our primary SCC explant models were all pathologically classified as well-differentiated lesions. This may explain the limited invasion in our primary SCC explant models. The invasion observed may also result from an *in vitro* artifact. When modeling invasion *in vitro*, the BM should essentially be fully formed and functional first, before any genuine invasion may develop. The dermal matrices of the models described in this thesis do not contain a fully intact BM prior to seeding the malignant epidermal cells. These cells may therefore have

entered the dermal matrix well before BM formation has occurred, thereby not actively crossing a functional BM and thus not meeting the definition of invasion. This phenomenon of opportunistic migration should not be equated with true invasion, but should probably rather be considered an *in vitro* artifact. This invasive phenomenon is, however, never seen in healthy skin models seeded with normal healthy epidermal keratinocytes. This indicates that the opportunistically migrating malignant epidermal cells are at least able to actively break down the dermal matrix. These cells may also have the ability of crossing a functional BM and thus have invasive capacity, but cannot be inferred from the present endpoint observations after two weeks of culture. Following the cultures during their entire culture period would answer this question. This approach is however hampered by practical limitations, as each observation requires termination of the culture. To surely avoid such artifacts, dermal matrices with a pre-existing BM may be used, such as de-epidermized dermis (DED).[22, 23] The use of healthy DED, which harbors a fully functional pre-existing native BM, would allow for seeding malignant cells on a pre-existing BM. However, DEDs offer limited flexibility as logistics to obtain the material for upscaled research purposes is challenging.

In conclusion, our primary SCC explants and SCC cell lines cultured on rat-tail collagen matrices seeded with normal fibroblasts show limited proliferation and invasion, but represent cytological and architectural atypia hallmarking primary SCC. As such, the *in vitro* SCC models described in **Chapter 2** of this thesis represent useful models. However, primary SCC explant models are subject to practical limitations. First, availability of primary SCC biopsies is limited and requires tight logistics with the outpatient clinic, thereby limiting flexibility. Second, culture difficulties include the risk of microorganism infections inherent to immune-suppressed patient material and the critical handling in placing the primary SCC biopsy in the correct physical orientation onto the dermal matrix in order for the SCC cells to expand. Although these *in vitro* SCC explant models may best represent the heterogeneity of primary SCC in small-scale experimental research, upscaling of these models for large-scale industrial SCC compound screening is not feasible.

Modulating the dermal microenvironment

The development of invasive cutaneous SCC is not simply accomplished by unrestricted proliferation of the epidermal cancer cell population, but results from the active collaboration of SCC cells and various dermal components. To further increase representation of the primary lesion by our *in vitro* cutaneous SCC models, we modulated the dermal microenvironment of these models. We focused on the fibroblasts and the

extracellular matrix as the two main components of the dermal microenvironment *in vitro*. Replacement of healthy fibroblasts (NHDFs) by SCC-associated fibroblasts (CAFs) in the dermal matrix of our *in vitro* SCC cell line models resulted in a decreased proliferation index of epidermal keratinocytes after two weeks of air-exposed culture, as described in **Chapter 3** of this thesis. If persistent during the entire culture, this decreased proliferation would result in reduced epidermal thickness. However, no significant changes in epidermal thickness were observed. CAFs are known to affect the phenotype of both normal and malignant epidermal keratinocytes in both two- and three-dimensional co-culture systems.[24-30] The cytological atypia characteristic for SCC cell line models was not influenced by CAFs. However, terminal differentiation decreased in the epidermal compartment of CAF-based SCC cell line models, while architectural atypia increased. Moreover, we showed that invasion of SCC-12B2 cells dramatically increased when SCC-associated fibroblasts were used in the dermal matrix of *in vitro* SCC models instead of normal fibroblasts. Similar effects have never been described for cutaneous SCC, but are observed in *in vitro* models for oral SCC with transformed oral keratinocytes and immortalized and genetically engineered esophageal epithelial cells cultured with corresponding CAFs.[28, 31] Increased invasion in models cultured with SCC-associated fibroblasts coincided with a dramatic decrease in proliferation and terminal differentiation, which is in line with established reciprocal correlations between differentiation status of tumors and their potential to invade and metastasize.[19, 32] CAFs are therefore preferred in representative future *in vitro* SCC models. Furthermore, healthy skin models in which rat-tail collagen is replaced by normal human dermal fibroblast-derived matrix (FDM) result in a fully human dermal microenvironment more representative of *in vivo* human skin, as described in **Chapter 4** of this thesis. Therefore, replacement of rat-tail collagen matrix by primary SCC-associated fibroblast matrix (SCC-FDM) is recommended for future *in vitro* SCC models. However, SCC-associated fibroblasts are subject to limited passaging, as they retain their characteristic tumor-supportive features only in low passages *in vitro* (own observation confirmed by colleagues in the field by personal communication). The resulting need for primary cutaneous SCC material limits the availability of CAFs and their use in *in vitro* SCC models for large-scale industrial SCC compound screening.

Molecular profiling of primary SCC

Molecular profiling of primary cutaneous OTR-SCCs in comparison to its precursor lesions AK and normal skin as described in **Chapter 5** of this thesis allowed the further comparison of primary SCCs with their counterparts expanded *in vitro*. Based on mRNA expression profiles, SCC, AK and normal skin clustered in three distinct groups, with several thousands

of genes differentially expressed between the groups. The most prominent finding in primary SCCs was overexpression of the genes encoding intermediate filament keratins K16 and K17 in primary SCCs, which matched our findings in their cultured counterparts which showed abundant immunohistochemical staining of K16 and K17 that was retained throughout the entire explant culture period, as described in **Chapter 2** of this thesis. The pathways and genomic alterations marking the progression of precursor lesions to cutaneous SCC mainly concerned epidermal proliferation and differentiation, including keratins, S100 molecules and small proline-rich (SPRR) proteins. Furthermore, we demonstrated activation of RAS signaling in primary SCC biopsies, but not yet in AK, which has also been documented for SCCs of immune suppressed individuals.[33-35] The many differences in gene expression between our samples of SCC, AK and normal skin could not be explained by genomic alterations, as genome-wide SNP analysis showed very few copy number variations in SCC and AK, and these variations were unrelated to the observed gene expression changes.

Functional validation of *in vitro* SCC models

In order to test the applicability of *in vitro* SCC models as drug screening tools, they need to be functionally validated with active compounds. As enrichment of genes upregulated in the RAS pathway was found in our molecular profiling of primary SCCs as described in **Chapter 5** of this thesis, we used our *in vitro* SCC cell line models to functionally modulate this pathway, which was presented in **Chapter 6** of this thesis. An important upstream factor of RAS includes the transmembrane tyrosine kinase epidermal growth factor receptor (EGFR). Upregulated EGFR signaling was consistently found in cutaneous SCCs, rendering this receptor a potential treatment target that is currently under clinical investigation for cutaneous SCC. We therefore investigated the effects of epidermal growth factor (EGF) and erlotinib, a small molecule inhibitor of the EGF receptor (EGFR) tyrosine kinase upstream of RAS. Treatment of *in vitro* SCC models with lower concentrations of EGF significantly increased proliferation, whereas higher EGF concentrations arrested epidermal proliferation after two weeks of culture. EGF-treated *in vitro* SCC models showed a consistent and dose-dependent increase of cytological and architectural atypia. Erlotinib appeared an effective inhibitor of proliferation and invasion in the *in vitro* SCC models within the time-span of our experiments, reinforcing the supposed effects of this compound in cutaneous SCC and indicating potential of our *in vitro* SCC models for drug screening purposes.[36, 37]

Future perspective on *in vitro* SCC models in drug development

Treatment associated with the high and rising prevalence of cutaneous SCC puts an increasingly high financial burden on society, marking a pressing need for advancements in skin cancer drug development. For screening of novel therapeutic compounds, representative models of human cutaneous SCC are required. Such models need not only be representative of human cutaneous SCC, but should also allow for high-throughput screening at limited cost. The *in vitro* cutaneous SCC models presented in this thesis add to the models available for therapeutic screening, as exemplified by testing the effect of the tyrosine kinase inhibitor erlotinib on proliferation and invasion of SCC *in vitro* in **Chapter 6**. In addition to the use of cutaneous SCC cell lines for drug screening purposes, the use of primary SCC biopsies harboring natural heterogeneity increases its representation of primary SCC, but compromises its reproducibility, thereby strongly limiting high-throughput screening. Cell line based models on the other hand offer great availability and reproducibility, but limited representation of primary SCC. Replacement of the dermal ECM by CAF-derived matrix (SCC-FDM) would result in an optimal tumor microenvironment. The *in vitro* SCC models described in this thesis have different strengths in terms of representation, high-throughput options and cost-effectiveness, as schematically displayed in Figure 1.

Undoubtedly, representation of primary SCC is the most vital demand for a reliable *in vitro* SCC model, whereas high-throughput options and low cost are of secondary interest. As no *in vitro* model recapitulates all features of cutaneous SCC, the model of choice for screening novel therapeutic compounds should be a model representing the specific SCC characteristic targeted by the compounds. Moreover, *in vitro* models are perfectly suitable for serial or parallel testing set-ups, as to assess the effect of compounds on multiple SCC features, each represented by different *in vitro* models, ranging from simple and non-expensive two-dimensional monolayer and co-culture systems to more advanced three-dimensional multi-cellular models that structurally and functionally mimic the full microenvironment of native human skin. This approach not only applies to *in vitro* skin cancer models, but also to *in vitro* models representing other skin conditions for which currently no representative models are available for compound testing, including atopic dermatitis and skin ageing.

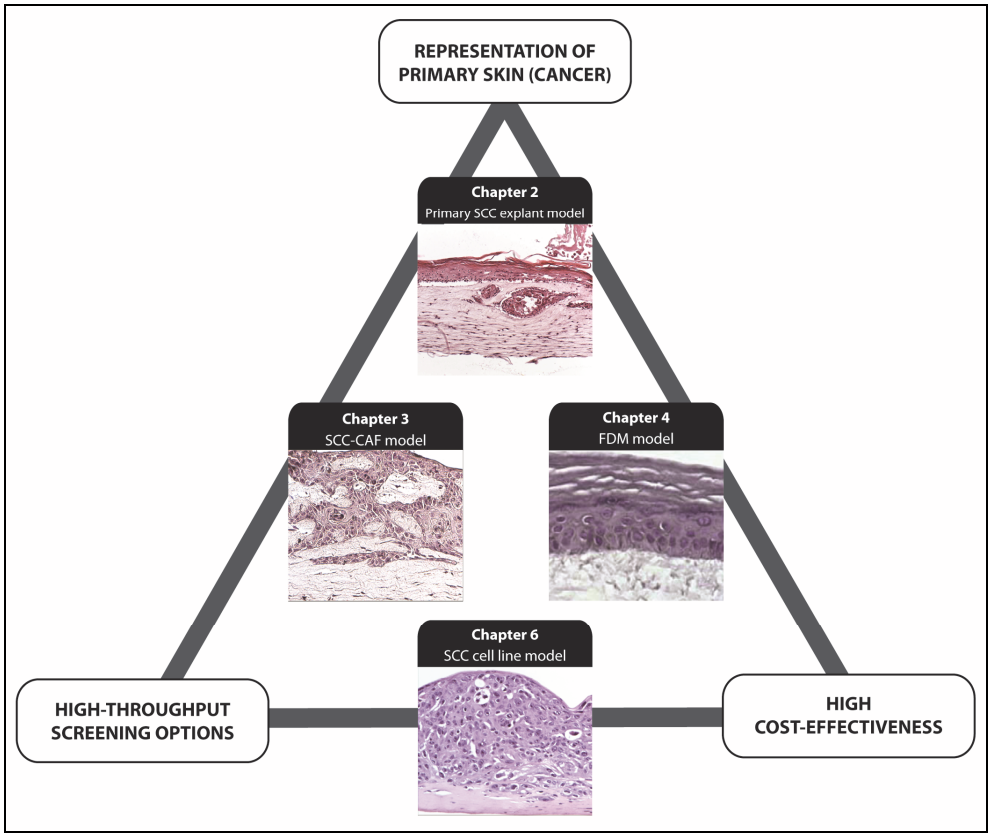

Figure 1 | Relevance of presented *in vitro* human skin (cancer) models in terms of representation, high-throughput screening and cost-effectiveness.

References

1. Glick, A. A new xenotransplantation model reveals tumor-initiating cells in cutaneous squamous cell carcinoma. *J Invest Dermatol* 132, 261-2 (2012).
2. Rheinwald, J.G. & Beckett, M.A. Defective terminal differentiation in culture as a consistent and selectable character of malignant human keratinocytes. *Cell* 22, 629-632 (1980).
3. Watt, S.A. et al. Integrative mRNA profiling comparing cultured primary cells with clinical samples reveals PLK1 and C20orf20 as therapeutic targets in cutaneous squamous cell carcinoma. *Oncogene* (2011).
4. Borchers, A.H. et al. Fibroblast-directed expression and localization of 92-kDa type IV collagenase along the tumor-stroma interface in an in vitro three-dimensional model of human squamous cell carcinoma. *Mol Carcinog* 19, 258-66 (1997).
5. Gioeli, D., Conway, K. & Weissman, B.E. Localization and characterization of a chromosome 11 tumor suppressor gene using organotypic raft cultures. *Cancer Res* 57, 1157-65 (1997).
6. Martins, V.L. et al. Increased invasive behaviour in cutaneous squamous cell carcinoma with loss of basement-membrane type VII collagen. *J Cell Sci* 122, 1788-99 (2009).
7. Obrigkeit, D.H. et al. Effects of photodynamic therapy evaluated in a novel three-dimensional squamous cell carcinoma organ construct of the skin. *Photochem Photobiol* 85, 272-8 (2009).
8. Ponec, M., Weerheim, A., Kempenaar, J., Elias, P.M. & Williams, M.L. Differentiation of cultured human keratinocytes: effect of culture conditions on lipid composition of normal vs. malignant cells. *In Vitro Cell Dev Biol* 25, 689-96 (1989).
9. Conscience, I. et al. P16 is overexpressed in cutaneous carcinomas located on sun-exposed areas. *Eur J Dermatol* 16, 518-22 (2006).
10. El Ghalbzouri, A., Gibbs, S., Lamme, E., Van Blitterswijk, C.A. & Ponec, M. Effect of fibroblasts on epidermal regeneration. *Br.J.Dermatol.* 147, 230-243 (2002).
11. Talghini, S., Halimi, M. & Baybordi, H. Expression of P27, Ki67 and P53 in squamous cell carcinoma, actinic keratosis and Bowen disease. *Pak J Biol Sci* 12, 929-33 (2009).
12. Fernandez-Figueras, M.T. et al. Prognostic significance of p27Kip1, p45Skp2 and Ki67 expression profiles in Merkel cell carcinoma, extracutaneous small cell carcinoma, and cutaneous squamous cell carcinoma. *Histopathology* 46, 614-21 (2005).
13. Suomela, S. et al. CCHCR1 is up-regulated in skin cancer and associated with EGFR expression. *PLoS One* 4, e6030 (2009).
14. Hautier, A. et al. Assessment of organ culture for the conservation of human skin allografts. *Cell Tissue Bank* 9, 19-29 (2008).
15. Richard, G., De, L.V., Didona, B., Bale, S.J. & Compton, J.G. Keratin 13 point mutation underlies the hereditary mucosal epithelial disorder white sponge nevus. *Nat.Genet.* 11, 453-455 (1995).
16. Freedberg, I.M., Tomic-Canic, M., Komine, M. & Blumenberg, M. Keratins and the keratinocyte activation cycle. *J.Invest Dermatol.* 116, 633-640 (2001).
17. Moll, R., Franke, W.W., Schiller, D.L., Geiger, B. & Krepler, R. The catalog of human cytokeratins: patterns of expression in normal epithelia, tumors and cultured cells. *Cell* 31, 11-24 (1982).
18. Yoshikawa, K., Katagata, Y. & Kondo, S. Relative amounts of keratin 17 are higher than those of keratin 16 in hair-follicle-derived tumors in comparison with nonfollicular epithelial skin tumors. *J.Invest Dermatol.* 104, 396-400 (1995).
19. Cassarino, D.S., Derienzo, D.P. & Barr, R.J. Cutaneous squamous cell carcinoma: a comprehensive clinicopathologic classification. Part one. *J.Cutan.Pathol.* 33, 191-206 (2006).
20. Oguro, K. et al. Immunohistochemical alterations in basement membrane components of squamous cell carcinoma. *J.Invest Dermatol.* 96, 250-254 (1991).
21. Tsuboi, R. et al. Comparison of proteinase activities in squamous cell carcinoma, basal cell epithelioma, and seborrheic keratosis. *J.Invest Dermatol.* 90, 869-872 (1988).
22. Dekker, S.K. et al. Skin equivalent: an attractive model to evaluate early melanoma metastasis. *Melanoma Res* 10, 127-40 (2000).
23. Ponec, M. Reconstruction of human epidermis on de-epidermized dermis: Expression of differentiation-specific protein markers and lipid composition. *Toxicol In Vitro* 5, 597-606 (1991).
24. Lacina, L. et al. Stromal fibroblasts from basal cell carcinoma affect phenotype of normal keratinocytes. *Br J Dermatol* 156, 819-29 (2007).
25. Desmouliere, A., Guyot, C. & Gabbiani, G. The stroma reaction myofibroblast: a key player in

the control of tumor cell behavior. *Int.J.Dev.Biol.* 48, 509-517 (2004).
26. Kalluri, R. & Zeisberg, M. Fibroblasts in cancer. *Nat.Rev.Cancer* 6, 392-401 (2006).
27. Lengyel, E. et al. Induction of M(r) 92,000 type IV collagenase expression in a squamous cell carcinoma cell line by fibroblasts. *Cancer Res.* 55, 963-967 (1995).
28. Okawa, T. et al. The functional interplay between EGFR overexpression, hTERT activation, and p53 mutation in esophageal epithelial cells with activation of stromal fibroblasts induces tumor development, invasion, and differentiation. *Genes Dev.* 21, 2788-2803 (2007).
29. Ostman, A. & Augsten, M. Cancer-associated fibroblasts and tumor growth--bystanders turning into key players. *Curr.Opin.Genet.Dev.* 19, 67-73 (2009).
30. Atula, S., Grenman, R. & Syrjanen, S. Fibroblasts can modulate the phenotype of malignant epithelial cells in vitro. *Exp Cell Res* 235, 180-7 (1997).
31. Costea, D.E., Kulasekara, K., Neppelberg, E., Johannessen, A.C. & Vintermyr, O.K. Species-specific fibroblasts required for triggering invasiveness of partially transformed oral keratinocytes. *Am.J.Pathol.* 168, 1889-1897 (2006).
32. Liotta, L.A. et al. Metastatic potential correlates with enzymatic degradation of basement membrane collagen. *Nature* 284, 67-68 (1980).
33. Pelisson, I., Soler, C., Chardonnet, Y., Euvrard, S. & Schmitt, D. A possible role for human papillomaviruses and c-myc, c-Ha-ras, and p53 gene alterations in malignant cutaneous lesions from renal transplant recipients. *Cancer Detect Prev* 20, 20-30 (1996).
34. Toll, A. et al. Epidermal growth factor receptor gene numerical aberrations are frequent events in actinic keratoses and invasive cutaneous squamous cell carcinomas. *Exp Dermatol* 19, 151-3 (2010).
35. van der Schroeff, J.G., Evers, L.M., Boot, A.J. & Bos, J.L. Ras oncogene mutations in basal cell carcinomas and squamous cell carcinomas of human skin. *J Invest Dermatol* 94, 423-5 (1990).
36. Amini, S., Viera, M.H., Valins, W. & Berman, B. Nonsurgical innovations in the treatment of nonmelanoma skin cancer. *J Clin Aesthet Dermatol* 3, 20-34 (2010).
37. Mendelsohn, J. & Baselga, J. Status of epidermal growth factor receptor antagonists in the biology and treatment of cancer. *J.Clin.Oncol.* 21, 2787-2799 (2003).

7

8

Nederlandse samenvatting

List of publications

Curriculum vitae

Short summary

Nederlandse samenvatting

Huidkanker

Huidkanker is de meest voorkomende vorm van kanker bij mensen met een blanke huid. Het aantal patiënten met huidkanker neemt elk jaar toe. In Nederland werden in het jaar 2000 meer dan 20.000 nieuwe gevallen van huidkanker geconstateerd. In 2009 was dat aantal al met 80% toegenomen naar 37.000 nieuwe gevallen per jaar. Ongeveer 15% van alle patiënten met huidkanker heeft een plaveiselcelcarcinoom. Het plaveiselcelcarcinoom is een snelgroeiende en kwaadaardige vorm van huidkanker. Plaveiselcelcarcinomen van de huid vormen een groot probleem voor patiënten die een orgaantransplantatie hebben ondergaan en die medicijnen krijgen ter onderdrukking van hun immuunsysteem om afstoting van het nieuwe orgaan te voorkomen. Het risico op het ontstaan van plaveiselcelcarcinomen is voor deze groep mensen ongeveer 70 keer hoger dan bij de algemene bevolking. Daarnaast hebben deze patiënten ongeveer 75% kans op het ontstaan van een tweede plaveiselcelcarcinoom binnen vijf jaar na de eerste, terwijl dit risico bij de algemene bevolking gemiddeld 20% is. Behalve bij orgaantransplantatie-patiënten, komt het plaveiselcelcarcinoom van huid ook vaker voor bij mensen bij wie het immuunsysteem op een andere manier is onderdrukt, bijvoorbeeld door genetische immuundeficiënties of chemotherapie. Andere risicofactoren zijn blootstelling aan ultraviolette (UV) straling van de zon of zonnebank, radiotherapie en roken. Van deze risicofactoren is blootstelling aan UV-straling de meest bekende en meest relevante voor zowel de algemene bevolking als voor orgaantransplantatiepatiënten. Plaveiselcel-carcinomen komen dan ook het meest voor op lichaamsdelen die veel aan de zon zijn blootgesteld, zoals het gezicht en de armen. Daarnaast zijn er ook risicofactoren die niets te maken hebben met blootstelling, zoals een hoge leeftijd, het mannelijk geslacht en een lichte huidskleur. Plaveiselcelcarcinomen worden meestal verwijderd uit de huid. Bij vroegtijdige behandeling heeft het plaveiselcelcarcinoom een gunstig vooruitzicht en deze vorm van huidkanker is zelden dodelijk. Echter, omdat dit type huidkanker zo vaak voorkomt op zonbeschenen en dus zichtbare huid, kan (het verwijderen van) een plaveiselcelcarcinoom cosmetisch misvormend zijn, wat een grote negatieve invloed kan hebben op de kwaliteit van leven van de patiënt. De kosten voor behandeling van plaveiselcelcarcinomen zijn aanzienlijk. Zo heeft de directe behandeling van plaveiselcelcarcinomen de Verenigde Staten in 2004 maar liefst 1.5 miljard dollar gekost . De sterk toenemende incidentie van plaveiselcelcarcinoom en de kosten van behandeling vormen een groeiend probleem voor de maatschappij.

Proliferatie, differentiatie en invasie

Een plaveiselcelcarcinoom ontstaat uit de bovenste laag cellen van de huid. De menselijke huid bestaat uit drie lagen. Van buiten naar binnen zijn dit de opperhuid (epidermis), de lederhuid (dermis) en het onderhuids bindweefsel (subcutis). De opperhuid bestaat uit epidermale huidcellen (keratinocyten). De keratinocyten in de opperhuid bestaan uit basale cellen en plaveiselcellen. De basale cellen vormen de onderkant van de opperhuid. Daar ontstaan nieuwe huidcellen. Het proces van celdeling in de opperhuid noemt men *epidermale proliferatie*. In de loop van de tijd groeien basale cellen uit tot volwassen plaveiselcellen. Daarbij verhuizen de cellen geleidelijk van de onderste naar de bovenste laag van de opperhuid. Uiteindelijk verhoornen de plaveiselcellen en sterven zij af in de hoornlaag, die de opperhuid bedekt en beschermt tegen invloeden van buitenaf. Gedurende dit proces veranderen de opperhuidcellen ook van vorm: de ronde of ovale basale cellen veranderen in hoekige en uiteindelijk platte plaveiselcellen voordat ze sterven en als huidschilfers worden afgestoten. Dit gehele proces van het uitgroeien van basale cellen tot het afstoten van dode plaveiselcellen noemt men *epidermale differentiatie*. De aanmaak van nieuwe cellen en de afstoting van dode cellen houden elkaar voortdurend in evenwicht. Bij het ontstaan van een plaveiselcelcarcinoom is dit evenwicht verstoord: de proliferatie van de plaveiselcellen gaat sneller dan normaal en er ontstaat een woekering van cellen in de opperhuid. Ook de differentiatie van de cellen raakt hierbij verstoord. De ontregelde celdeling is het gevolg van schade aan DNA in de huidcellen, meestal veroorzaakt door UV-straling. Zulke DNA-schade kan leiden tot veranderingen in genen die coderen voor eiwitten die de celdeling in de huid reguleren, zoals het eiwit p53 en de epidermale groeifactor receptor (EGFR). UV-straling veroorzaakt behalve DNA-schade ook onderdrukking van het immuunsysteem van de huid, waardoor de huid minder goed in staat is om de beschadigde plaveiselcellen op te ruimen. Een plaveiselcelcarcinoom ontstaat in de opperhuid, maar uiteindelijk raakt ook de lederhuid betrokken. De lederhuid bestaat uit bindweefsel, voornamelijk collageen, met daarin dermale huidcellen (fibroblasten). De opperhuid wordt van de lederhuid gescheiden door de basaalmembraan. Dit is een zone die bestaat uit veel verschillende eiwitten die beide huidlagen stevig met elkaar verbinden en die tegelijkertijd een strikte barrière vormt tussen beide compartimenten. De kwaadaardige cellen van een plaveiselcelcarcinoom zijn in staat om deze basaalmembraan te doorbreken en de lederhuid in te groeien. Tijdens dit proces, dat men *invasie* noemt, hebben de keratinocyten in de opperhuid veel interactie met de fibroblasten in de lederhuid. Deze huidkanker-geassocieerde fibroblasten scheiden enerzijds stoffen uit die de plaveiselcellen harder laten groeien en hen meer mobiliteit geven, en anderzijds scheiden ze stoffen uit die de basaalmembraan en het bindweefsel in de lederhuid kunnen afbreken zodat de plaveiselcellen er makkelijker in kunnen groeien.

Van gezonde huid tot plaveiselcelcarcinoom

Een plaveiselcelcarcinoom ontstaat door onherstelbare schade die zich in de loop van de tijd ophoopt in het DNA van de opperhuidcellen. Deze opgebouwde DNA-schade kan op zichzelf tot een plaveiselcelcarcinoom leiden, maar de tumor kan ook voortkomen uit *actinische keratose*, een voorloperstadium waarin beschadigde plaveiselcellen al afwijkend gedrag vertonen, maar waarbij nog geen invasie optreedt. In **hoofdstuk 5** van dit proefschrift onderzochten we de verschillen in genexpressie tussen normale huid, actinische keratose en plaveiselcelcarcinomen van orgaantransplantatiepatiënten bij wie het immuunsysteem werd onderdrukt met medicijnen. Tussen de drie groepen bleken enkele duizenden genen in verschillende mate tot expressie te komen. De grootste verschillen werden gevonden in de expressie van genen waarvan bekend is dat ze betrokken zijn bij epidermale proliferatie en differentiatie in de huid. Bij plaveiselcelcarcinomen vonden we veel veranderingen in groepen genen waarvan bekend is dat ze betrokken zijn bij het ontstaan van kanker. Deze veranderingen waren in mindere mate aanwezig bij actinische keratosen en afwezig bij normale huid.

In vivo en *in vitro* studiemodellen voor het plaveiselcelcarcinoom

De enige directe manier om de ontwikkeling van menselijke plaveiselcelcarcinomen beter te begrijpen en om geneesmiddelen tegen dit type huidkanker te ontwikkelen, is bestudering en behandeling van plaveiselcelcarcinomen bij patiënten. Dergelijk klinisch onderzoek kent echter ethische bezwaren en technische beperkingen. Daarom zijn er indirecte studiemodellen, waarbij men onderscheid maakt tussen *in vivo* en *in vitro* modellen. *In vivo* modellen zijn intacte, levende wezens waarin de ziekte wordt bestudeerd zonder mensen te schaden. Traditionele *in vivo* modellen voor het plaveiselcelcarcinoom van de menselijke huid zijn muizen waarbij men huidkanker veroorzaakt door hen bloot te stellen aan chemische stoffen of UV-straling, of die men genetisch zo verandert dat ze snel plaveiselcelcarcinomen in de huid ontwikkelen. Ook zijn er modellen waarbij men menselijke huidkankercellen injecteert bij muizen die genetisch zo veranderd zijn dat ze geen intact imuunsysteem meer hebben. Deze verschillende *in vivo* modellen hebben in de afgelopen decennia bijgedragen aan de huidige inzichten en behandelmogelijkheden voor het plaveiselcelcarcinoom. Echter, de mate waarin de gebruikte *in vivo* modellen het menselijke plaveiselcelcarcinoom benaderen is beperkt. Dit is het gevolg van grote verschillen tussen de huid van muizen en die van mensen. Zo is de huid van muizen dunner dan die van de mens, vormt de muizenhuid geen littekens na verwonding en vernieuwt de huid van een muis veel sneller dan die van de mens. Daarnaast is het gebruik van *in vivo* modellen onderwerp van ethische discussies. Onderzoekers zijn verplicht om de schade die zij de dieren tijdens een experiment zullen toebrengen af te wegen tegen de verwachte toename in wetenschappelijke kennis.

Daarom moeten zij bij het ontwerpen van dierproeven zoveel mogelijk rekening houden met de drie V's: vermindering, verfijning en vervanging van dierproeven. Bij vermindering van dierproeven is het de bedoeling dat men een bepaalde hoeveelheid informatie verkrijgt met minder dieren. Bij verfijning vermindert men de schade die de dieren wordt toegebracht om pijn, lijden en angst bij de dieren te minimaliseren. Bij vervanging van dierproeven bereikt men een wetenschappelijk doel zonder daarbij enige wetenschappelijke procedure op dieren uit te voeren. Onderzoekers die *in vivo* modellen willen gebruiken voor een experiment, zijn dus verplicht om alternatieven te gebruiken als deze beschikbaar zijn. Dergelijke alternatieven zijn vaak *in vitro* modellen. Dit zijn stukjes van een levend organisme die uit hun biologische context zijn gehaald. Ze zijn daardoor makkelijker te bestuderen en te manipuleren dan wanneer ze nog in het organisme zouden zitten. Dit zijn bijvoorbeeld menselijke huidkankercellen die in een kweekbakje in leven worden gehouden. Er zijn tweedimensionale en driedimensionale *in vitro* kweeksystemen. Waar tweedimensionale modellen slechts één laag cellen bevatten, zijn driedimensionale kweekmodellen opgebouwd uit meerdere cellagen. Voor het *in vitro* onderzoeken van huidkanker bestaan tweedimensionale modellen meestal uit cellijnen die zijn geïsoleerd uit stukjes menselijke huidkanker. Hiermee kan men de kwaadaardige opperhuidcellen los van de omgeving en van andere cellen bestuderen. Om juist de interactie tussen de huidkankercellen en de biologische omgeving te kunnen bestuderen, is het onderzoek beschreven in dit proefschrift gericht op het ontwikkelen van representatieve driedimensionale *in vitro* modellen voor plaveiselcelcarcinomen van de menselijke huid.

Driedimensionale *in vitro* huidkankermodellen

Om de biologisch relevante context zoveel mogelijk te benaderen, zijn driedimensionale *in vitro* huidkankermodellen opgebouwd uit een nagebootste lederhuid (dermaal equivalent) met levende dermale fibroblasten met daar bovenop een laag epidermale keratinocyten die de opperhuid vormen. Tussen de opperhuid en de lederhuid bevindt zich een intacte basaalmembraan. De opperhuid van een gezond *in vitro* huidmodel bestaat uit meerdere lagen gezonde menselijke keratinocyten, die samen een volledig intacte opperhuid vormen, inclusief de afschilferende hoornlaag. De opperhuid van een *in vitro* huidkankermodel bestaat uit menselijke huidkankercellen. Deze cellen vormen geen normale opperhuid, maar een doorgaans ongeorganiseerde en snel groeiende laag cellen die vergelijkbaar is met een plaveiselcelcarcinoom. De lederhuid van een gezond *in vitro* huidmodel bestaat meestal uit een bindweefsel-achtige laag collageenvezels van menselijke of dierlijke oorsprong, uit celvrije lederhuid van huiddonoren of uit een synthetische matrix van niet-levende, draadachtige vezels. In een nagebootste lederhuid worden meestal levende menselijke fibroblasten gebracht. Het maken van een *in vitro*

huid(kanker)model duurt minimaal drie weken. Eerst worden de fibroblasten in de lederhuid van het model gekweekt. Dit duurt één tot vier weken, afhankelijk van het type matrix dat men gebruikt. Daarna wordt de opperhuid op de lederhuid gekweekt. Eerst wordt het hele model enkele dagen gekweekt onder een vloeibare laag kweekmedium, zodat alle cellen voldoende voedingsstoffen krijgen om te groeien. Daarna wordt het model gedurende minimaal twee weken aan de lucht gekweekt en alleen aan de onderkant van kweekmedium voorzien, net zoals menselijke huid(kanker) ook voortdurend blootstaat aan de lucht en vanaf de onderkant gevoed wordt. In deze kweekfase vindt de vorming van een gedifferentieerde opperhuid plaats. Afhankelijk van het type huidmodel, kan deze *air-exposed* kweekfase twee tot twintig weken duren. De samenstelling van de opperhuid, lederhuid, het kweekmedium en de kweekcondities kunnen allemaal naar wens worden aangepast.

Sleutelen aan de *in vitro* opperhuid

Uit de literatuur is bekend dat men *in vitro* huidkankermodellen kweekt met cellijnen verkregen uit menselijke plaveiselcelcarcinomen van de huid. Zulke cellijnen bestaan uit uitsluitend identieke huidkankercellen. Een plaveiselcelcarcinoom bestaat meestal uit allemaal verschillende populaties huidkankercellen en is daarmee heterogeen. Huidkankermodellen die met cellijnen gekweekt worden hebben als groot experimenteel voordeel dat ze zeer reproduceerbaar zijn. Het nadeel van deze modellen is echter dat ze niet de heterogeniteit van een plaveiselcelcarcinoom vertonen zoals die bij een patiënt aanwezig is. In **Hoofdstuk 2** van dit proefschrift hebben we voor het eerst laten zien dat het ook mogelijk is om een *in vitro* huidkankermodel te genereren met in de opperhuid primaire menselijke plaveiselcelcarcinomen, waarin de volledige heterogeniteit van de tumorcellen nog aanwezig is. De plaveiselcelcarcinomen die hiervoor gebruikt zijn, waren goed gedifferentieerde tumoren afkomstig van orgaantransplantatiepatiënten bij wie het immuunsysteem onderdrukt werd met medicijnen. De primaire *in vitro* huidkankermodellen bleken op meerdere fronten vergelijkbaar met originele plaveiselcelcarcinomen. Zo had de opperhuid van de *in vitro* huidkankermodellen een afwijkend differentiatiepatroon dat overeenkomsten vertoont met de differentiatie van echte plaveiselcelcarcinomen. De eiwitten keratine 4 (K4), K13, K16 en K17, die aanwezig zijn in primaire plaveiselcelcarcinomen, bleken ook in de *in vitro* huidkankermodellen aanwezig. Een andere overeenkomst was de vorming van nesten met plaveiselcellen in de lederhuid van de modellen. Hoewel geen uitgebreide invasie werd waargenomen, bleken subpopulaties van de primaire tumorcellen in staat om in een *in vitro* lederhuid te groeien, ook op plaatsen die relatief ver van de originele tumor vandaan lagen. De basaalmembraan van deze modellen was intact en scheidde zowel de epidermis als de ingegroeide celnesten van het dermaal equivalent. Dit doet vermoeden dat de

basaalmembraan niet is doorbroken door de plaveiselcellen uit de primaire tumoren. Mogelijk zijn de plaveiselcellen reeds in de lederhuid gegroeid voordat de basaalmembraan goed en wel gevormd was. Een andere mogelijkheid is dat de ogenschijnlijk invasieve nesten van plaveiselcellen in de lederhuid toch nog in verbinding staan met de opperhuid, maar dat dit in de bekeken doorsneden niet waargenomen is. Ook moet rekening gehouden worden met het feit dat het moment waarop de modellen zijn geanalyseerd de staat weergeeft waarin het model zich na twee weken kweken bevindt. De beperkte proliferatieve en invasieve eigenschappen van de op primaire plaveiselcelcarcinomen gebaseerde *in vitro* huidkankermodellen kunnen het gevolg zijn van de goed gedifferentieerde aard van de primaire tumoren in combinatie met een op gezonde lederhuid lijkende *in vitro* lederhuid, voorzien van levende gezonde fibroblasten. Daarom hebben we in het onderzoek beschreven in **hoofdstuk 3** en **hoofdstuk 4** van dit proefschrift de samenstelling van de lederhuid veranderd.

Sleutelen aan de *in vitro* lederhuid

Waar we in **hoofdstuk 2** gebruik maakten van gezonde fibroblasten in de lederhuid, hebben we in het onderzoek beschreven in **hoofdstuk 3** fibroblasten gebruikt die uit primaire menselijke plaveiselcelcarcinomen afkomstig waren. Als opperhuid maakten we gebruik van twee verschillende cellijnen van het menselijk plaveiselcelcarcinoom. De resulterende *in vitro* huidkankermodellen vertoonden een sterk toegenomen invasie ten opzichte van de modellen met gezonde fibroblasten in de lederhuid. Dit suggereert dat huidkanker-geassocieerde fibroblasten inderdaad een belangrijke bijdrage leveren aan met name het invasieve aspect van huidkanker. Het is de eerste keer dat dergelijke effecten zijn waargenomen met fibroblasten uit plaveiselcelcarcinomen van de huid. Naast het veranderen van de fibroblasten in de lederhuid, hebben we ook de samenstelling van de lederhuid zelf veranderd, zoals beschreven in **hoofdstuk 4** van dit proefschrift. In plaats van collageen afkomstig uit rattenstaarten hebben we gezonde menselijke fibroblasten hun eigen bindweefsel-matrix laten aanmaken, zoals dat in de menselijke huid ook gebeurt. Als opperhuid hebben we hierbij gekozen voor gezonde keratinocyten, die onder invloed van de volledig menselijke lederhuid de menselijke huid nog dichter benaderde en in plaats van de gebruikelijke acht weken maar liefst twintig weken intact bleef. Toekomstig onderzoek zal zich richten op het genereren van *in vitro* huidkankermodellen met een lederhuid die gemaakt is door fibroblasten afkomstig uit plaveiselcelcarcinomen.

Functionele validatie van *in vitro* huidkankermodellen

Om na te gaan of *in vitro* huidkankermodellen geschikt zijn om nieuwe medicijnen tegen huidkanker te testen, hebben we in het onderzoek beschreven in **hoofstuk 6** van dit proefschrift het geneesmiddel erlotinib op deze modellen getest. Erlotinib is een medicijn dat de epidermale groeifactor receptor (EGFR) remt. EGFR is een belangrijk eiwit bij epidermale proliferatie, differentiatie en de ontwikkeling van plaveiselcelcarcinomen. Het middel erlotinib wordt momenteel gebruikt voor patiënten met een bepaald type longkanker, waarin EGFR ook een rol speelt. Om de effecten van dit middel op de huid te bestuderen, hebben we *in vitro* huidkankermodellen gemaakt met plaveiselcelcarcinoom-cellijnen in de opperhuid, die vervolgens hebben behandeld met erlotinib. Waar de *in vitro* huidkankermodellen zonder behandeling een dikke en sterk prolifererende epidermis met tumorcellen vormden die sterke invasie vertoonden, zorgde behandeling met erlotinib ervoor dat de epidermis met tumorcellen nog maar enkele cellagen dun was en er veel minder invasie optrad. Een opvallend gegeven was dat de gezonde *in vitro* huidmodellen die als controle dienden, door de behandeling met erlotinib een sterke toename in schilfering van de hoornlaag vertoonden. Dit leek een *in vitro* manifestatie van een sterk schilferende huid die gezien wordt bij patiënten met longkanker die behandeld worden met erlotinib. Behalve een bevestiging van de toepasbaarheid van *in vitro* huidkankermodellen om het effect van medicijnen tegen huidkanker te screenen, hebben we ook laten zien dat deze modellen geschikt zijn om bijwerkingen van medicijnen te bestuderen die zich uiten in de huid.

In vitro huidkankermodellen voor ontwikkeling van medicijnen

Om in de grote behoefte aan nieuwe behandelingsmogelijkheden voor het plaveiselcelcarcinoom van de huid te voorzien, moeten er nieuwe medicijnen tegen huidkanker worden ontwikkeld en getest op relevante modellen. Zulke modellen moeten niet alleen representatief zijn voor het plaveiselcelcarcinoom bij de mens, maar ze dienen ook geschikt te zijn voor het op grote schaal testen van medicijnen tegen zo laag mogelijke kosten. De *in vitro* huidkankermodellen die in dit proefschrift zijn gepresenteerd vergroten het arsenaal aan beschikbare *in vitro* modellen voor het screenen van medicijnen tegen huidkanker. Het gebruik van plaveiselcelcarcinoom-cellijnen in de opperhuid van *in vitro* huidkankermodellen zorgt voor een hoge reproduceerbaarheid en beschikbaarheid van huidmodellen en zijn daarmee erg geschikt voor het op grotere schaal screenen van nieuwe medicijnen. Wanneer men kiest voor primaire plaveiselcelcarcinomen in de opperhuid van *in vitro* huidkankermodellen verliest men deze reproduceerbaarheid, maar is wel de natuurlijke heterogeniteit van het plaveiselcelcarcinoom in het model aanwezig. Omdat men voor zulke modellen afhankelijk is van primaire plaveiselcelcarcinomen van patiënten, zijn deze modellen niet geschikt voor toepassing op grote schaal. Afhankelijk

van het type medicijn en het stadium van ontwikkeling waarin het medicijn zich bevindt, kan men dus kiezen voor verschillende *in vitro* huidkankermodellen. Verschillende twee- en driedimensionale *in vitro* modellen kunnen ook gecombineerd worden om uiteindelijk een volledig beeld te krijgen van de effecten van een medicijn op de menselijke huid zonder daarbij gebruik te maken van diermodellen.

List of publications

van Doorn R, Zoutman WH, Dijkman R, de Menezes RX, **Commandeur S**, Mulder AA, van der Velden PA, Vermeer MH, Willemze R, Yan PS, Huang TH, Tensen CP. *Epigenetic profiling of cutaneous T-cell lymphoma: promoter hypermethylation of multiple tumor suppressor genes including BCL7a, PTPRG, and p73.* J Clin Oncol. 2005 Jun 10;23(17):3886-96.

Commandeur S, van Beusekom HM, van der Giessen WJ. Polymers, drug release, and drug-eluting stents. J Interv Cardiol. 2006 Dec;19(6):500-6. Review.

Michiels JJ, **Commandeur S**, Hoogenboom GJ, Wegman JJ, Scholten L, van Rijssel RH, De Raeve H. *JAK2(V617F) positive early stage myeloproliferative disease (essential thrombocythemia) as the cause of portal vein thrombosis in two middle-aged women: therapeutic implications in view of the literature.* Ann Hematol. 2007 Nov;86(11):793-800. Review.

El Ghalbzouri A, **Commandeur S**, Rietveld MH, Mulder AA, Willemze R. *Replacement of animal-derived collagen matrix by human fibroblast-derived dermal matrix for human skin equivalent products.* Biomaterials. 2009 Jan;30(1):71-8.

Commandeur S, de Gruijl FR, Willemze R, Tensen CP, El Ghalbzouri A. *An in vitro three-dimensional model of primary human cutaneous squamous cell carcinoma.* Exp Dermatol. 2009 Oct;18(10):849-56.

El Ghalbzouri A, **Commandeur S**. *In vitro disease models: human skin equivalents for research purposes*. ALTEX 27; 2010 special issue:317-320.

Commandeur S, Ho SH, De Gruijl FR, Willemze R, Tensen CP, El Ghalbzouri A. *Functional characterization of cancer associated fibroblasts of human cutaneous squamous cell carcinoma.* Exp Dermatol. 2011 Sep;20(9):737-42.

Commandeur S, Van Drongelen V, De Gruijl FR, Willemze R, El Ghalbzouri A. *Epidermal growth factor receptor activation and inhibition in 3D in vitro models of normal skin and human cutaneous squamous cell carcinoma in vitro.* Cancer Science (accepted).

Hameetman L, **Commandeur S**, Bouwes Bavinck JN, Wisgerhof HC, De Gruijl FR, Willemze R, Mullenders L, Tensen CP, Vrieling H. *Gene expression analysis of squamous cell carcinoma of immunosuppressed transplant recipients.* Submitted.

Emanuel RM, Dueck AC, Geyer HL, Kiladjian JJ, Slot S, Zweegman S, Te Boekhorst PA, **Commandeur S**, Schouten HC, Sackmann F, Kerguelen Fuentes A, Hernández-Maraver D, Pahl HL, Griesshammer M, Stegelmann F, Doehner K, Lehmann T, Bonatz K, Reiter A, Boyer F, Etienne G, Ianotto JC, Ranta D, Roy L, Cahn JY, Harrison CN, Radia D, Muxi P, Maldonado N, Besses C, Cervantes F, Johansson PL, Barbui T, Barosi G, Vannucchi AM, Passamonti F, Andreasson B, Ferarri ML, Rambaldi A, Samuelsson J, Birgegard G, Tefferi A, Mesa RA. *Myeloproliferative Neoplasm (MPN) Symptom Assessment Form Total Symptom Score: Prospective International Assessment of an Abbreviated Symptom Burden Scoring System Among Patients With MPNs.* J Clin Oncol. 2012 Oct 15.

Curriculum vitae

Suzan Commandeur werd geboren op 18 februari 1983 te Delft. Zij groeide op in Naaldwijk en Maassluis en volgde het voorbereidend wetenschappelijk onderwijs (vwo) aan het CSG Aquamarijn te Vlaardingen. Na het behalen van het eindexamen atheneum in 2001, begon zij in datzelfde jaar aan de bacheloropleiding Life Science & Technology aan de Technische Universiteit Delft en de Universiteit Leiden. Ter afsluiting van deze opleiding liep zij stage bij de afdeling Dermatologie van het Leids Universitair Medisch Centrum (LUMC) en deed daar onderzoek naar DNA-methylatie in cutane T-cel lymfomen onder leiding van Dr. Remco van Doorn. Zij vervolgende het Life Science & Technology opleidingstraject in 2003 met de gelijknamige masteropleiding. Ter afsluiting van deze opleiding liep zij een onderzoeksstage bij de afdeling Experimentele Cardiologie in het Erasmus MC te Rotterdam onder leiding van Dr. Heleen van Beusekom. Hier deed zij onderzoek naar regeneratie van menselijke hartcellen met biodegradeerbare, injecteerbare biomaterialen. In het kader van ditzelfde onderzoek liep zij een bedrijfsstage bij de afdeling Business Development van OctoPlus B.V. in Leiden onder leiding van Gerben Moolhuizen MBA, waar ze de marktaspecten van biodegradeerbare microsferen voor hartregeneratie onderzocht in een business case. In 2006 studeerde zij *cum laude* af aan de masteropleiding Life Science & Technology met een specialisatie in *functional genomics*.

In 2006 startte zij met het in dit proefschrift beschreven promotieonderzoek naar de ontwikkeling van een *in vitro* huidkankermodel aan de afdeling Dermatologie van het LUMC onder leiding van Dr. Abdoel El Ghalbzouri, Dr. Frank de Gruijl, Dr. Kees Tensen en Prof. Dr. Rein Willemze. Dit promotieonderzoek werd in 2009 bekroond tot ZonMw Parelproject. Gedurende haar promotieonderzoek begeleidde zij drie studenten Biomedische Wetenschappen bij hun afstudeerstages. In deze periode bouwde zij tevens een netwerk op van contacten bij belangenorganisaties in het veld van alternatieven voor dierproeven. Daarnaast deed zij gedurende een jaar onderzoek naar huidmelanomen onder leiding van Dr. Nelleke Gruis. In die periode begeleidde ze een student Biomedische Wetenschappen bij de ontwikkeling van een *in vitro* model voor huidmelanomen.

Tenslotte heeft zij zich tijdens haar promotieonderzoek samen met haar co-promotor Dr. Abdoel El Ghalbzouri gericht op de commercialisering van *in vitro* huidmodellen door deelname aan de Venture Challenge van het Netherlands Genomics Initiative (NGI) in 2009. Vanaf 2011 werkte zij als *operational manager* op een NGI Life Sciences Pre-Seed Grant aan de verdere commerciële toepassing van *in vitro* huidmodellen binnen de afdeling Dermatologie van het LUMC te Leiden. Momenteel is zij in dienst bij Aeon Astron Europe B.V. als *senior product specialist human skin equivalents* om commercialisering van

de Leidse *in vitro* huidmodellen, waaronder de in dit proefschrift beschreven *in vitro* huidkankermodellen, concreet uit te bouwen in nauwe samenwerking met de afdeling Dermatologie van het LUMC.

Naast haar opleiding en promotieonderzoek is Suzan sinds 2003 actief als vrijwilliger en later bestuurslid informatievoorziening bij de MPN Stichting; de Nederlandse patiënten-organisatie voor mensen met de myeloproliferatieve neoplasieën (MPN) essentiële trombocytemie, polycythaemia vera en myelofibrose.

Short summary

Organotypic *in vitro* models of human cutaneous squamous cell carcinoma

Skin cancer is the most common type of cancer in fair-skinned populations. Cutaneous squamous cell carcinoma (SCC) comprises about 15% of all skin cancer diagnoses. Treatment associated with the high and rising prevalence of cutaneous SCC puts an increasingly high financial burden on society, marking a pressing need for advancements in skin cancer drug development. For screening of novel therapeutic compounds, representative models of human cutaneous SCC are required.

The aim of the research described in this thesis was to develop a representative *in vitro* model of human SCC for screening potential therapeutic compounds, without the unnecessary use of animals. To this end, we generated several three-dimensional *in vitro* SCC models in which the malignant epidermal cancer cells were either represented by intact primary human cutaneous or by established, spontaneously immortalized human cutaneous SCC cell lines. The dermal microenvironment in our models was seeded with either primary normal human dermal fibroblasts or primary fibroblasts associated with SCCs. In verifying human cutaneous SCC representation in these *in vitro models*, we focused on hyperproliferation, cytological and architectural atypia and invasion as three main features of primary SCC.

The *in vitro* skin cancer models presented in this thesis add to the spectrum of available *in vitro* models for therapeutic screening.